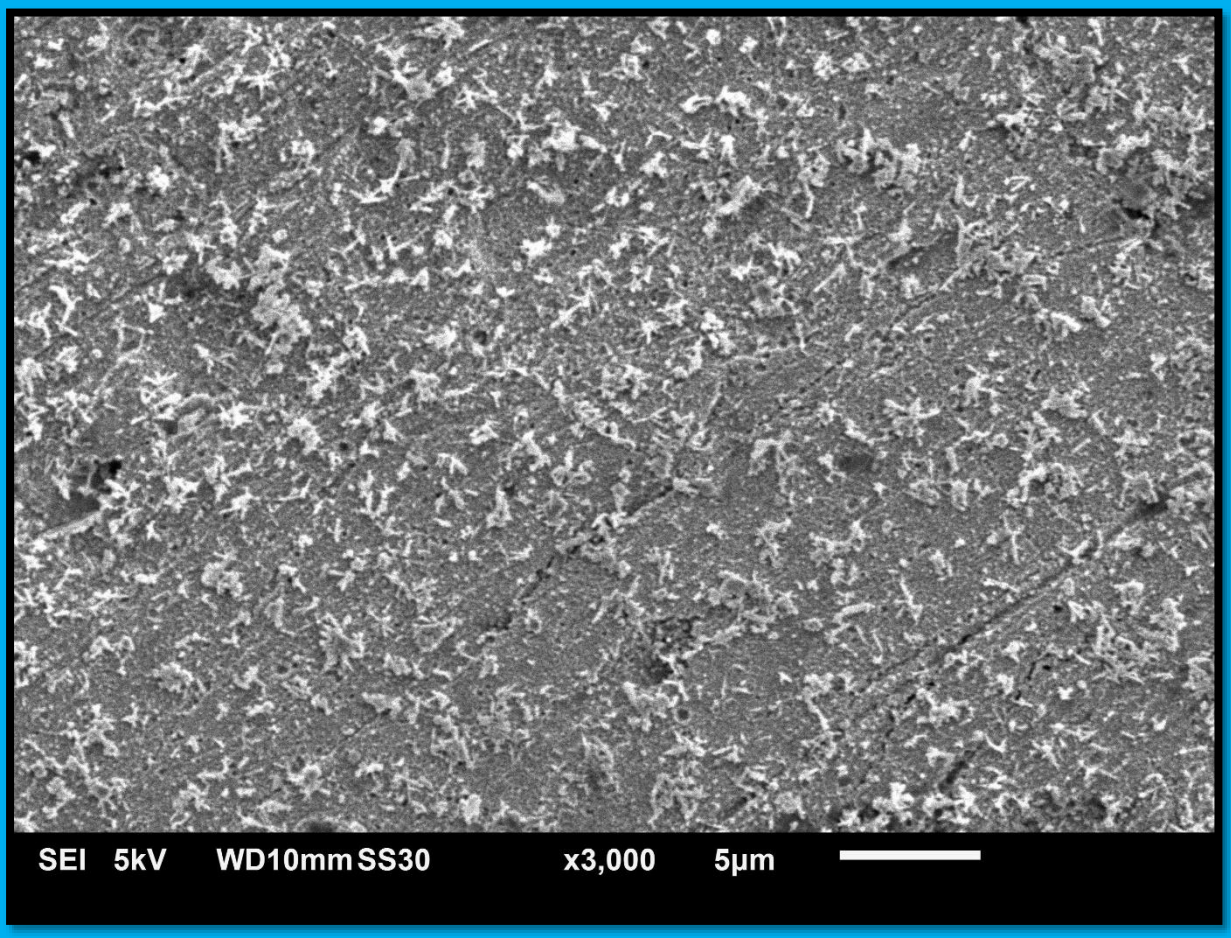

Electrocatalytic reduction of CO_2 in Deep Eutectic Solvents

TU Delft

ADRIANA RIOJA CABANILLAS

Electrocatalytic reduction of CO_2 in Deep Eutectic Solvents

By

Adriana Rioja Cabanillas

in partial fulfilment of the requirements for the degree of

Master of Science
in Sustainable Energy Technology

at the Delft University of Technology,
to be defended publicly on 16 August 2017 at 13:00 PM.

Daily Supervisor:	Dr. Isis Ledezma-Yanez	TU Delft
Responsible Supervisor:	Prof. dr Wiebren de Jong	TU Delft
Thesis committee:	Prof. dr. Fokko Mulder	TU Delft
	Dr. Wim Haije	TU Delft
	Dr. Remco HartKamp	TU Delft


TU Delft

CONTENTS

LIST OF FIGURES

LIST OF ABREVATIONS

ATR	Attenuated Total Reflction
CA	Citric Acid
CE	Counter Electrode
DEA	Diethanolamine
DES	Deep Eutectic Solvent
DL	Double Layer
F	Fructose
FTIR	Fourier Transform Infrared Spectroscopy
HBA	Hydrogen Bond Acceptor
HBD	Hydrogen Bond Donor
HER	Hydrogen Evolution Reaction
IL	Ionic liquid
LTTM	Low Transition Temperature Mixture
RE	Reference Electrode
SERS	Surface Enhanced Raman Spectroscopy
SEIRAS	Surface Enhanced Infrared Absorption
TBA-Cl	Tetrabutylammonium Chloride
UPD	Underpotential deposition
WE	Working Electrode

LIST OF SYMBOLS

δ	Bending of a functional group.
ν	Stretching of a functional group.

ABSTRACT

Energy demand is constantly increasing and the use of fossil fuels causes an accumulation of carbon dioxide (CO_2) which is an important environmental problem that needs to be solved. A promising solution to this problem would be the electrochemical reduction of CO_2 to useful products, using the surplus of electricity from renewable sources. This would be a way of storing this excess of electricity in chemical bonds. However, this has not reached high efficiency and selectivity needed for establishing its use. For this process, the CO_2 is usually dissolved in an aqueous electrolyte. This thesis proposes the new approach, using Deep Eutectic Solvents (DES) which would capture a higher concentration of CO_2 helping to make the whole process more efficient. However, not all salt mixtures reach the eutectic point and therefore, the solvents formed are a low-transition temperature mixtures (LTTMs) of the selected salts.

Experimental work was performed to find out if these solvents can be used for electrochemical carbon dioxide reduction. Non-reported LTTMs were synthetized; they were formed with mixtures of the hydrogen bond donor citric acid (CA), fructose (F) and diethanolamine (DEA) with the hydrogen bond acceptor tetrabutylammonium chloride (TBA-Cl) and different quantities of water, which was found necessary to carry out electrochemistry since the solvents formed were too viscous, and this water has an important effect in the electrocatalytic reduction of CO_2 as proton source and charge carrier.

These solvents were characterized electrochemically, performing studies to find out on which metallic surface they behave better (wider working potential window, low degree of decomposition and adsorption) and how different water quantities affect this process. These studies were performed using cyclic voltammetry. From this, it was seen that the solvents are more stable during electrochemical process in presence of copper. Moreover, the solvent formed by DEA:TBA-Cl:H_2O in the molar proportions 1:1:1,375 was found to have interesting features that resemble CO_2 reduction. As result, this solvent was further analysed using electrochemical in-situ Fourier-Transformed Infrared (FTIR) spectroscopy in surface-enhanced attenuated total reflectance configuration. With this, it was seen that the carbon dioxide was captured by the solvent and that there are visible changes when applying potential. Remarkably, the data shows the formation of a dimer OCCO on the Cu electrode surface, stabilized by the solvent.

This project shows for the first time the electrochemical reduction of CO_2 in LTTMs, evaluating different solvents, metals and water quantities. Determining that the carbon dioxide reduction is possible with the solvent DEA:TBA-Cl:H_2O in the molar proportions 1:1:1,375 in a copper polycrystalline electrode.

1 INTRODUCTION

Energy demand keeps increasing and the use of fossil fuels is causing an accumulation of carbon dioxide (CO_2) in the atmosphere and oceans which is an important environmental problem. It is a very stable gas that is the major contributor to the so-called greenhouse gas effect [1]–[3].

The International Panel on Climate Change (IPCC) in the Fifth Assessment Report (AR5) states:
"The atmospheric concentrations of carbon dioxide, methane and nitrous oxide have increased to levels unprecedented in at least the last 800,000 years. Carbon dioxide concentrations have increased by 40% since pre-industrial times, primarily from fossil fuel emission and secondarily from net land use change emissions. The ocean has absorbed about 30% of the emitted anthropogenic carbon dioxide, causing ocean acidification"[3].

The concentration of carbon dioxide in the atmosphere from 420 000 years ago up to date can be seen in Figure 1-1. It is clear that humans are the cause of the accumulation of CO_2. So it is our responsibility to find solutions for this.

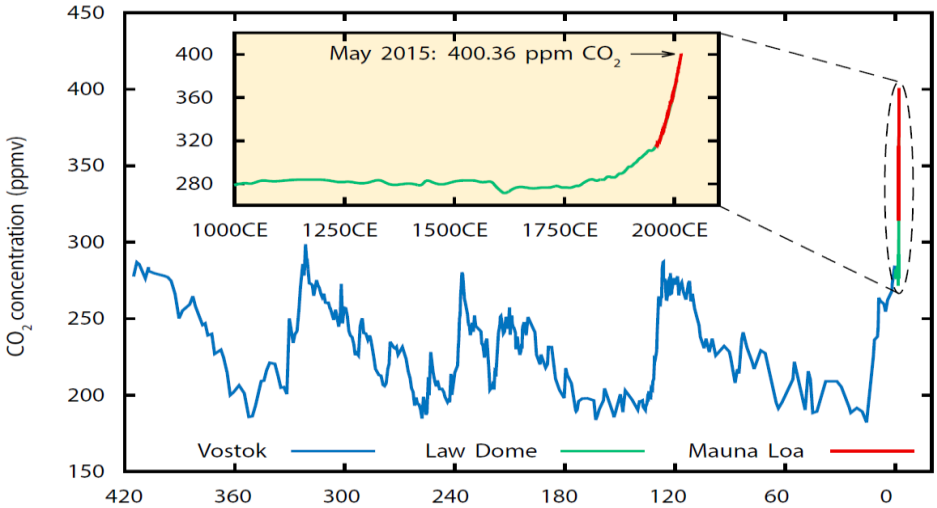

Figure 1-1. Atmospheric CO_2 concentration since 420 000 years ago (in zoom since the year 1000). Figure merges information from antartic Vostok and Law Dome and updated data from the Mauna Loa Observatory in Hawaii [4], [5] **.**

Some proposed solution to reduce the carbon dioxide emissions is to capture and store it, for example, geologically, in oil fields, depleted gas fields, and saline formations. However, this can be very expensive, and generate some risks [6], [7].

An option to reduce the emissions could be to reuse the carbon dioxide, by converting it into other products using CO_2 hydrogenation, CO_2 reacts with H_2 at high temperatures and pressures to produce long chain hydrocarbons. This process has drawn lot of attention, studies have been published and some promising results have been obtained in pilot plants. However, the high pressures and temperatures needed that lead to high costs and the need of hydrogen generated by a renewable source make it not very attractive [8], [9].

Another option could be the conversion of carbon dioxide at room temperature and atmospheric pressure using solar light, this is referred as photocatalysis. In this process, a semiconductor is used as catalyst to take in solar energy and generate electrons and protons which are needed for the reduction of carbon dioxide. Nevertheless, this process has materials and stability issues[10], [11].

A more interesting option could be the electrochemical conversion of carbon dioxide into fuels and chemicals using energy from renewable sources as solar or wind. These sources are intermittent and not very predictable, so it is difficult to match the production with the demand and they are usually far from where the consumption is needed. This makes clear the need of a storage system. This would be a way of storing the excess energy of these intermittent sources for a long term period as chemical fuel. This option has the advantages of a high reactivity under room temperature and atmospheric pressure and a good adaptation to small and large scale processes.

Electrochemistry uses the reactions occurring between the surface of the working electrode, which is the electron conductor, and the electrolyte, with the reactive species dissolved, which is the ionic conductor. Electrons are transferred between these two media by the effect of an applied potential. For making this possible there is a water oxidation followed by the carbon dioxide reduction. But this is a very complex process. Even though there have been numerous studies to develop high performance electrochemical CO_2 reduction systems, these systems did not yield to a commercial application since they have problems with the stability, efficiency and product selectivity [12].

This thesis addresses the problem of improving the efficiency by the approach of finding an electrolyte that would have higher CO_2 solubility that could be used for electrocatalytic carbon dioxide reduction.

The main goal is finding out if Deep Eutectic solvents (DES) can be used for electrocatalytic CO_2 reduction, which has not been tried before. DES can be defined as a eutectic mixture of two or more solids that are liquid at room temperature. If this were possible the efficiency could be increased since these solvents would have a higher solubility than aqueous electrolytes.

The proposed research questions to achieve the described purpose are the following,
Main research question:

- Can DES be used for Electrocatalytic reduction of CO_2?

Sub-questions:

- Can DES be used for electrochemistry?
- Is the DES stable in presence of a determined metallic electrode catalyst?
- Does DES need water addition?
- Does water have an effect in the catalysis?

These questions are addressed with two main experimental studies, electrochemical characterization and in-situ electrochemical spectroscopy. The electrochemical characterization is subdivided in two parts the characterization of metallic surfaces in contact with the solvents and the water effect study.

This thesis follows a classical structure in which the background is presented upfront, followed by the different experimental studies, their results and discussions and a closing chapter containing the conclusions and recommendations.

Chapter 2 gives the background required for the understanding of the thesis. Some fundamental electrochemical concepts are explained. A general overview of how the electrochemical reduction of carbon dioxide works, what are the main problems and the main research lines to improve the problems. The chapter finishes with an overview of ionic liquids and deep eutectic solvents.

Chapter 3 shows experimental work that was chosen to perform with the objective of finding out the previously described research goals. In it, the components used to prepare the solvents, their molar proportions and their preparation procedure are explained. The two main studies are described including their objective, techniques, instruments, materials and procedures used.

Chapter 4 includes the experimental results and the discussion from the two studies: electrochemical characterization and in-situ electrochemical spectroscopy. At the end of each section a brief conclusion is included that helps to understand which information was obtained from the study, preparing the reader in the use of that selected information for the following study.

Chapter 5 presents the conclusions result of the two experimental studies performed, which evaluated different solvents, metals and water quantities. Determining that the carbon dioxide reduction is possible for one of the solvents using copper polycrystalline electrode. Recommendations for future work are included too.

The Appendix compiles the work done to improve the electrode catalyst with the formation of nanostructures, which represents prospects for future work. Problems encountered related to the spectroelectrochemical technique that was proposed to be used in this work are explained (Raman-SERS). Raw data from some measurements are included as well.

2 BACKGROUND

2.1 Electrochemical Fundamentals

It is necessary to consider that for a reaction on the electrode surface to occur, there are three processes involved which are mass transport, a heterogeneous step and a homogeneous step. This can be seen in Figure 2-1.

The mass transport step includes diffusion which can be defined as the movement of the species due to a concentration gradient and it takes place when there is a chemical change at the surface. It includes migration which can be explained as the movement of the species caused by a potential gradient, this process occurs when the external current must be balanced by the transfer of ions at the electrolyte. Moreover, it also includes convection which can be described as the movement of species because of mechanical forces.

The heterogeneous step includes processes as charge transfer, adsorption and desorption, nucleation, crystal growth and surface diffusion. The adsorption of reactants and intermediates is a necessary step for the reaction to occur. In electrocatalysis, the binding energy of adsorption of intermediates is very important since this offers a lower activation energy pathway.
Homogeneous steps include the chemical reactions that occur in the solution.

It should be said that the rate of the transfer of electrons between the electrode and the electrolyte depends mainly on the applied voltage and the strength of the adsorbed intermediates. Nevertheless, physical processes (non-faradaic processes, steric impediment, London forces, Van der Waals forces, etc) might contribute as well, making this process more complex. The overall reaction rate will then be limited by the slowest step [13], [14].

Another effect that should be considered in electrochemistry is the separation between positive and negative charges that occurs at the interface between electrode and electrolyte, this concept is referred as electrical double layer [14], [15].

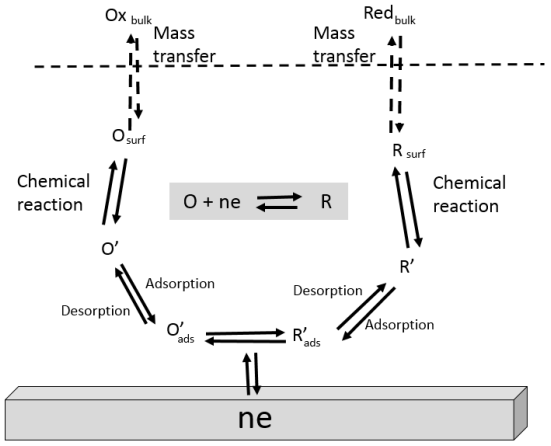

Figure 2-1. Schematic of the processes occurring at the electrode/electrolyte interface. Adapted from [13]**.**

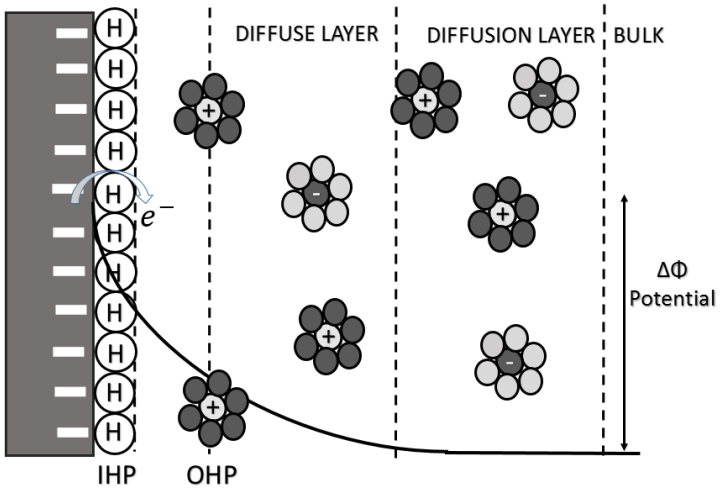

Figure 2-2. Schematic representation of the electrical double layer.

According to the concept, the interface layer can be separated in three zones which are the metal layer, the inner layer and the diffuse layer, this could be seen in Figure 2-2. The metal layer is homogeneous and its extra charge is in a two-dimensional layer close to the solution.

The inner layer accommodates solvent molecules and partial monolayer of neutral molecules or specifically adsorbed ions. These specifically adsorbed ions are mainly anions, but cations could also specifically adsorb. Specifically adsorbed ions are speculated to be not solvated, particularly in the direction of the metal and their centres localization delimits the position of the Inner Helmholtz Plane (IHP).

The diffuse layer is the zone within the bulk and the outer Helmholtz plane (OHP), which is defined as the closest approach of non-specifically adsorbed species. In this layer there is an equilibrium between thermal motion and the long range coulombic forces of the ions with the electrode charge.

2.2 Carbon dioxide electrochemical reduction

Main reactions involved in the electrochemical reduction of carbon dioxide are shown in Table 1.

Table 1. Reactions in the electrochemical reduction of carbon dioxide.

$2H^+ + 2e^- \rightarrow H_2$	**(Equation 1)**
$CO_2 + H^+ + 2e^- \rightarrow HCOO^-$	**(Equation 2)**
$CO_2 + 2H^+ + 2e^- \rightarrow CO + H_2O$	**(Equation 3)**
$CO_2 + 6H^+ + 6e^- \rightarrow CH_3OH + H_2O$	**(Equation 4)**
$CO_2 + 8H^+ + 8e^- \rightarrow CH_4 + 2H_2O$	**(Equation 5)**
$2CO_2 + 12H^+ + 12e^- \rightarrow C_2H_4 + 4H_2O$	**(Equation 6)**

For these reactions to happen an energy input is necessary in the form of electricity. Moreover, they present kinetic barriers that need to be reduced by the utilization of catalysts. However, even using a catalyst, they need an excess of voltage called

overpotential because the interactions between intermediates and solvent are complex and there is no catalyst to date that can catalyse the reduction of carbon dioxide in a spontaneous way.

Another aspect to take into account is the reduction of the water to form hydrogen, called hydrogen evolution reaction (HER), (Equation 1),which is triggered at similar potentials as the carbon dioxide reduction reaction and lowers significantly the faradaic efficiency of the process [14], [16], [17].

It is important to know that the reactions are dependent of the local conditions at the electrode surface like pH and carbon dioxide concentration. These conditions are influenced by buffer strength, degree of mass transport, temperature and pressure [16],[18]. In addition, other factors like the type and amount of other ions in solution could also have an effect in the distribution of products [16].

Besides, it is necessary to note that the electrolyte solution which is close to the electrode is not in equilibrium during the process. For instance, in aqueous electrolytes OH^- is derived from HER, which increases the pH of this region when compared to the bulk electrolyte [13], [14] , [17], [19].

To improve this process, research is needed in both the electrolyte and the catalyst.

First breakthrough happened in 1985 when Hori et al. reported that methane (CH_4) and ethylene (C_2H_4) together with hydrogen (H_2), formic acid (HCOOH), and carbon monoxide (CO) were the main products for carbon dioxide when copper was used as catalyst [20]. Hori et al. reported products as function of applied potential can be seen in Figure 2-3.

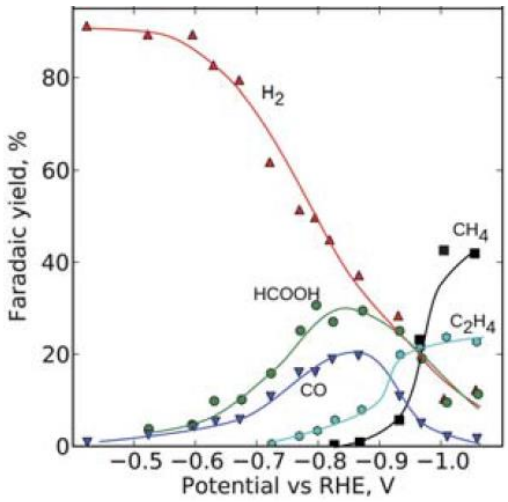

Figure 2-3. Experimental product distribution on a Cu electrode on 0,1 M $KHCO_3$ (pH 6,8) at 18,5 ºC [20]**,** [21]**.**

Peterson et al, reported a computational hydrogen electrode (CHE) model using density functional theory (DFT) which explains the pathways to the products reported by Hori et al. on carbon dioxide reduction on copper surfaces, and which agrees with different experimental studies reported [20],[22], [23]. They reported that in the pathway related to H_2 evolution, protons bind to the same sites as O and OH, being that the reason for a need of a potential of -0,3 V to remove the OH and allow H_2 production. Regarding the HCOOH, they proposed two pathways. The first one, being the cause for lower

overvoltage formic acid production. On it, a proton-electron pair is adsorbed together with carbon dioxide as carboxyl group, to this a second proton-electron pair is added which results in the production at -0,41 V. The second one, being the cause of higher overvoltage production. In this case, carbon dioxide is adsorbed as formate (OCHO) which then desorbs as HCOOH at -0,61 V. According to their model, the key step for CH_4 and C_2H_4 formation is the hydrogenation of previously adsorbed CO to form adsorbed CHO at -0,74 V. The CH_4 pathway suggests that CHO adsorbed together with a proton electron pair originates formaldehyde (H_2CO) that binds weakly, and afterwards is deprotonated to form methoxy (OCH_3), which positions the methyl group away from the electrode surface. A proton from the solution takes this group producing methane. For C_2H_4 they suggested that includes the creation of the C-C bond non-electrochemically on the electrode surface so it could not be explained by their model [21].

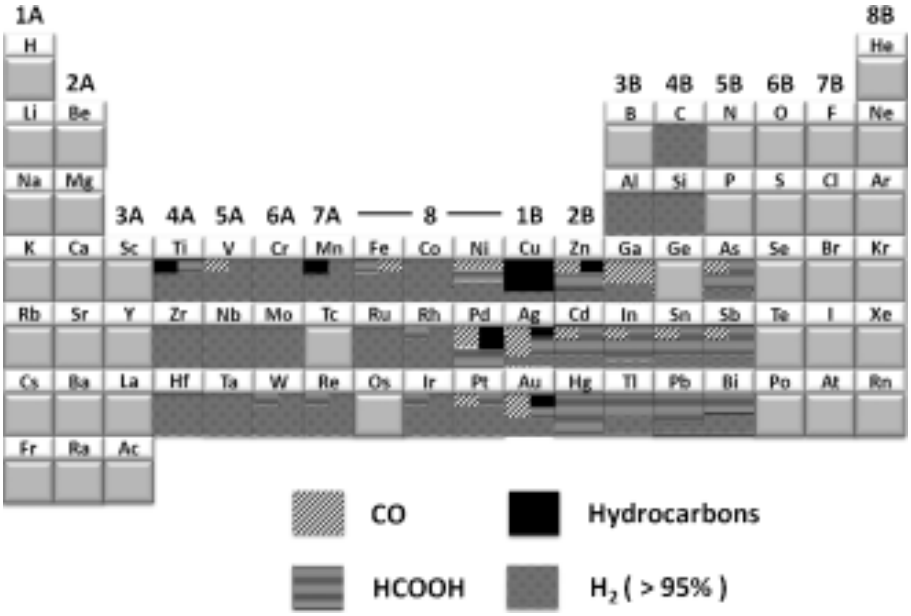

Figure 2-4. Periodic table showing CO_2 reduction products at ambient conditions [24]**.**

There have been several reports that studied the products of carbon dioxide reduction in different transition metals. On Figure 2-4, a periodic table showing the carbon dioxide reduction products of each element can be seen. It is reported that electrodes that have a high hydrogen overvoltage and a small CO adsorption strength of CO as mercury (Hg), cadmium (Cd) lead (Pb), titanium (Ti), indium (In) and tin (Sn) are able to reduce the carbon dioxide with high current efficiency. Nevertheless, they are considered bad catalysts since they mainly produce formate, where there is no rupture of the bond between carbon and oxygen present at carbon dioxide. Besides, they are highly toxic and should not be considered for scaling up options, although they can serve as dopant e.g in copper-based alloys [12].

In addition, electrodes which have a low hydrogen overvoltage and a high CO adsorption strength, as platinum (Pt), nickel (Ni) and iron (Fe) are able to reduce carbon dioxide to form CO [17], [19].

Additionally, electrodes which possess a medium hydrogen overvoltage and a weak CO adsorption are able to catalyze the rupture of the bond between carbon and oxygen that is

present in carbon dioxide; however, they allow the CO to desorb, i.e. gold (Au), silver (Ag), zinc (Zn) and copper (Cu). With Ag, Au and Zn being able to produce CO with high current efficiencies but only Cu having the ability to reduce the CO into other products with notable amounts [16], [25],[26].

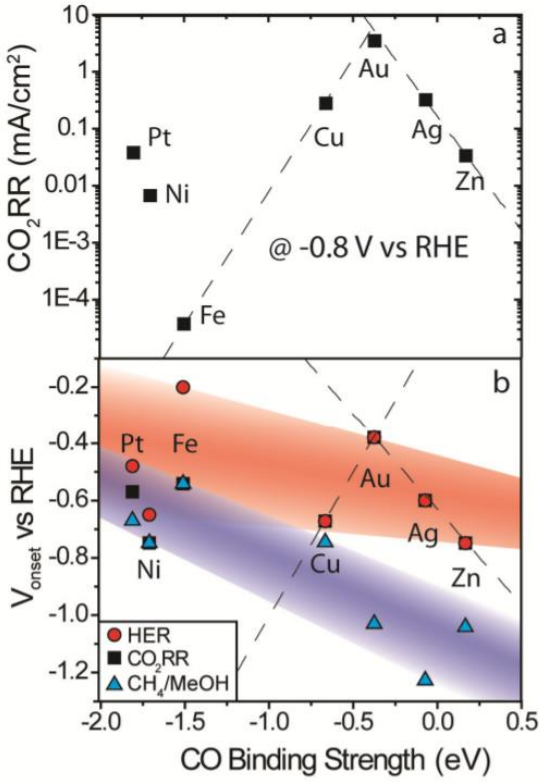

Figure 2-5. Volcano plot for CO binding strength on different metals [27].

It is generally believed that the carbon dioxide reduction depends on the binding energy of CO which is identified as a very important intermediate on this process [17], [18], [21]. On Figure 2-5, the volcano plot for CO binding energy in different metals can be seen. The binding strength of CO is plotted against the current density and onset potential for some metals. This plot follows the Sabatier principle, which states that there is an optimum binding energy for the intermediates of a reaction. It can be seen that Au is close to the top volcano plot, suggesting that its binding energy is close to the optimum, neither too strong, nor too weak. Taking this into account, some reports suggest that the catalyst research needs to study elements with binding energies between Cu and Au. Trying to find a catalyst with higher current density for CO_2 reduction products and earlier onset potential [27].

In the effort to increase the efficiency and selectivity of this process by improving the catalyst there is a research line which involves the development of nanostructured catalysts. This presents a promising way of controlling the reactions and products, since they present higher catalytic surface area and larger portion of low coordinated sites compared to flat surfaces which have full coordinates sites.

Another research line which is directed towards electrochemical reduction of carbon dioxide at non-aqueous solution would result interesting since the hydrogen evolution reaction is suppressed, the concentration of water could be adapted to requirements which

would make easier the mechanistic study. The solubility of CO_2 is increased compared to aqueous solutions, and this could improve significantly the selectivity [16], [13], [28].

Examples of solvents studied could be propylene carbonate (PC), acetonitrile (AC), DMF, dimethyl sulfoxide and methanol [16]. For instance, Haynes and Sawyer reported the reduction of CO_2 to CO and formate at Au in DMSO [29]. In addition, Saveant et al. researched reduction of CO_2 at Hg and Pb in H2O-DMF finding the main products of CO, HCOOH and $(COOH)_2$ [30], [31]. As well, Tyssee et al showed that CO_2 is reduced to oxalic acid in HF in DMF [32].

Recent publications reported that the electrochemical reduction of CO_2 in non-aqueous solvents increases significantly the CO_2 solubility but the absence of protons leads to extremely high overpotentials. But if small quantities of water are added the overpotential is reduced and the CO_2 solubility does not vary much from the dry non-aqueous solvent. [32]. The reduction of CO_2 is significantly dependent on the presence of water, even if just in trace amounts, it was reported that acetonitrile in a system with water acts as weak protic solvent with water playing the main role [28]. Moreover, it is reported that the main mechanism for CO_2 reduction in non-protic solvents and in the presence of water leads to carbonates and bicarbonates [28].

2.3 Ionic Liquids

Ionic liquids (ILs) can be defined as salt mixtures that are composed entirely of ions [33] [34]. An important characteristic of ILs is that they have very low vapour pressures that allows them to be stable at high temperatures. Another decisive property is that they are designer solvents, meaning that their properties can be modified with different combinations of cations and anions [33] [34]. The cations are generally organic structures of low symmetry, meanwhile most common anions are weak basic inorganic or organic compounds that have a diffuse or protected negative charge [13] [35]. Examples of used cations and anions can be seen in Figure 2-6 and Figure 2-7.

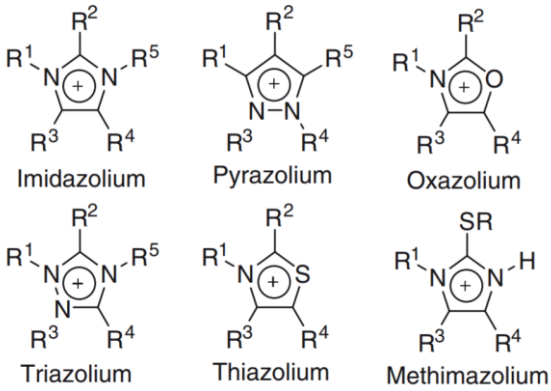

Figure 2-6. Example of cations used to form ILs [36]**.**

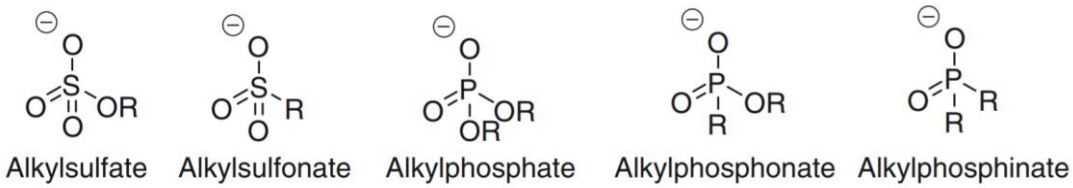

Figure 2-7. Example of anions used to form ILs [36]**.**

Due to their unique properties and tunability, they have quickly shown improved roles as solvents, electrolytes, catalysts and reagents. For example, in the fields of biofuel production [37], [33], in gas separation and capture [38]–[40] and extraction [33] [41].

Ionic liquids have proved to be useful for carbon dioxide capture and electro-reduction. There have been some experimental and theoretical studies of electrocatalytic carbon dioxide reduction in ILs and they report that the unique physicochemical properties can improve activity and selectivity. Regarding experimental studies, screening studies were carried out, trying different combinations of these solvents. Examples of ILs that have been studied several times are imidazolium-based ILs, especially [BMIm][BF4], [EMIm][BF4], or [BMIm][Br] [42]. For example, Rosen et al. reported a system containing [EMIm][BF4], which has low overpotentials and high faradaic efficiency. They explained this as a cause that the IL suppresses the hydrogen formation and provides a low energy pathway for the conversion of CO_2 to CO through the formation of an adsorbed CO_2-EMIm complex [43]. Moreover, studies focused in the characteristics of ionic liquids at the interface between electrode and solvent. Some of them agree that the main driving force for improved activity in these systems are the cations at the electrode surface [35], [42], [44]–[46].

ILs have the disadvantages that the ions are very expensive, as well as the processes to synthesize them, so their application on a large scale would not be possible. Moreover, some of them can be toxic and non biodegradable [33], [34], [47], [48].

2.4 Deep Eutectic Solvents

A eutectic mixture is a specific composition of two or more phase-immiscible solid components that experience a complete change of phase to liquid at a specific temperature, called eutectic point, which is the minimum melting point in the whole set of compositions [49],[50] . The formation happens when the atoms are small enough to locate themselves in the interstitial space of a composite network formed by larger atoms, which causes an interference in the crystalline pattern that decreases electrostatic forces causing a reduction of the freezing point [49].

A Deep eutectic solvent (DES) can be defined as a eutectic mixture of two or more solids that are liquid at room temperature. To this definition, it should be added that it can also be formed by liquids which have a melting point close to room temperature. They are formed by hydrogen bond donor (HBDs) and hydrogen bond acceptors (HBAs) which usually are Lewis or Brønsted acids and bases which can contain a variety of anionic and/or cationic species [50] [51] [52].

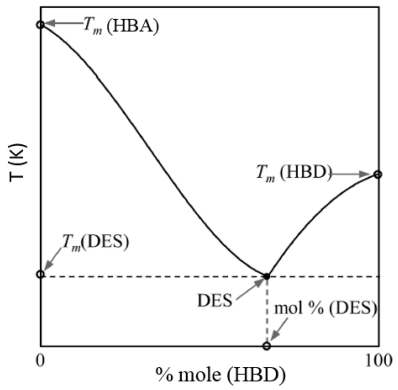

Figure 2-**8. Phase diagram for the formation of a DES** [51]**.**

It should be mentioned that some of the mixtures do not show a specific eutectic point but a glass transition temperature point, which are therefore called low-transition-temperature-mixtures (LTTMs) [53], [54]. Most common structures of HBDs and HBAs used for DES and LTTMs can be seen in Figure 2-9 and Figure 2-10 respectively.

DES main advantages, when compared to ILs, are their low-cost synthesis and they are usually derived from natural sources which makes them nontoxic and totally biodegradables [47], [48],[50], [52].

A disadvantage of DES is their high viscosity that make them difficult to use for some applications. A possible solution is the addition of a small quantity of water which is known to reduce the viscosity and increase the conductivity [55], [56]. However, it was reported that the H-bonding interactions are weakened by the gradual addition of water until they disappear with the addition of 50% (v/v) water addition [55].

First DES was reported in 2002 formed by the combination of choline chloride and urea in the molar proportions 1:2 [51], [57]. Since then, there have been several studies, lot of them are based on the mixture of choline chloride with HBDs [58], [59]. Others have been based in for example: imidazolium [60], ammonium [61],[62] and phosphonium [63].

The research of DESs used for materials in energy and environmental applications is considered to be in its first stages. The main proposed applications of this solvents are metal processing (metal electropolishing, metal extraction and processing of metal oxides, metal electrodeposition) and synthesis media (purifying and manufacturing biodiesel, transformations of unprotected sugars, cellulose and starch, biological transformations, gas adsorption, isothermal synthesis)[49], [51], [64].

Moreover, there have been some studies reporting DES and LTTMs for capture of carbon dioxide [50], [65] ,[66], [67]. For example, a DES has been reported containing monoethanolamine hydrochloride-ethylenediamine uptake of 33,7 wt%, which captures the carbon dioxide via carbamate formation, this is irreversible and needs heat to desorb it [67]. Ternary DES comprised of choline chloride, glycerol and the superbase: 1,5-diazabicyclo[4.3.0] non-5-ene(DBN) reports a capture of 2,3-2,4 mmol of CO_2 per gram of DES (10 wt%) [66]. Furthermore, a study in carbon dioxide capture with LTTMs was reported based on the HBD lactic acid and in HDAs tetramethylammonium chloride, tetraethylammonium chloride, and tetrabutylammonium chloride, reporting that the highest CO_2 solubility was obtained with the mixture of lactic acid and tetrabutylammonium chloride in the molar proportions 1:2 [54].

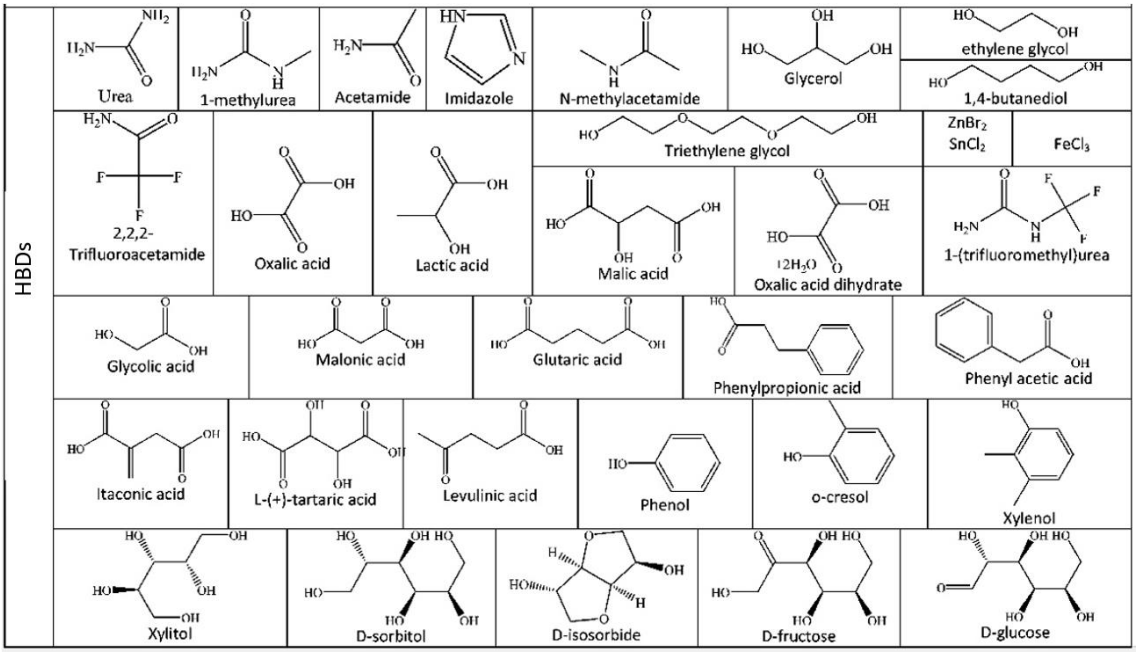

Figure 2-9. Common structures of HBDs used in DESs or LTTMs [51]**.**

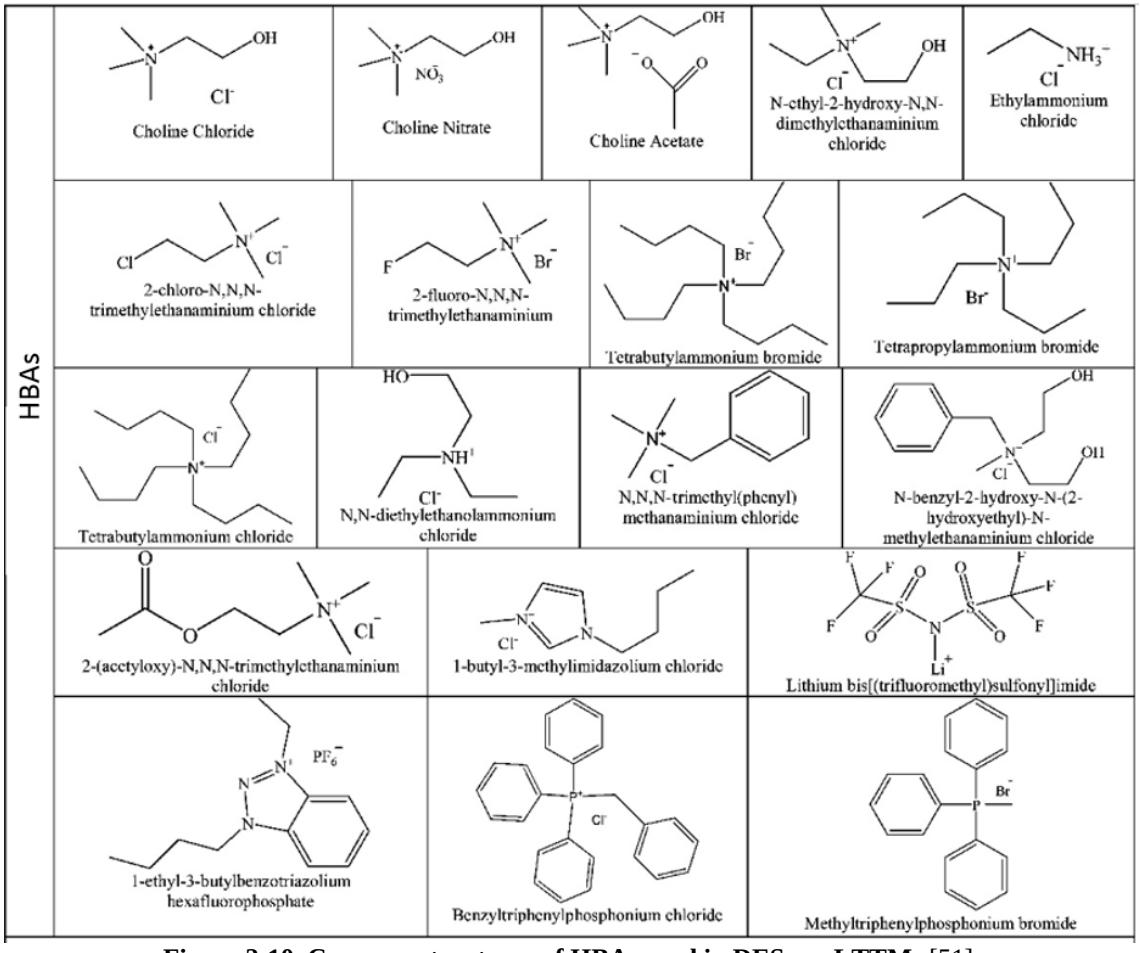

Figure 2-10. Common structures of HBAs used in DESs or LTTMs [51]**.**

3 EXPERIMENTAL

In this chapter, all the information regarding the experimental work is given. The components forming the new compositions (DES-LTTMs) that have not been reported before are described and the procedure to prepare them is explained. The main studies performed are described (Electrochemical characterization and In-situ electrochemical Spectroscopy), explaining why each technique was chosen, their fundamentals and their specific used configurations and set-ups together with every material needed for it.

3.1 SOLVENTS

It is important to note that even the objective is to use DES, it was out of the scope of the project to perform experiments to check if these solvents in the used proportions fulfil all the characteristics required to be deep eutectic solvents. Most probably they formed LTTMs. To avoid misinterpretations, they will be referred as solvents during this sections.

As it was mentioned in section 2.4, DES and LTTMs are formed by a hydrogen bond donor and a hydrogen bond acceptor. The HBDs chosen to form the solvents were citric acid, fructose and diethanolamine. Their structure can be seen in Figure 3-1. On it, the protons that could be reduced and the functional groups can be observed. It should be noted that carbonyl groups (C=O) could help in the capture of carbon dioxide [68], and this is one of the reasons why these compounds were chosen, along with their easy accessibility and biodegradability.

Citric acid (CA), is a weak organic acid, which has three carboxylic acid groups (COOH), which leads to three pKa values, and one hydroxyl group (OH). It occurs naturally in fruits and vegetables with largest amount in citrus fruits as oranges, lemons and limes.
It is mainly produced by fermentation of carbohydrates such as molasses, corn sugar or cane, or extracted from citrus fruits. Its main uses are in food industry as flavouring agent, pH modifier and in cleaning solutions. (Citric acid monohydrate, from Merck was used).

Fructose (F), is a polyhydroxideketone which has five hydroxyl groups (OH) and a carbonyl group (C=O). It is naturally found in honey, tree and vine fruits, berries and root vegetables. It is commercially derived from sugar cane, sugar beets and maize. In food industry it is commonly used as additive for taste enhancement. (Fructose 99 % from Sigma-Aldrich was used).

Diethanolamine (DEA), is a weak organic base, an amino alcohol which has two hydroxyl groups (OH) and an amine group. It is mainly produced from the reaction of ethylene oxide with aqueous ammonia. It is commonly used in the preparation of soaps and surfactants, agricultural chemicals and textile processing and as absorbent for capturing CO_2. (Diethanolamine BioUltra 99,5 % from Sigma-Aldrich was used). The relevant physicochemical properties of these HBDs are shown in Table 2.

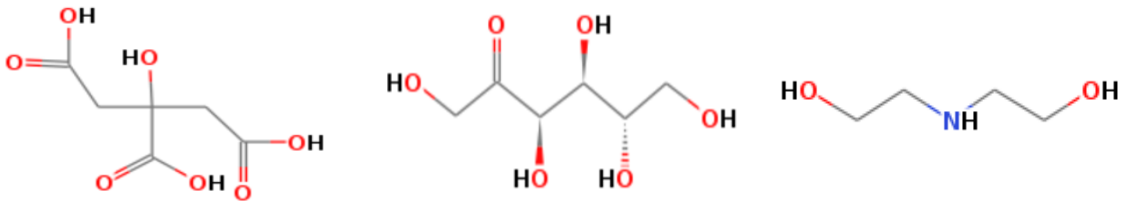

Citric Acid (CA) **Fructose (F)** **Diethanolamine (DEA)**

Figure 3-1. Hydrogen bond donors used [69].

Table 2. Main properties of the hydrogen bond donors used [69], [70].

	Citric Acid	Fructose	Diethanolamine
Molecular Formula	$C_6H_8O_7$	$C_6H_{12}O_6$	$C_4H_{11}NO_2$
Molecular Weight (g/mol)	192,123	180,156	105,137
Hydrogen Bond donor count	4	5	3
Hydrogen Bond acceptor count	7	6	3
Melting Point (ºC)	152	103	28
pKa	3,13; 4,76; 6,4	12,03	8,96

For all solvents tetrabutylammonium chloride (TBA-Cl) was chosen as the hydrogen bond acceptor. It is a vastly used cation in electrochemistry due to its stability. It is reported that the bulkiness of the tetrahedral ammonium ion pushes away the chloride ion from the cation, and this decrease in electrostatic interaction causes these anions to be more nucleophilic [71]. It is believed that these properties could help stabilize the formation of intermediates from CO_2 reduction. (Tetrabutylammonium chloride 97 % from Sigma-Aldrich was used). Its structure and properties can be seen in Figure 3-2 and Table 3.

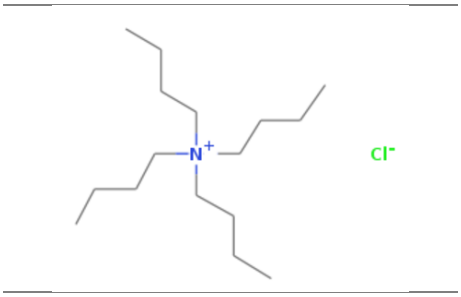

Tetrabutylammonium Chloride (TBA-Cl)

Figure 3-2. Hydrogen bond acceptor used [69].

Table 3. Main properties of the hydrogen bond acceptor used [69],[70].

	Tetrabutylammonium Chloride
Molecular Formula	$C_{16}H_{36}ClN$
Molecular Weight (g/mol)	277,921
Hydrogen Bond donor count	0
Hydrogen Bond acceptor count	1
Melting Point (ºC)	53

In order to prepare the solvent, both components were weighted and placed in a volumetric flask. This mixture is heated with constant magnetic stirring and temperature control until the solvent is formed.

When the solvent is formed, a determined ultrapure water quantity is added and it is stirred until a homogeneous solvent is obtained. Then, it is left to cool down to room temperature before it is transferred to the electrochemical cells where the experiment will be performed. The solvent was daily prepared before each experiment. Using an "old" solvent would have the consequence of an increase in the water content.

3.2 Electrochemical Characterization

The electrochemical characterization has the objective of studying the electrochemical behavior of different solvents. In order to do so, it was divided into two main parts. First, different metals as electrode were studied to identify the solvent performance for each metal. Secondly, after choosing one metal with an improved performance, the effect of the water in the solvent and the electrochemistry was studied, adding different quantities of water to regulate pH/proton availability and comparing the different results. The solvent stability was also characterized.

The metals used were gold, copper, palladium and platinum. These metals were selected since they show interesting electroreduction capacity for carbon dioxide in aqueous solution and therefore these catalysts were expected to show electrocatalytic activity towards CO_2 reduction in the proposed solvents [16],[26],[27].

These studies were carried out performing cyclic voltammetry in a three-electrode cell configuration, using a potentiostat. The potentiostat (Metrohm Autolab) was used. This is an electronic instrument which is connected to the three electrode electrochemical cell: working, counter and reference.

Figure 3-3. Picture of the electrochemical cell, showing RE, WE, CE.

The working electrode (WE) is the electrode on which surface the reaction is occurring.

Counter electrode (CE), is used to close the circuit in the cell. Due to the fact that the current flows between it and the working electrode, its area should be bigger than the working electrode so it does not act as a limiting factor in the kinetics of the electrochemical process under investigation.

The reference electrode (RE), is an electrode which has a stable and well-known electrode potential and it is used as a reference for the process. During the experiments attention was paid to place the reference electrode close to the working electrode to lower the system resistance and ohmic drop.

As previously mentioned, the technique chosen to use in the potentiostat was cyclic voltammetry. Cyclic voltammetry is the usual technique used for electrochemical characterization because the potential at which the faradaic processes occur are easily obtained and interpreted. The processes can be related to the changes observed in the peaks between the first and subsequent cycles. Because of that, this technique is considered useful to identify adsorption and desorption processes, solvent decomposition and redox processes.

In this technique, the potential is swept in time between two values E_1 and E_2, when E_2 is reached the sweep is reversed until the initial potential value E_1. The measured current at the working electrode is plotted versus the applied potential. This can be observed in Figure 3-4. The measured current is usually normalised by the active area of the electrode surface. Then obtaining a plot of potential versus current density (J). In an ideal redox process, the peaks will appear as it is shown in Figure 3-4. However, for non-ideal electrochemical processes (the vast majority) the electrochemical features are distributed in a very different way and are limited by the composition of the electrolyte. In this work, the cyclic voltammograms show upper and lower potential limit, resembling a horizontal sigmoid, with steep oxidation currents owed to metallic dissolution and reduction currents reported as water discharge, water decomposition or hydrogen formation from water, representing well-known phenomena in classic electrochemistry.

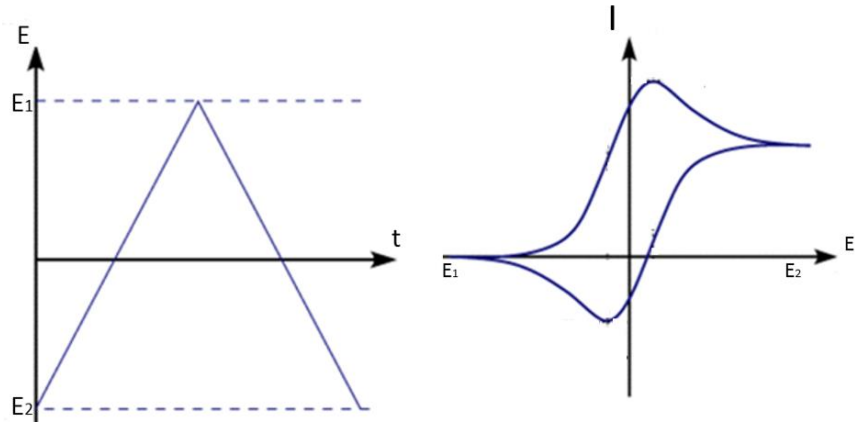

Figure 3-4. Cyclic voltammetry. Potential-time profile (left). Cyclic voltammogram (right). Adapted from [72]**.**

In order to carry out these studies, the solvents were saturated either with carbon dioxide or argon before each measurement. Argon gas was used to remove oxygen present in the solvent and as an inert gas. These two atmospheres were utilized to characterize the solvent both in the presence of carbon dioxide and without it. By comparing these voltammetries, it would be easier to identify if there are features in the voltammetry in presence of CO_2 which do not appear in presence of Ar and that are consequently caused by carbon dioxide reduction or interaction with the solvent.

It is necessary to point out that every experiment was repeated several times to assure the reproducibility of the results presented. The voltammograms were cycled twice, from it

just the second cycle will be shown when there is no significant difference between them, if there is any difference, both cycles will be shown.

Materials

To carry out these experiments two identical glass cells with Teflon caps were used, one to perform experiments in argon atmosphere and the other one for experiments in presence of carbon dioxide. The solvent was divided into two identical quantities for each cell. The cells used had a capacity of 10 mL and the dimensions of 24 mm of diameter and 62 mm height.

The material was boiled weekly with a mixture of acid sulfonitric mixture 1:1 and rinsed three times with ultrapure water. After it is boiled five times in water to eliminate sulfates and nitrates.

Each Cyclic Voltammetry curve was measured in one of the cells with three electrodes connected to the potentiostat as previously described. The WE consisted of a metal wire with a diameter of 3 mm assembled into a solvent resistant PCTFE plastic body. Their dimensions are 7,5 cm length and 5 mm of outer diameter. The electrode was polished manually before every experiment using alumina suspension in water with the different grain sizes of 1 µm, 0,3 µm and 0,05 µm. After polishing, the electrode was sonicated during 10 minutes in ultrapure water to remove possible residues of the alumina suspension. The electrode was dried using air. The RE used was a leakless miniature Ag/AgCl electrode, with a carbon membrane to allow ion migration.

As counter electrodes, a gold wire was used for the WE copper and gold, and a platinum wire was used for the WE palladium and platinum. Before every experiment, the CE was flame annealed to remove the impurities and cooled using water quenching (three times). All these materials can be seen in Figure 3-5.

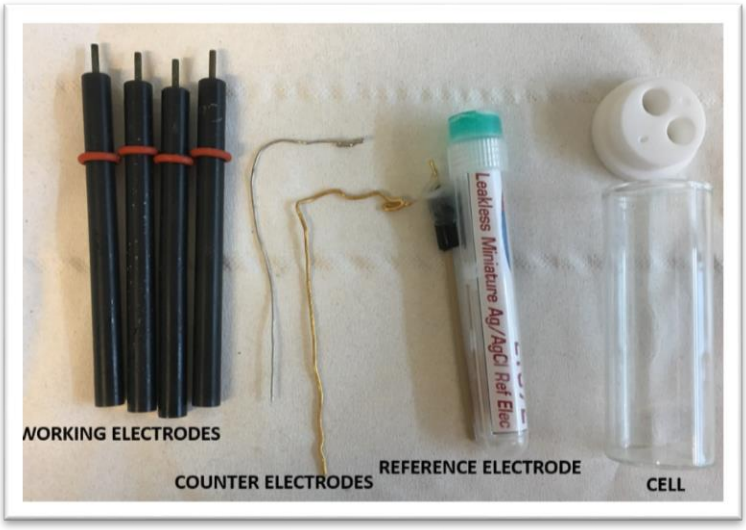

Figure 3-5. Materials used for electrochemical characterization.

3.3 In-situ Electrochemical Spectroscopy

This study is done in order to get information about molecules adsorbed in the electrode surface, intermediates and possible desorbing products in the electrocatalytic reduction of carbon dioxide in the solvent.

3.3.1 Raman

Raman spectroscopy is a technique based on inelastic scattering of monochromatic light. The energy of photons proceeding from a laser are absorbed by the molecules and then reemitted, if the energy at which they are reemitted is shifted up or down in comparison with the original this is referred as Raman effect [73],[74].

The specific technique desired was Surface Enhanced Raman Spectroscopy (SERS). This technique is based in the amplification of Raman signals through the interaction of the light with metals, which originates amplifications of the laser field by excitations referred as plasmon resonances. For this amplification to work the molecules should be absorbed in the surface or very close to it. In order to have these plasmon resonances, usually roughened metals or metals containing nanoparticles are used. Sometimes simply the metal are used too [74]. The different electrodes surfaces tried for plasmon enhancement are described in Appendix B.

The study objective of this technique was to research how the solvent adsorbs on the surface of the catalyst and how this affects in the formation of CO, which as it was previously explained is a key step in the formation of further reduction products.

Materials

Raman spectrometer available was a model RamanRXN2 from Kaiser optical systems. Laser wavelength is 532 nm, 100 mW with a CCD detector. The probe used was an immersion optic, VIS probe with a sapphire window.

The cell was a bottle with customized holes in its Teflon lid, for the three electrodes and the laser probe. The WE consisted of a copper disc of of diameter 250 mm welded to a copper wire, covered by a non-conductive gel Omega bond except for the upper surface, used as active electrode surface. For RE, the Ag/AgCl leakless electrode previously described in section 3.2 was used. For the CE we used a gold coil with a higher surface area than the WE. This is illustrated in Figure 3-6. The whole electrochemical setup was placed inside a Faradaic cage, sealed with tape to prevent light to enter the box.

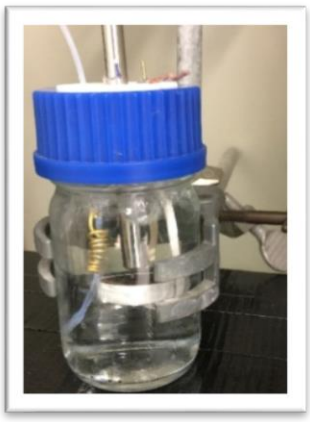

Figure 3-6. Raman setup components.

3.3.2 FTIR (ATR-SEIRAS)

FTIR technique is based on the principle that all the atoms in a molecule which are at a temperature above absolute zero are in vibration with respect to each other. When the molecules are exposed to IR source, if the frequency of the IR radiation is the same as the vibration frequency of the atoms, the molecule absorbs the radiation [14].

It is important to know that each compound induces many bands at different wavelengths. This is caused by the different functional groups that are present in each molecule and the different types of vibration between the atoms. The main vibrations are symmetric and asymmetric stretching, in plane bending vibrations, as scissoring and rocking in and out of plane, as well as bending vibrations like wagging and twisting.

The IR region is situated at the low energy side of the electromagnetic spectrum and usually compounds absorb IR radiation in the mid-infrared region which ranges from wavenumber of 4000 cm^{-1} to 400 cm^{-1}. This range can be divided in two regions, one containing wavenumber between 4000 cm^{-1} and around 1300 cm^{-1}, that is called functional group region. In it, bands are characteristic of a type of bond and consequently, this region can be used to identify if a specific functional group is there. The second region that go until wavenumber 400 cm^{-1} is called fingerprint region. Bands in this region are caused by complex deformations of the molecule, most of the bending vibrations (some stretching) occurs, so it is not useful to identify functional groups, but it shows characteristic bands for each compound that are unique and can be used to identify molecules with similar functional groups, and it is used to identify adsorbed intermediates, which is the purpose of this study.

The interpretation of the spectra follows Planck's equation, which presents the relation between energy and frequency. At higher frequencies, higher vibrational energy are in relation with the strength of the bonds between the atoms. For example, a double bond between two atoms would be at higher wavenumber than a single bond between the same atoms.

This technique was used in situ. Electrochemical in situ FTIR spectroscopy studies the changes in the spectrum with applied potential which is very useful to identify the molecules adsorbed, intermediates and desorbing products at the surface and the surrounding electrolyte during the catalytic process, all within the perimeters of the electrical double layer.

Attenuated total reflection (ATR) was used which is a surface sensitive FTIR technique. It consists of IR light that penetrates through a crystal of IR transparent material and bounces in the crystal just penetrating few μm into the liquid [75]. This can be observed in Figure 3-7. A higher number of bounces have a greater contact with the molecules that translates into a higher intensity.

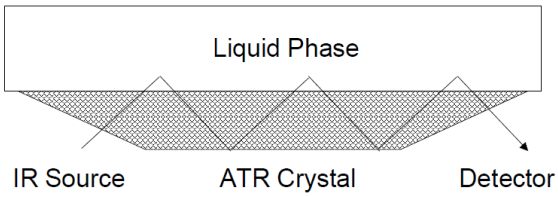

Figure 3-7. ATR principle [75].

More specifically surface-enhanced Infrared Absorption (SEIRAS) with ATR configuration was used. SEIRAS uses a vacuum evaporated metal film as working electrode. Analogously to SERS which was explained previously, it is based in the effect that molecules in the metal surface show higher infrared absorption than measurements without the metal. The enhancement greatly depends on the morphology of the metal surface [75].

All the spectra were obtained by averaging 100 scans with 4 cm^{-1} resolution. The spectra were averaged while imposing a determined potential, in a potential working window in which the experimentalist knows that a Faradaic process is occurring.

For the SEIRAS spectra, first, a background spectrum was obtained in open circuit voltage configuration. Then, the potential was varied and each sample was obtained. The final spectra are represented as absorbance, following $A=-\log(R/R_o)$ where R and R_o are the reflectance corresponding to the spectra collected at the sample and at reference potential. In these difference spectra, negative bands (pointing down) are the species that were on the electrode surface or near it at the reference potential and when the potential is applied they are leaving this region. Positive bands (pointing up) are species which are forming or are going toward the electrode surface [28].

Materials

To be able to use this technique in situ for the WE a copper film was deposited on top of the crystal. This crystal is placed in a holder and with an electrochemical cell on top. The cell has two holes in its lid to introduce the RE and CE, and the connection between the deposited WE and the potentiostat was made using a copper tape which was positioned under the o-ring and pressed between the cell body and the prism's base.

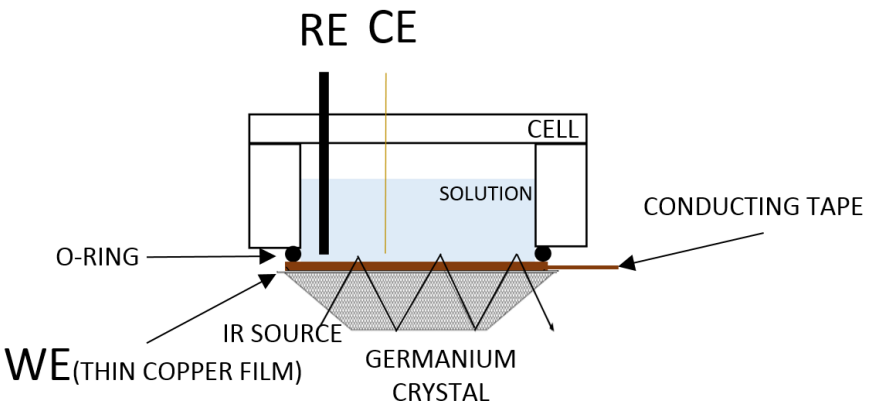

Figure 3-8. Transverse section of the schematic representation of SEIRAS configuration.

Germanium crystal beveled at 60º was used as IR transparent material. In this case, metallic copper was deposited using the technique physical vapor deposition (PVD). For this technique, a piece of the metal required is placed in the tungsten holder, it generates a high vacuum and applying certain current in between the two nods connected by the tungsten holder. The metallic piece is molten and vaporized, and the vapors are carried towards the germanium crystal where it is condensed forming a thin film. The thickness of this film can be controlled by a quartz crystal microbalance. The result is a thin metallic foil of few nanometer in thickness (10 to 15 nm).

The RE used was a leakless miniature Ag/AgCl electrode, with a carbon membrane to allow ion migration.

As CE, a gold wire was used. Before every experiment, the CE was flame-annealed to remove the impurities, and cooled using water quenching repetitively.

The solvent was bubbled with CO_2 until saturation before the experiment. No bubbling was done during measuring.

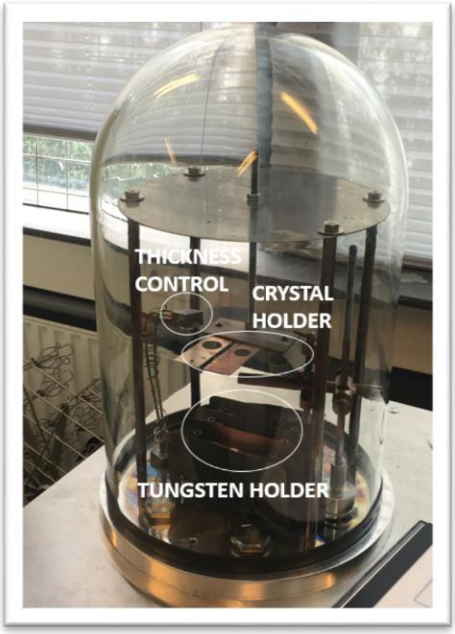

Figure 3-9. PVD machine.

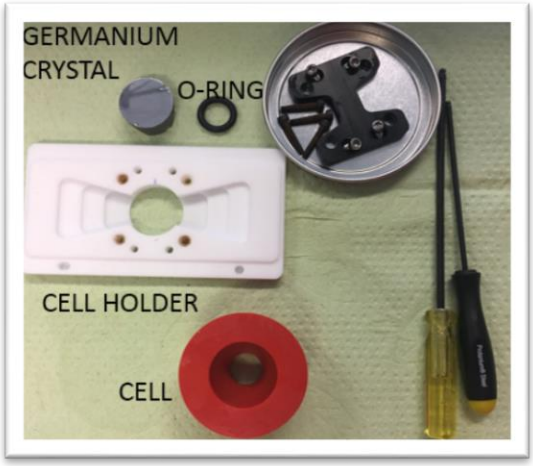

Figure 3-10. Parts of the set-up used for FTIR.

4 RESULTS AND DISSCUSIONS

In this chapter the experimental results from the electrochemical characterization and the in-situ electrochemical spectroscopy are presented and discussed. Since the findings of the studies determine the choice of parameters in posterior studies, some conclusions are included at the end of each section to better understand which information is obtained from the results and used in posterior studies.

4.1 Electrochemical Characterization

As it was previously mentioned the electrochemical characterization was divided into two studies. First, the characterization of metallic electrode surfaces in contact with different solvents was done. The metals used were gold, copper, palladium and platinum. Performance of these metals was judged in terms of stability and of the absence of evident features associated to proton reduction from the hydrogen bond donor or solvent adsorption. Second, the water study was performed using the chosen metal, this was done regulating the proton availability with different water quantities. The stability during several cycles was studied as well.

4.1.1 Characterization of metallic electrode surfaces in contact with the different solvents

In this section, different metals were studied for the solvents formed by CA:TBA-Cl:H_2O and F:TBA-Cl:H_2O, both solvents had the molar proportion 1:1:27,5.

In this study, a screening was done to find the working potential windows for each system. The working potential windows give an indication of the regions of electrochemical stability. Different working potential windows were used as well to explore the limits at which H_2 formation from water and dissolution of the surfaces start. Just the ones considered relevant are presented below.

The voltammograms were analysed to discover if the solvent is stable in the presence of each metal electrode. Moreover, every feature was carefully analysed, trying to correlate them to the processes occurring in the system. Special attention was paid to features that could resemble the adsorption or reduction of carbon dioxide. This study had as well the purpose of seeing if any metal showed better performance than the rest in terms of stability and of the absence of features associated to proton reduction from the hydrogen bond donor or solvent adsorption and then it could be chosen for further studies.

CA:TBA-Cl: H_2O

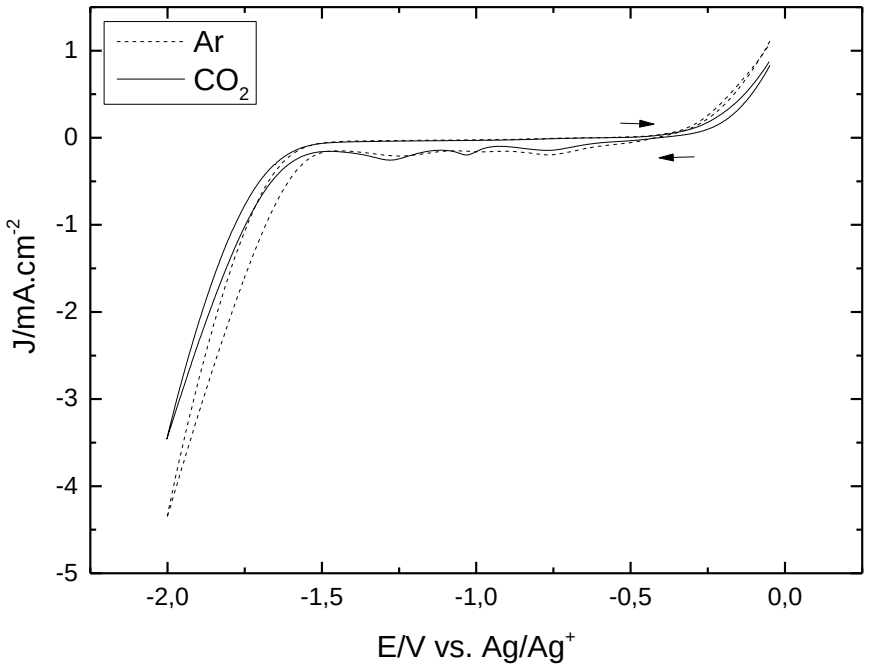

Figure 4-1. Cyclic voltammograms for a polycrystalline gold electrode, in CA:TBA-Cl:H_2O with molar proportions 1:1:27,5, in saturated Ar and CO_2, scan rate: 0,1V/s, working window: 0V -2V.

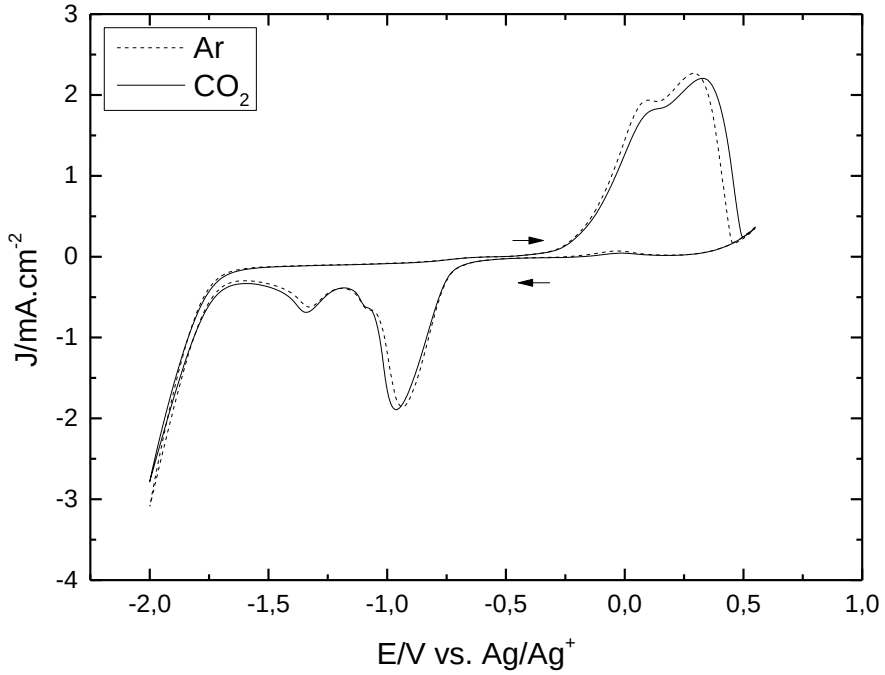

Figure 4-2. Cyclic voltammograms for a polycrystalline gold electrode, in CA:TBA-Cl:H_2O with molar proportions 1:1:27,5, in saturated Ar and CO_2, scan rate: 0,1 V/s, working window: 0,6 V -2 V.

Figure 4-1 and Figure 4-2 present cyclic voltammograms for a polycrystalline gold electrode in the solvent formed by CA:TBA-Cl:H_2O with two different potential windows in order to explore if the working window limits are a cause of the solvent decomposition or catalyst modification. In this case, it can be seen in Figure 4-2, that when the working window is expanded until a potential of 0,6 V, features are observed at potential of 0,1 V and 0,3 V, this could be because the gold catalyst forms oxides and oxyhydroxides. This oxides require usually large overpotentials to be formed, but in presence of this solvent they can be seen at low overpontentials. Their reduction can be seen at potentials of -0,94 V, -1,1V -1,3 V. However, it is suggested that this reduction might be overlapped with proton reduction since when the working is shortened to 0 V (Figure 4-1) and there is no oxide and oxyhydroxide formation, there is a slight reduction at potential values of -0,8 V, -1 V and -1,3 V [76]. Moreover, the H_2 formation from water can be observed which an onset potential around -1,6 V.

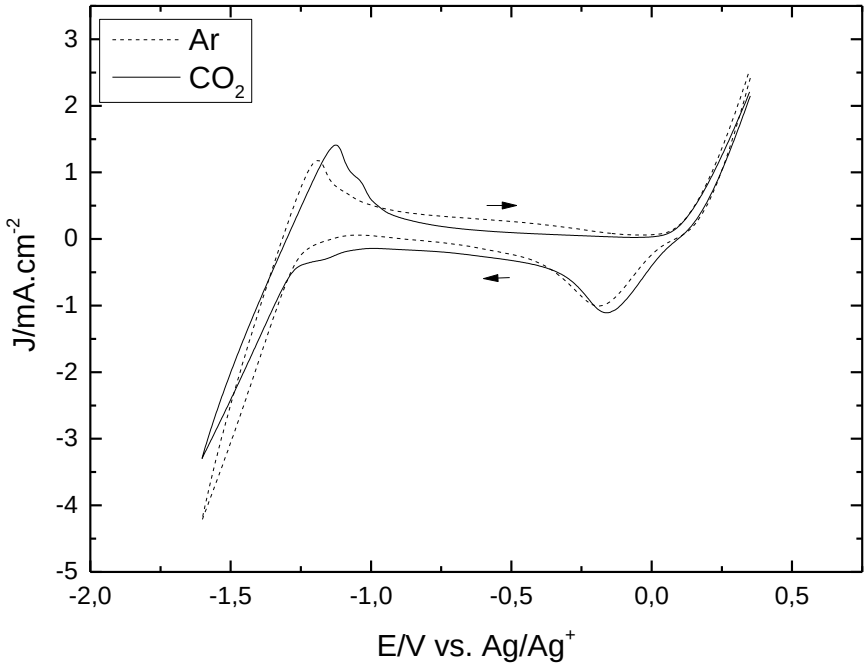

Figure 4-3. Cyclic voltammograms for a polycrystalline platinum electrode, in CA:TBA-Cl: H_2O with molar proportions 1:1:27,5, in saturated Ar and CO_2, scan rate: 0,1V/s, working window 0,4 V -1,6 V.

Figure 4-3 exhibits cyclic voltammogram for a polycrystalline platinum electrode in the solvent formed by CA:TBA-Cl:H_2O. Similar features can be observed for argon than for carbon dioxide but slightly displaced in potential. First, a feature at a potential of -0,2 V in argon and -0,15 V in carbon dioxide can be seen, it is attributed to the reduction of oxides. The H_2 formation from water reaction has an onset potential of -1,1 V for argon and -1,25 V for CO_2. Another feature can be recognized at a potential around -1,1 V just in carbon dioxide. Moreover, in the reverse cycle just in carbon dioxide a feature can be observed in a potential of -1 V. This suggest the formation of underpotentially deposited hydrogen (H-UPD) with the peak from hydrogen oxidation at -1,1 V [77]. This is remarkable, in a solvent mixture in which water is not the target solvent. Underpotential

hydrogen deposition occurs when the hydrogen is deposited at a potential lower than its equilibrium reduction potential [78].

In Figure 4-4 the cyclic voltammogram for a polycrystalline palladium electrode in the solvent formed by CA:TBA-Cl:H_2O is displayed. For argon there is a feature at the potential -0,3 V which could be considered due to solvent adsorption since in the reverse cycle, there is one at -0,4 V that could be due to solvent desorption. Another feature at -1 V, can be observed in both argon and carbon dioxide atmospheres that is attributed to proton reduction. Moreover, H_2 formation from water can be seen with an onset potential of -1,2 V. In presence of carbon dioxide the voltammetry is tilted. Since the configuration of the cell and the distances between the electrodes were ensured to be the same, this tilting is proposed to be due to ohmic drop caused by the competition of species in the surface which hinders electron transfer.

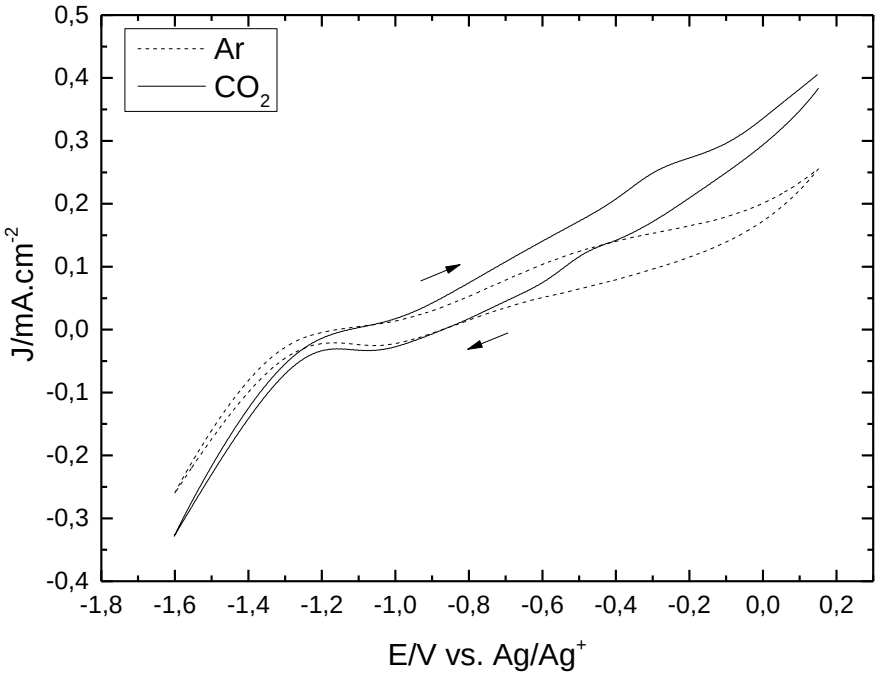

Figure 4-4. Cyclic voltammograms for a polycrystalline palladium electrode, in CA:TBA-Cl: H_2O with molar proportions 1:1:27,5, in saturated Ar and CO_2, scan rate: 0,1V/s, working window 0V - 1,6 V.

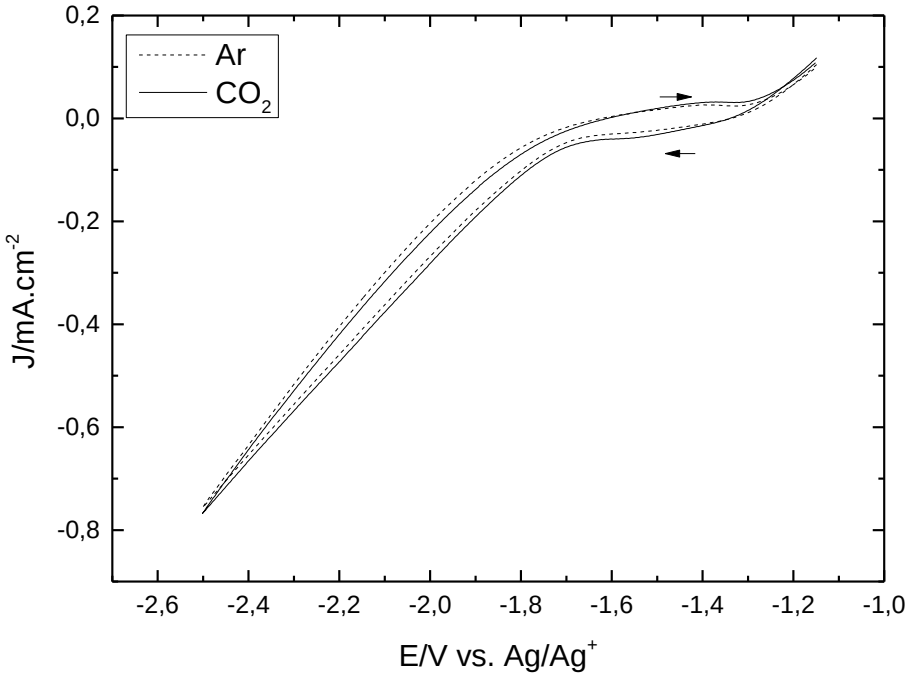

Figure 4-5. Cyclic voltammograms for a polycrystalline copper electrode, in CA:TBA-Cl: H_2O with molar proportions 1:1:27,5, in saturated Ar and CO_2, scan rate: 0,1V/s working window: -1,2V - 2,5V.

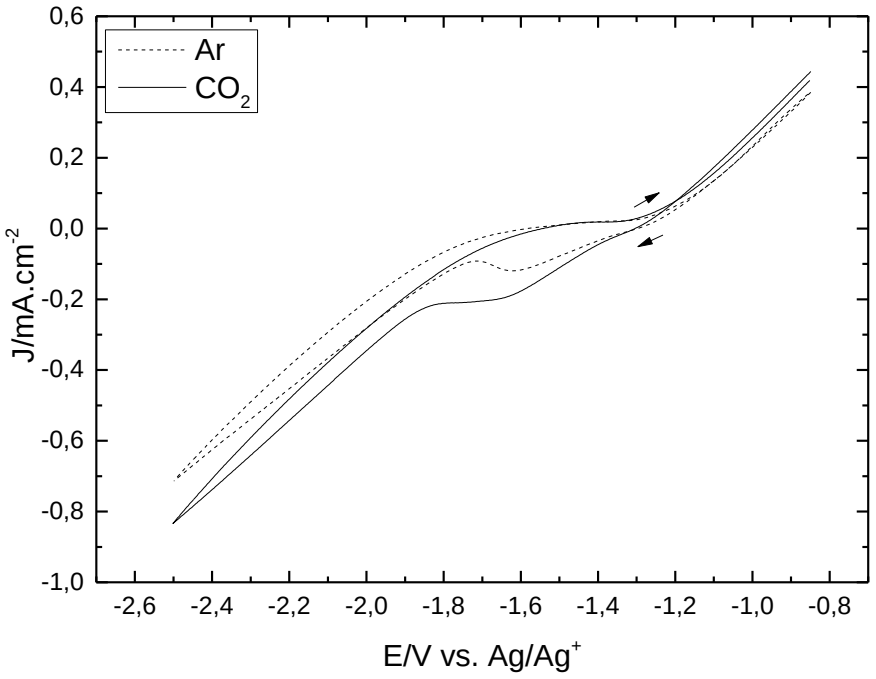

Figure 4-6. Cyclic voltammograms for a polycrystalline copper electrode, in CA:TBA-Cl: H_2O with molar proportions 1:1:27,5, in saturated Ar and CO_2, scan rate: 0,1V/s, working window -0,8V -2,5V.

Figure 4-5 and Figure 4-6 show cyclic voltammograms for a polycrystalline copper electrode in the solvent formed by CA:TBA-Cl:H_2O . It can be seen that H_2 formation from water has an onset potential of -1,65 V for Figure 4-5 and -1,85 V for Figure 4-6. When the working window is expanded to positive potentials (Figure 4-6), it can be seen that from potentials above -1,2 V there is copper dissolution [72]. This leads to a higher surface area which translates in more active sites available for reactions to occur.

F:TBA-Cl: H_2O

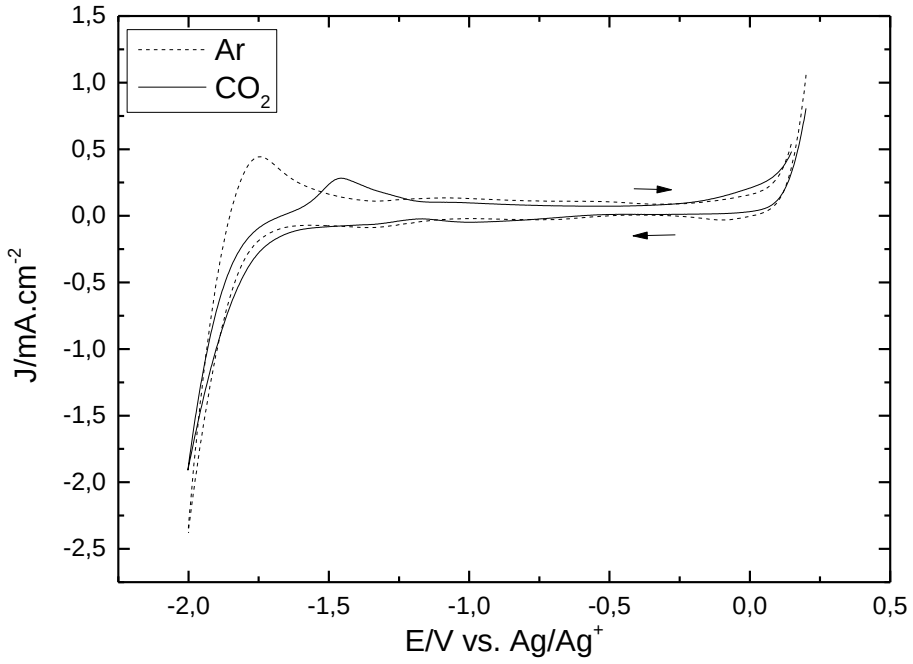

Figure 4-7. Cyclic voltammograms for a polycrystalline platinum electrode, in F:TBA-Cl: H_2O with molar proportions 1:1:27,5, in saturated Ar and CO_2, scan rate: 0,1V/s, working window: 0,2V -2V.

Figure 4-7 and Figure 4-8 present cyclic voltammograms for two different working windows with a polycrystalline platinum electrode in the solvent formed by F:TBA-Cl:H_2O.

In Figure 4-7, a feature can be observed at a potential of -1,3 V that suggests solvent adsorption. Another feature can be observed in the reverse cycle at a potential of -1,7 V for argon and -1,4 V for carbon dioxide, that could be caused by solvent desorption. Formation of H_2 from water can be seen with an onset potential of -1,6 V followed by hydrogen oxidation in the backwards scan.

In Figure 4-8, a feature can be observed at a potential of -0,2 V for both argon and carbon dioxide, this is due to reduction of Pt oxides. As well, another feature can be seen at a potential ca. -1,4 V for both carbon dioxide and argon, this suggests hydrogen adsorption, never shown before in another solvent than water-based electrolytes. The H_2 formation from water can be recognized with an onset potential of -1,7 V. Remarkably, there is H-UPD formation also in fructose, with an overpotential of ca. -1,5 V.

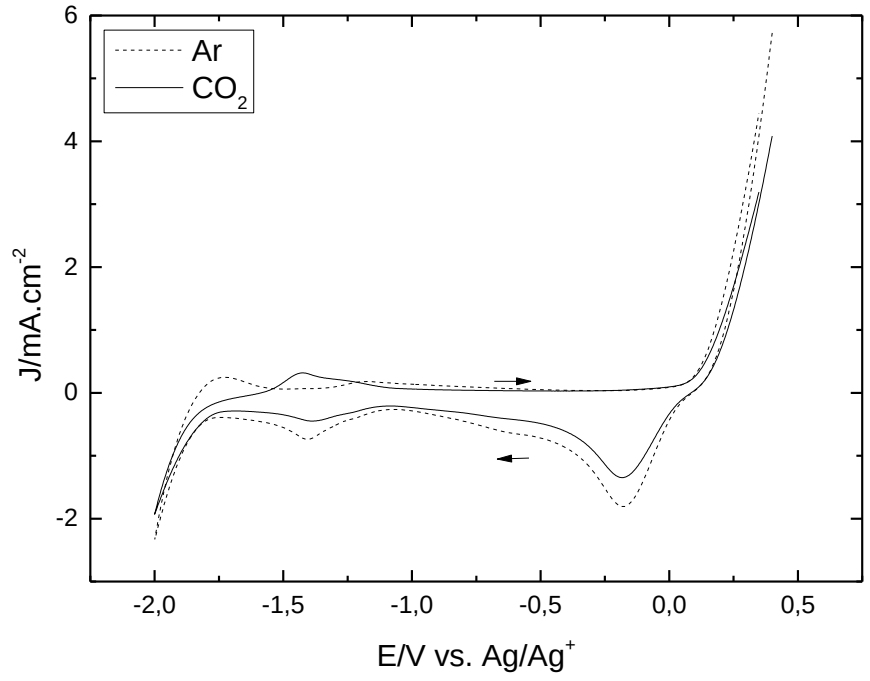

Figure 4-8. Cyclic voltammograms for a polycrystalline platinum electrode, in F:TBA-Cl: H_2O with molar proportions 1:1:27,5, in saturated Ar and CO_2, scan rate: 0,1V/s, working window: 0,4V -2V.

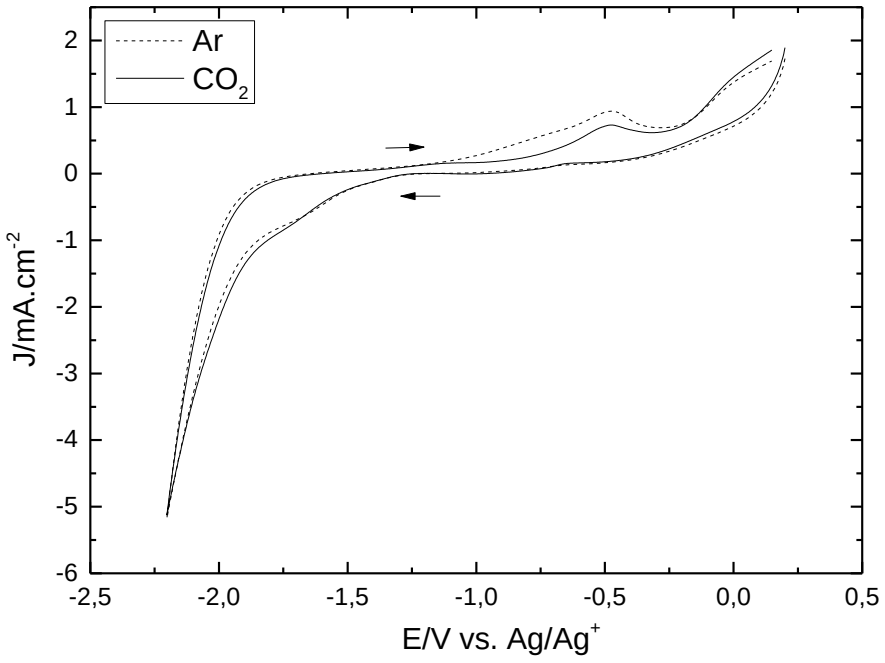

Figure 4-9. Cyclic voltammograms for a polycrystalline palladium electrode, in F:TBA-Cl: H_2O with molar proportions 1:1:27,5, in saturated Ar and CO_2, scan rate: 0,1V/s.

Figure 4-9 shows cyclic voltammograms for a polycrystalline platinum electrode in the solvent formed by F:TBA-Cl: H_2O. It can be observed the H_2 formation from water with an onset potential of -1,5 V, and in the reverse cycle a feature at -0,5 V can be seen, suggesting an oxidative process.

Figure 4-10 present cyclic voltammograms for a polycrystalline copper electrode in the solvent formed by F:TBA-Cl: H_2O. The H_2 formation from water can be observed with an onset potential of -1,95 V, and a feature can be seen for the reverse cycle in presence of argon at a potential of -1,13 V, and corresponds to copper oxide formation.

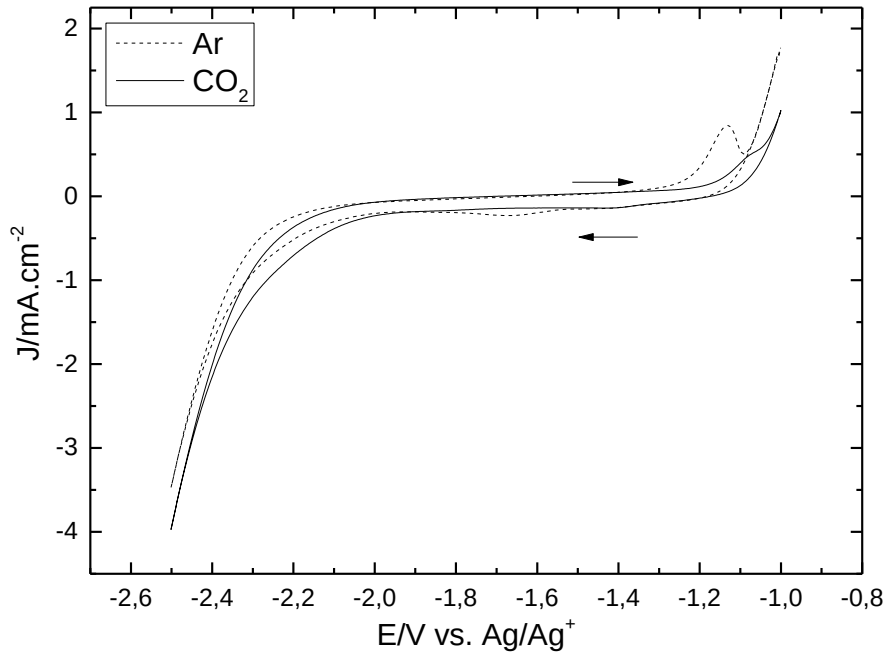

Figure 4-10. Cyclic voltammograms for a polycrystalline Copper electrode, in F:TBA-Cl: H_2O with molar proportions 1:1:27,5, in saturated Ar and CO_2, scan rate: 0,1V/s.

Conclusion

In the study, it was shown that both solvents in the molar proportions studied were conductive and utilizable to perform electrochemistry with the metal electrodes used. Besides, it can be noticed that the working windows are strongly dependent on how strong or weak is the interaction between the solvent and the catalyst.

When it comes to the specific metals, with respect to gold, it was observed in solvent formed by CA:TBA-Cl: H_2O that there was oxyhydroxide formation. In fructose, which has similar hydroxyl groups, a similar response was expected, so gold was discarded for more studies because it is not useful for electrocatalytic CO_2 reduction and the understanding of the formation of oxyhydroxides in this system is considered out of the scope of this study.

In platinum, the formation of H-UPD was seen as unexpected for a solvent with low proton availability. Also, H_2 formation from water and hydrogen oxidation were seen, contributing to the understanding of the role of these solvents. Palladium showed proton

reduction in presence of CA:TBA-Cl:H_2O and oxidation in presence of F:TBA-Cl:H_2O. Due to this interactions with the solvent, these metals were considered not useful for electrocatalytic carbon dioxide reduction. Moreover, Pt and Pd were expected to behave similarly regarding the H_2 formation from water, however the onset potential of Pd was behind of that of Pt for ca. 300 mV.

Furthermore, it was shown that the copper presents the "cleanest" voltammograms for both solvents, in the sense that there was not evident solvent adsorption and desorption or proton reduction from the hydrogen bond donor component. Comparing copper voltammograms from both solvents, the solvent formed by F:TBA-Cl:H_2O has wider working potential window, so it is chosen to keep the studies and CA: TBA-Cl:H_2O which a shorter one is discarded.

It was determined that there was no conclusive evidence of carbon dioxide reduction for any of the metals, suggesting that even with the presence of carbonyl groups, the pH could be in this case the dominant variable, being maybe too acidic to absorb enough carbon dioxide for further electro-reduction.

4.1.2 Water Effect Study

In this section, the effect of water is studied. This was done adding different water quantities to the solvent with different molar proportions.

Copper electrodes were used for this study; this choice was based on the previous screening of metals and their performance in the solvents that were discussed there.

The different working windows for each proportion were characterized. As well, the features were carefully analysed with special attention paid to the effects that water could have and the identification of possible adsorption or reduction of carbon dioxide. Also the stability over more cycles was studied.

F:TBA-Cl:H_2O

The solvent formed by F:TBA-Cl:H_2O was studied with the molar proportions 1:1; 1:1:6,785; 1:1:13,75 and 1:1:27,5.

In the following voltammograms, just the second cycle is shown since there are not significant differences between them, and this cycle is considered to be more stable.

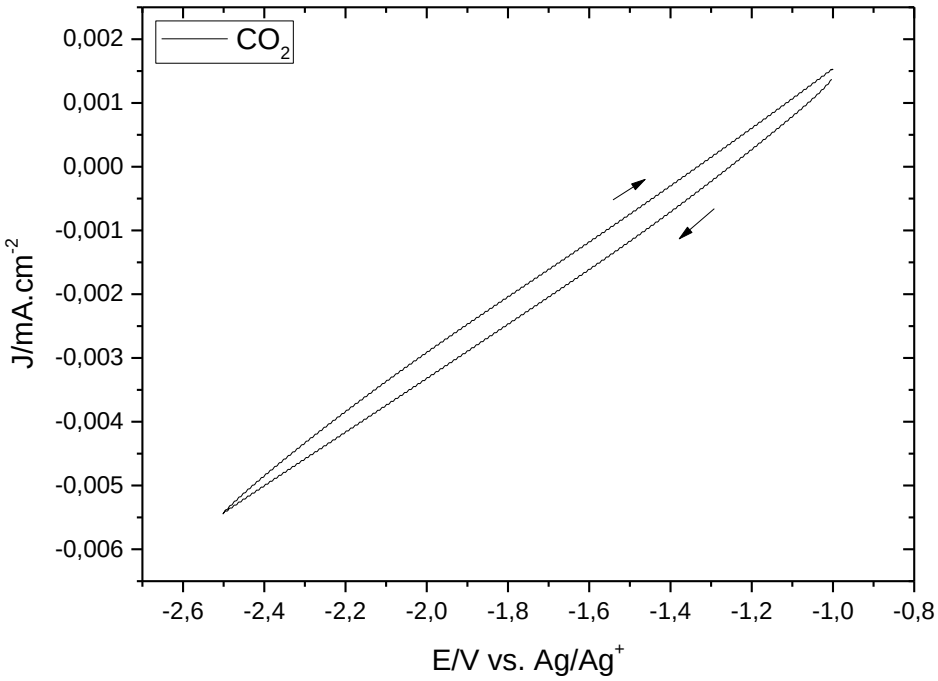

Figure 4-11. Cyclic voltammogram for a polycrystalline copper electrode, in F:TBA-Cl with molar proportion 1:1, CO_2 saturated, scan rate: 0,1V/s.

Figure 4-11 shows the cyclic voltammogram for a polycrystalline copper electrode in a solvent F:TBA-Cl with a molar proportion of 1:1, in presence of saturated carbon dioxide. It can be seen in this figure that the solvent has poor conductivity, as consequence, the solvent without water cannot be used for the purpose of electrochemistry.

Figure 4-12 and Figure 4-13 present the cyclic voltammograms for polycrystalline copper in the solvent F:TBA-Cl: H_2O with three different water quantities: 1:1:6,785; 1:1:13,75;

1:1:27,5, in both argon and carbon dioxide saturated solutions. Two working windows were studied from -1 V to -2,5 V and -1 V to -2,8 V. There are not significant features associated with proton reduction or solvent adsorption, nor carbon dioxide reduction. This indicates that the solvent is quite stable with or without CO_2 added. The working window is wide (up to 1.2 V), and the double layer is clean and thin, characteristic of a clean electrode surface. Still, there is a feature at a potential of -1,1 V in the reverse cycle in Figure 4-12 in the proportion 1:1:27,5 that resembles an oxidative process of the copper. This suggests that the water is the main source of oxygenated species for oxide formation on copper. The current for H_2 formation from water increases proportional to the water concentration. The current also increased for copper oxidation which is consistent with the formation of oxides. Furthermore, changes for the onset potential of H_2 formation from water, reaction can be observed in presence of CO_2.

Figure 4-14 shows the cyclic voltammograms for polycrystalline copper in the solvent F:TBA-Cl: H_2O with three different water quantities: 1:1:6,785; 1:1:13,75; 1:1:27,5, in an argon saturated solution and with both working windows. The current for H_2 formation has been shortened to show the significant features which become smaller if we use the complete scale. This is done with the objective of observing clearly if the water content affects in the oxidation or if otherwise is the solvent the one that dominates that process. As result, it can be observed that oxidation does not depend on the solvent but in the water content, with higher water content leading to higher copper oxidation.

When comparing the oxides region for each water quantity, each working window, it can be seen that with a bigger working window, that allows higher H_2 formation from water, copper redox couple is more reversible. This effect is also visible whenever more water is added with the same working window (see Figure 4-15). This may correspond to the availability of hydroxyl species in the double layer.

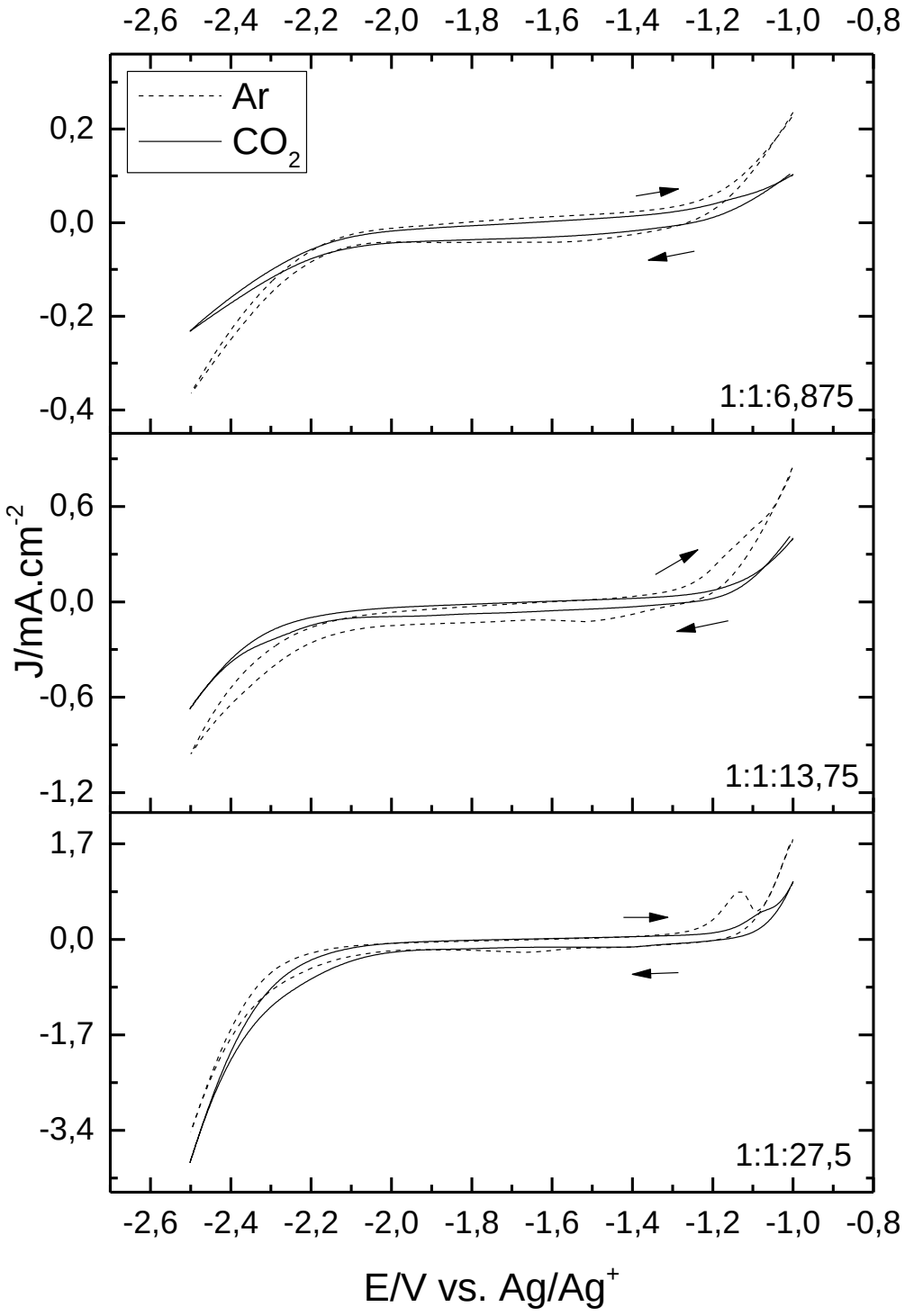

Figure 4-12. Cyclic voltammograms for a polycrystalline copper electrode, in F:TBA-Cl: H_2O with molar proportions 1:1:6,785, 1:1:13,75 and 1:1:27,5, in saturated Ar and CO_2, scan rate: 0,1V/s, working window , -1V -2,5V.

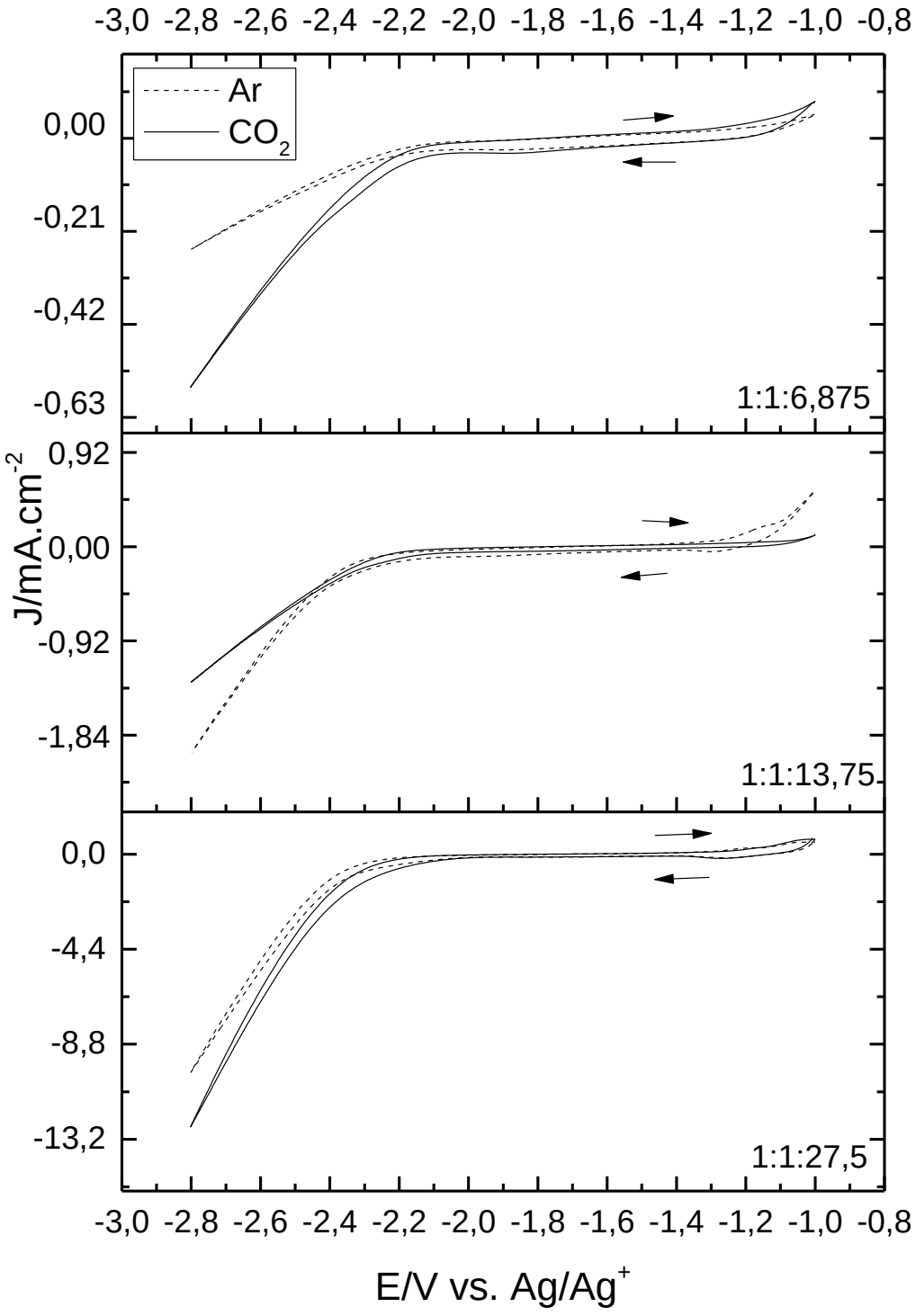

Figure 4-13. Cyclic voltammograms for a polycrystalline copper electrode, in F:TBA-Cl: H_2O with molar proportions 1:1:6,785, 1:1:13,75 and 1:1:27,5, in saturated Ar and CO_2, scan rate: 0,1V/s, working window , -1V -2,8V.

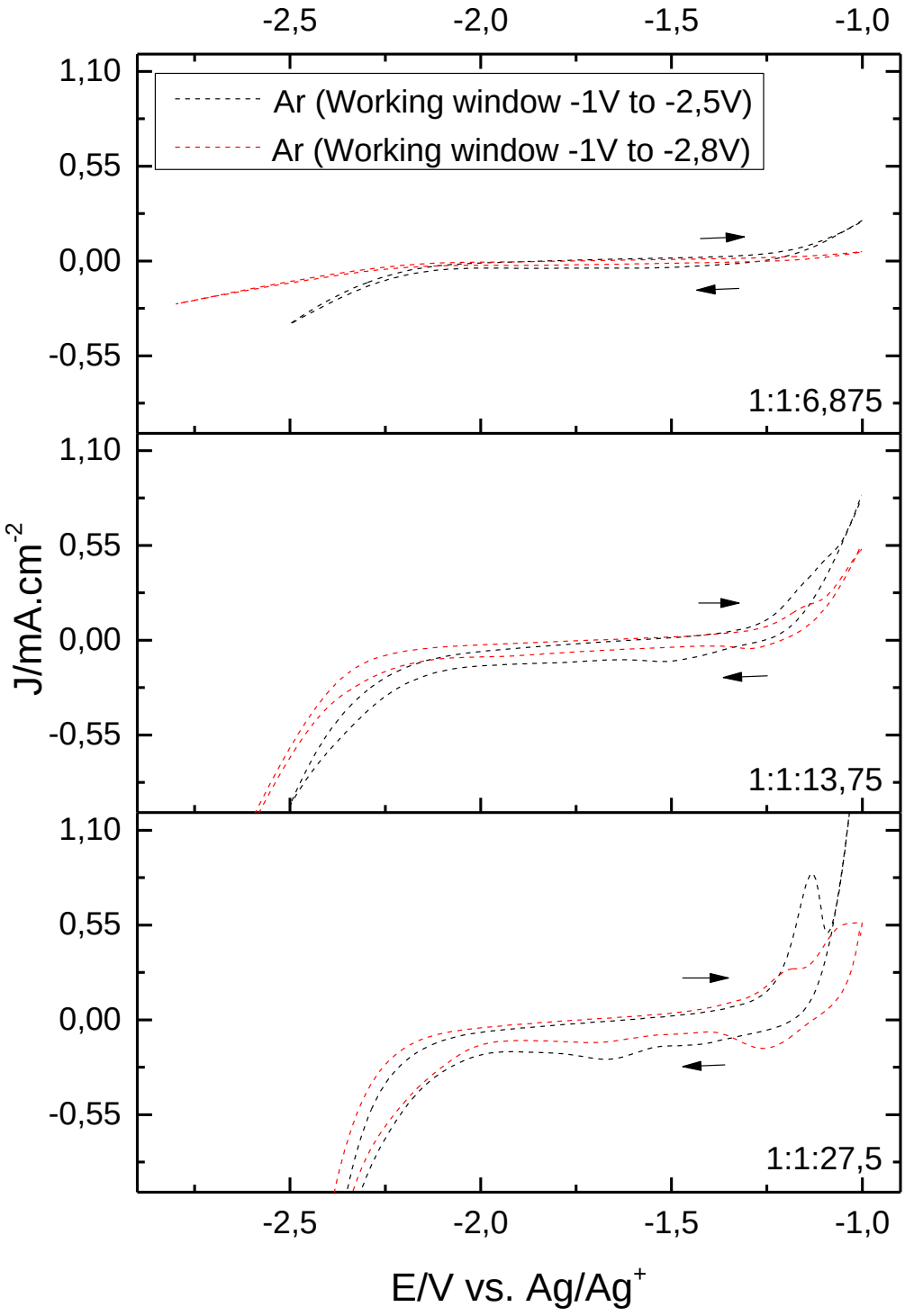

Figure 4-14. Cyclic voltammograms for a polycrystalline copper electrode, in F:TBA-Cl:H_2O with molar proportions 1:1:6,785, 1:1:13,75 and 1:1:27,5, in saturated Ar, scan rate: 0,1V/s, working window -1V -2,5V, -1V -2,8V.

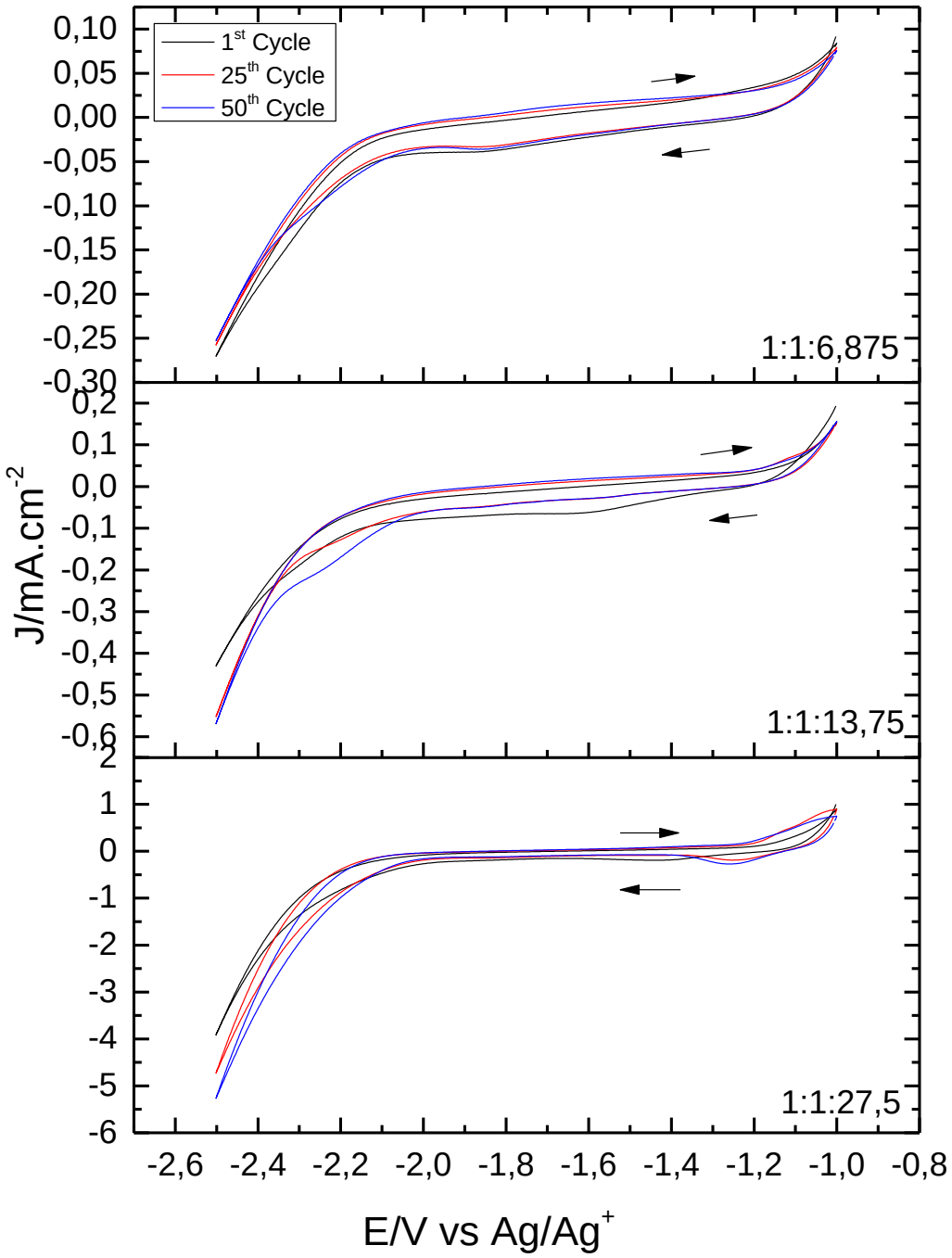

Figure 4-15. Cyclic voltammograms for a polycrystalline copper electrode, in F:TBA-Cl: H_2O with molar proportions 1:1:6,785, 1:1:13,75 and 1:1:28,5, in carbon dioxide saturated atmospheres, scan rate: 0,1V/s, working window: -1V -2,5V.

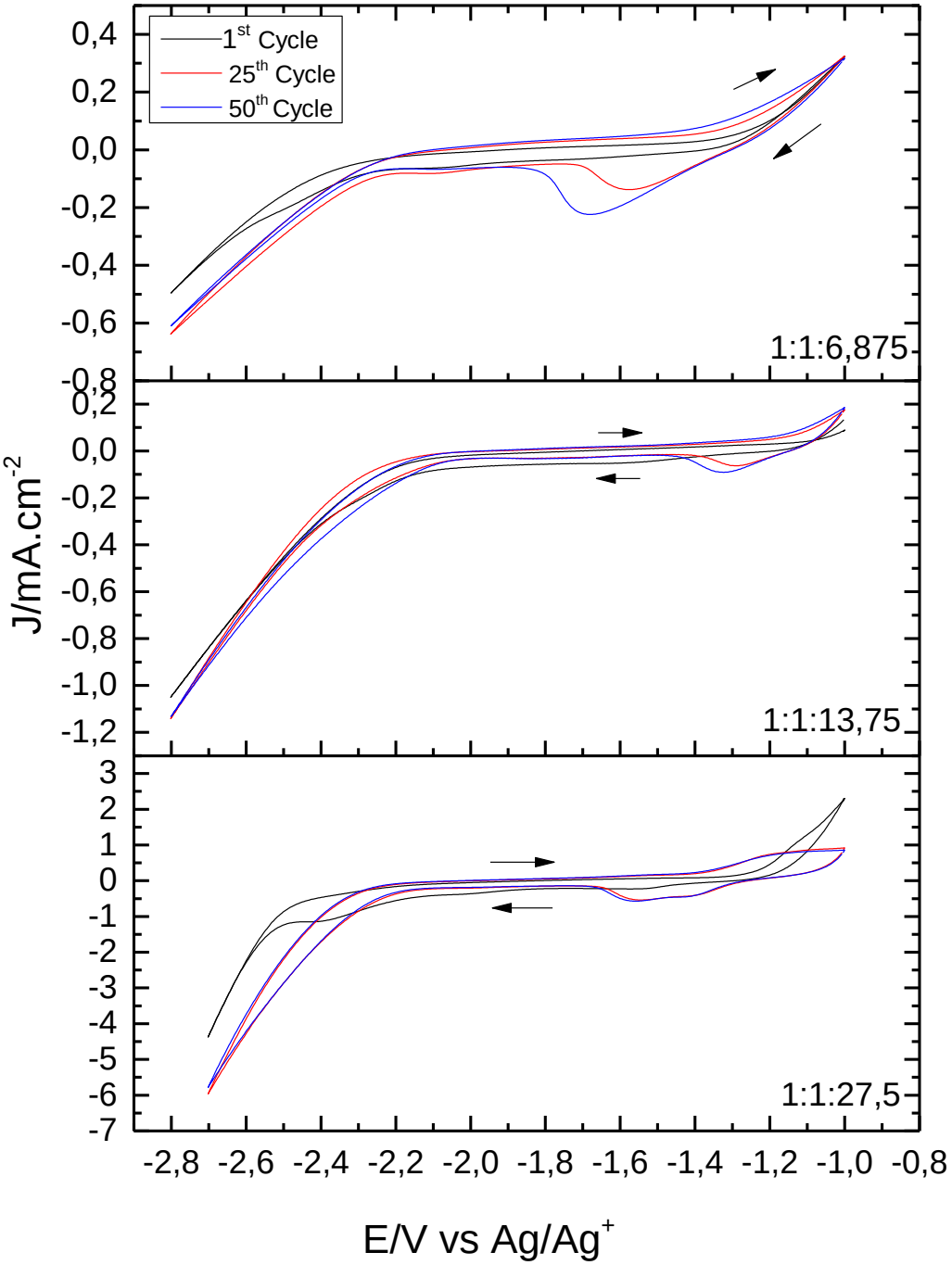

Figure 4-16. Cyclic voltammograms for a polycrystalline copper electrode, in F:TBA-Cl: H_2O with molar proportions 1:1:6,785, 1:1:13,75 and 1:1:28,5, in carbon dioxide saturated atmospheres, scan rate: 0,1V/s, working window -1V -2,8V.

Figure 4-15 and Figure 4-16 present cyclic voltammograms for fifty cycles in polycrystalline copper in the solvent F:TBA-Cl:H_2O with three different water quantities: 1:1:6,785; 1:1:13,75; 1:1:27,5, in carbon dioxide saturated solution and with different working windows respectively.
It can be seen that the more water content, the more noticeable becomes the potential shift of the onset potential for H_2 formation from water due too local pH change in the electrode interface.

In later cycles there are features that resemble proton reduction, showing that a bigger working window towards negative potential promotes proton reduction from the fructose. This could be due to the bigger H_2 formation from water that cleans the catalytic active sites and causes a reorganization of the solvent molecules on the surface that facilitates the proton reduction.

Conclusion
In this study, "clean" voltammograms were obtained, meaning with this that no proton reduction from the fructose or adsorption/desorption of the solvent in the first cycle is observed for any of the working windows studied. However, when studying its stability cycling it fifty times, it was seen than only the smaller working window with the smaller water quantities did not lead to adsorption/desorption of the solvent or proton reduction from the fructose. Furthermore, a difference in Ar and CO_2 atmospheres was observed but no apparent sign of CO_2 reduction is featured.

It was also seen that the addition of more water promotes copper oxidation, especially in bigger cathodic windows, due to generation of hydroxyl groups from water decomposition. The dissolution of this copper oxides leads to a loss of material, and as consequence there is a roughening of the surface, which translates in more surface area and active sites available for electrochemical reactions.

Afterwards, pH was measured by the student Zheng who is currently working in the physico-chemical characterization of several DESs and LTTMs. The solvent in the molar proportion 1:1:6,875 showed a pH of 4,6 and the solvent in the molar proportions 1:1:13,75 and 1:1:27,5 had a pH of 4.

In conclusion, with this study it is proven that low pH and high proton availability in the water-containing solvents is not suitable for CO_2 reduction, even using the best catalyst, because of a carbon dioxide dissolution impediment, highlighting the role of pH and electrolyte. Solvent with a higher pH would be needed to capture more carbon dioxide that could then subsequently adsorb on the surface and be reduced.

DEA:TBA-Cl:H_2O

In this section, the solvent formed by DEA:TBA-Cl:H_2O was studied following the conclusion on the previous section which highlighted the importance of a high pH for improving the carbon dioxide solubility which is needed for subsequent reduction. The pH of the solvent was previously measured by the student Zheng, as part of his current project on physico-chemical characterization of several DESs and LTTMs, showing promising values for carbon dioxide capture. This can be seen in Table 4. However, this solvent presented the risk of forming a strong bond with the CO_2 molecule which would require higher energy input for the catalysis.

In the graphs below, both the first and second cycle are presented since it is considered that they show distinctive information.

Table 4. pH of the solvent with different proportions under Ar and CO_2 atmospheres.

DEA:TBA-Cl: H_2O	Ar	CO_2
1:1:1,375	11,4	9,6
1:1:2,75	11,7	8,9

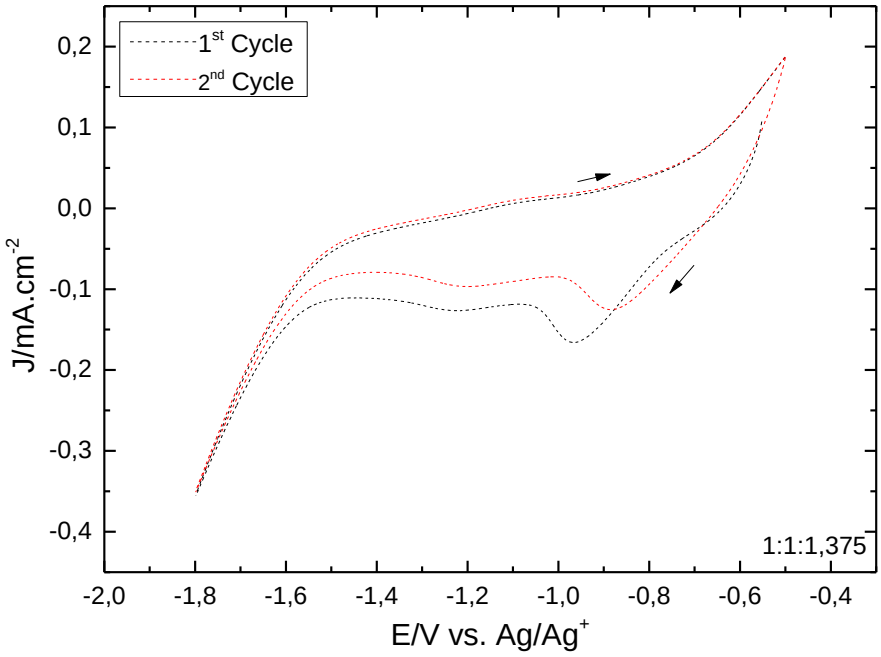

Figure 4-17. Cyclic voltammograms for a polycrystalline copper electrode in DEA:TBA-Cl: H_2O with molar proportion 1:1:1,375, argon saturation, scan rate: 0,1 V/s, working window: -0,5 V - 1,8V.

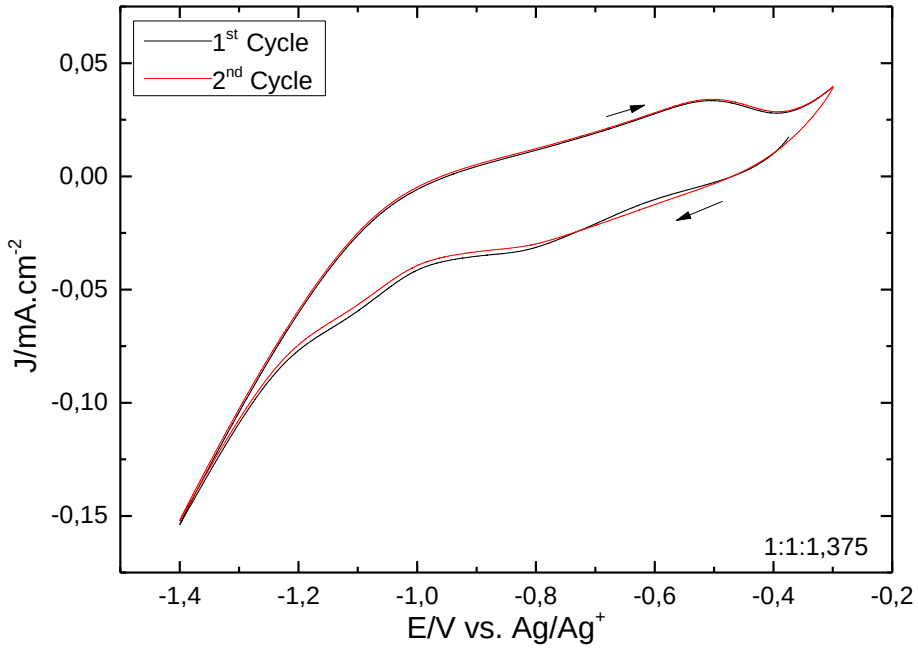

Figure 4-18. Cyclic voltammograms for a polycrystalline copper electrode in DEA:TBA-Cl: H_2O with molar proportion 1:1:1,375, carbon dioxide saturation, scan rate: 0,1 V/s, working window: -0,3 V -1,4 V.

Figure 4-17 presents the cyclic voltammogram for a polycrystalline copper electrode in the solvent formed by DEA:TBA-Cl:H_2O with the molar proportion of 1:1:1,375, which is saturated by argon atmosphere. On it, as it was previously said, both the first and second cycle are presented since it is considered that they are significantly different. In this figure, a reduction peak can be seen at the potential -0,95 V in the first cycle and at -0,87 V in the second one, and this could correspond to proton reduction. This reduction peak is shifted towards positive potentials in the second cycle, this is because in the first cycle the protons need more energy to be reduced due to instability of the double layer. Furthermore, another feature could be seen at around -1,22 V in the first cycle and at around -1,20 V in the second cycle, this could be solvent adsorption, due to the fact that in the reverse cycle there is feature at a potential of -1,1 V, which could be the desorption of the previously adsorbed species. The H_2 formation from water reaction can be observed, with and onset potential of -1,4 V.

Figure 4-18 shows the cyclic voltammogram for a polycrystalline copper electrode in the solvent formed by DEA:TBA-Cl:H_2O with the molar proportion of 1:1:1,375, which is saturated by carbon dioxide atmosphere. In this figure, a feature can be recognized around the potential -0,8 V in both the first and second cycle, this could be showing proton reduction. Moreover, a second feature at a potential of around -1,1 V, and with an onset potential of -0,96 V, this could be showing a proton reduction, but it is unlikely since it is in a very negative potential. Other possibility is that this presents either adsorption or reduction of carbon dioxide. In addition, the H_2 formation from water is found with an onset potential of -1,2 V.

When comparing Figure 4-17 and Figure 4-18, it is clearly seen that they are different, having the argon saturated solution a working potential window towards more negative potentials and higher current than the carbon dioxide solution. A shift in the working window towards more positive potentials in presence of carbon dioxide could be a consequence of the pH change. These differences strongly suggest that the solvent has captured the carbon dioxide. The shift in the onset potential for the H_2 formation from water might be evidence for a different process on the electrode surface, which may be caused by the CO_2.

Figure 4-19 displays the cyclic voltammograms for a polycrystalline copper electrode in. the solvent formed by DEA:TBA-Cl:H_2O with the molar proportion of 1:1:2,75, which is saturated by argon atmosphere. On it, it can be seen a feature at a potential of -2,1 V for the first cycle and at a potential of -1,7 V for the second one. This is due to proton reduction. It has a shift for the same reasons explained at Figure 4-17. In addition, there is another feature at around -2,1 V in the second cycle, that could be due to homoconjugation of the proton reduction. Homoconjugation is a process that occurs when the conjugate base is stabilized by the hydrogen bond to the acid [76], [79]. Additionally, the H_2 formation from water can be seen with an onset potential of -2,3 V.

Figure 4-20, exhibits the cyclic voltammogram for a polycrystalline copper electrode in the solvent formed by DEA:TBA-Cl:H_2O with the molar proportion of 1:1:2,75, which is saturated with carbon dioxide. A peak can be seen at a potential of -2 V with an onset potential of -1,9 V, which could be identified as carbon dioxide adsorption or reduction, analogously to Figure 4-18. Moreover, H_2 formation from water can be observed with an onset potential of -2,1 V. Solvent adsorption or reduction of protons is not observed as it is evident in the lower water quantity (Figure 4-18).
This could be due to rigid water networks at the electrode surface, preventing the adsorption of solvent molecules, since it has been reported that water can be the dominant solvent even when it is present in trace amounts [76], [80].

When comparing these voltammograms with the molar proportion 1:1:2,75 to the previous ones with the molar proportion 1:1:1,375 a shift towards cathodic potentials can be observed. Moreover the addition of water increased the conductivity of the electrolyte, consistent with previous observations.

The solvent stability was also studied in both water quantities, and under both argon and carbon dioxide saturated atmospheres. The electrode was subject to fifty oxidation/reduction cycles. This is presented in Figure 4-21, Figure 4-22, Figure 4-23 and Figure 4-24.

Figure 4-21 shows three cycles from a fifty cycles set of cyclic voltammograms for a polycrystalline copper electrode in the solvent formed by DEA:TBA-Cl:H_2O, with the molar proportion of 1:1:1,375, saturated with argon. As it can be seen, the solvent is remarkably and unexpectedly stable, having the same features discussed previously in the same potentials for the fifty cycles.

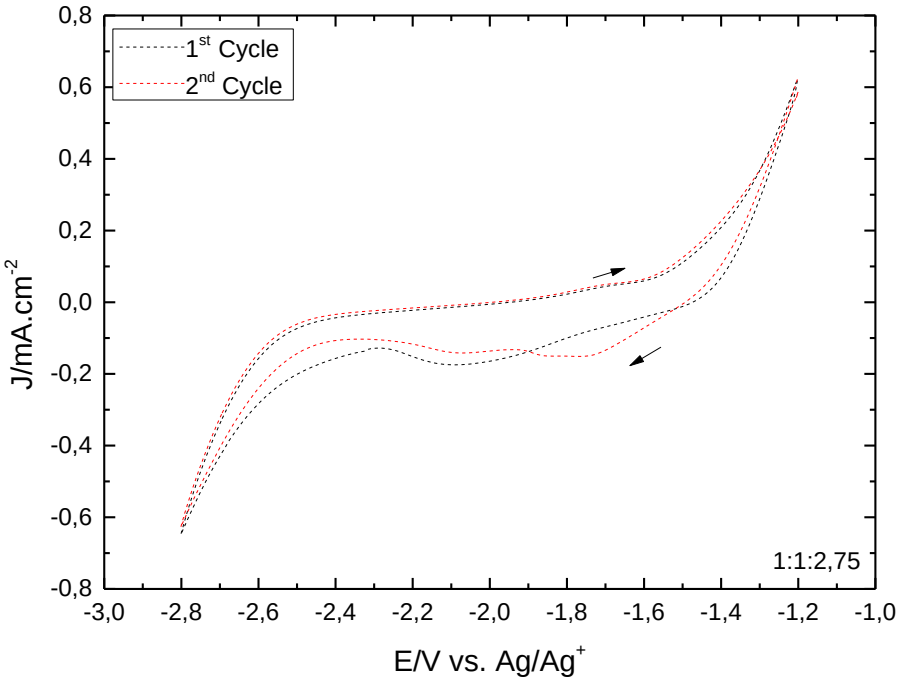

Figure 4-19. Cyclic voltammograms for a polycrystalline copper electrode in DEA:TBA-Cl:H_2O with molar proportion 1:1:2,75, argon saturation, scan rate: 0,1V/s, working window: -1,2 V -2,8 V.

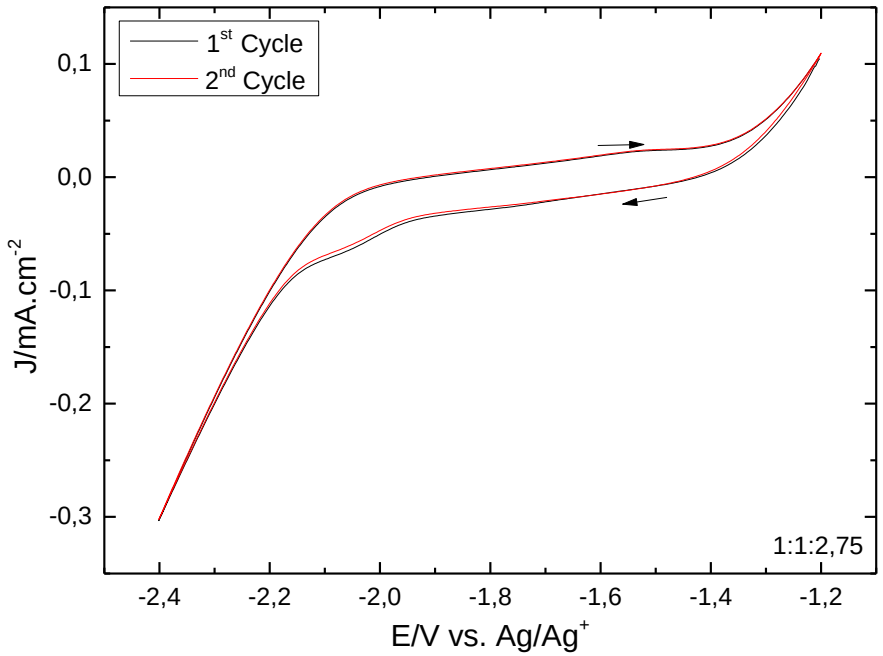

Figure 4-20. Cyclic voltammograms for a polycrystalline copper electrode in DEA:TBA-Cl:H_2O with molar proportion 1:1:2,75, carbon dioxide saturation, scan rate: 0,1V/s, working window: -1,2 V -2,4 V.

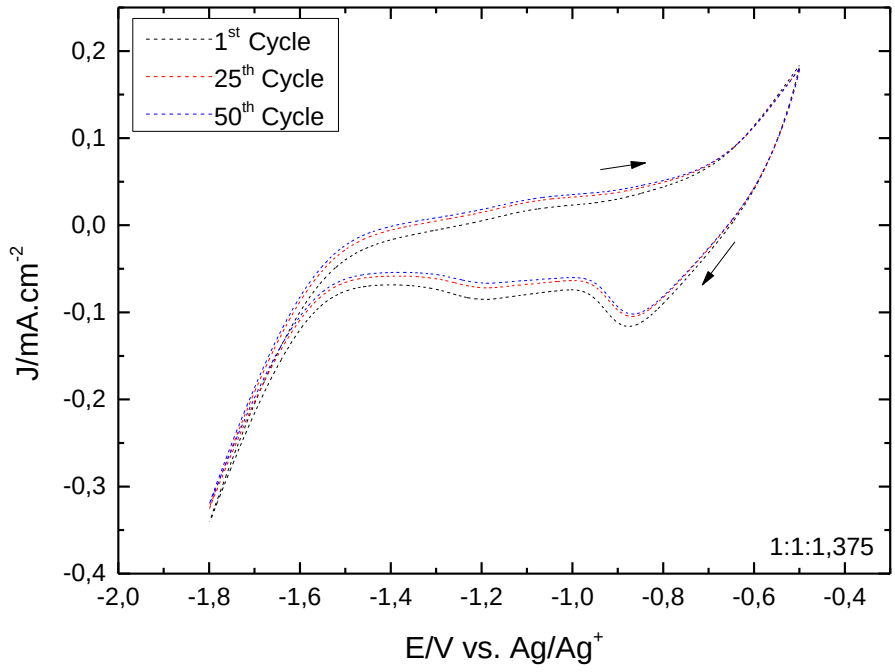

Figure 4-21. Cyclic voltammograms for a polycrystalline copper electrode in DEA:TBA-Cl: H_2O with molar proportion 1:1:1,375, argon saturation, scan rate: 0,1V/s, working window: -0,5 V -1,8V.

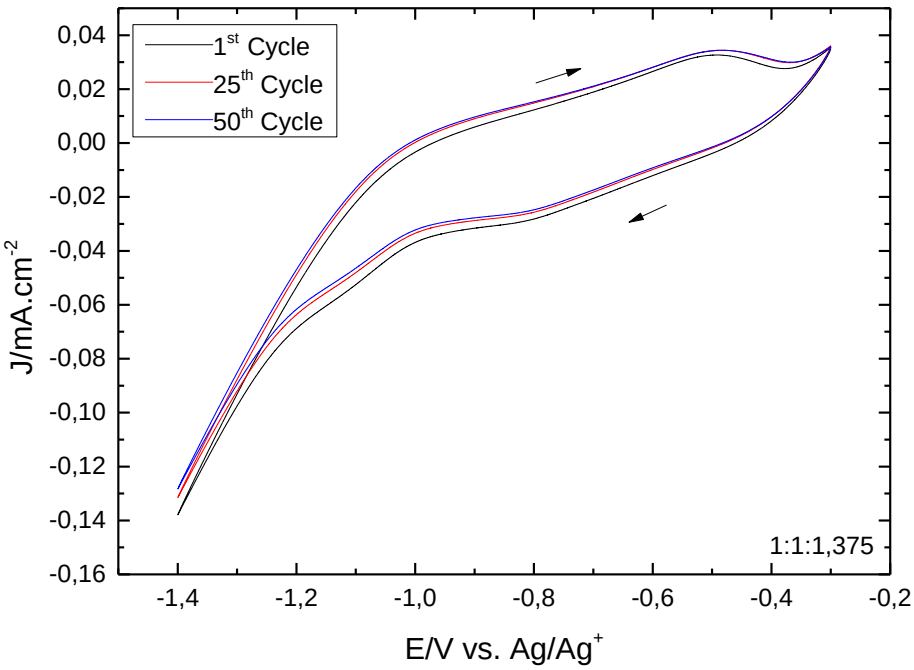

Figure 4-22. Cyclic voltammograms for a polycrystalline copper electrode in DEA:TBA-Cl: H_2O with molar proportion 1:1:1,375, carbon dioxide saturation, scan rate: 0,1V/s, working window: -0,3 V -1,4 V.

Figure 4-22 and Figure 4-24, exhibit three cycles from a fifty cycles set of cyclic voltammograms on a polycrystalline copper electrode in the solvent formed by DEA:TBA-Cl:H_2O, with molar proportions of 1:1:1,375 and 1:1:2,75 respectively. The solvent is under carbon dioxide atmosphere. The voltammograms show high stability with the same features at the same potentials along the whole set of cycles. This might mean that the complex formed between the solvent and the CO_2 is too strong and stable to allow the solvent to release the carbon dioxide for further reduction.

Figure 4-23 also shows three cycles from a fifty cycles set of cyclic voltammogram for a polycrystalline copper electrode in the solvent formed by DEA:TBA-Cl:H_2O with the molar proportion of 1:1:2,75, which is saturated by argon atmosphere. There is a feature at a potential of -1,8 V that suggests proton reduction, it shifts to negative potentials in higher cycles.

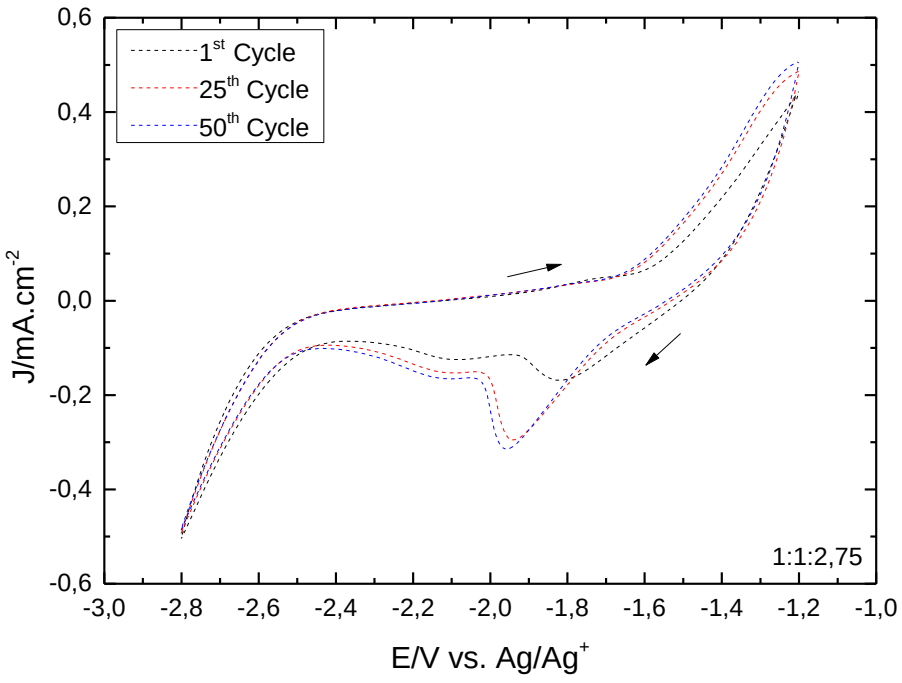

Figure 4-23. Cyclic voltammograms for a polycrystalline copper electrode in DEA:TBA-Cl: H_2O with molar proportion 1:1:2,75, argon saturation, scan rate: 0,1V/s, working window: -1,2 V -2,8 V.

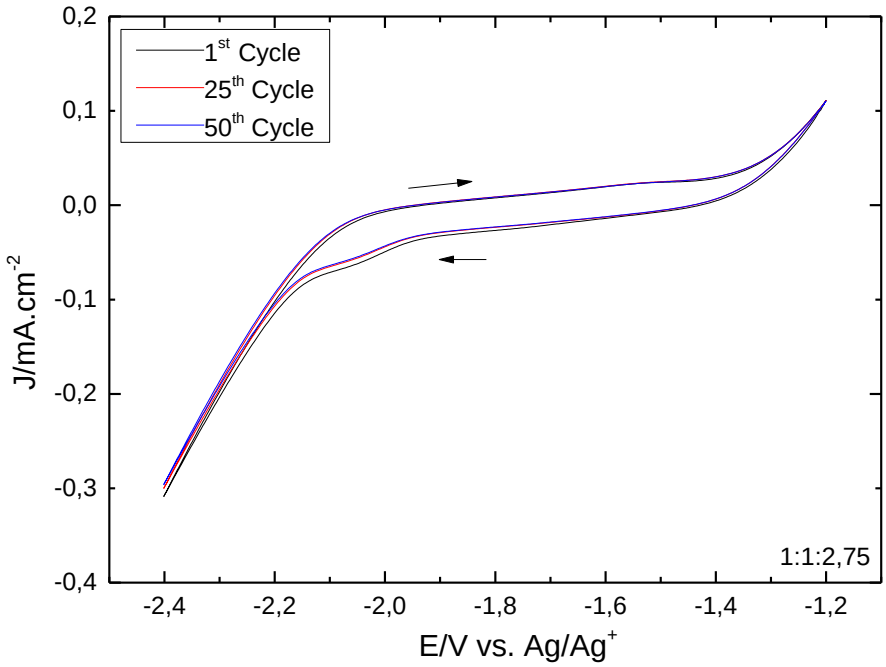

Figure 4-24. Cyclic voltammograms for a polycrystalline copper electrode in DEA:TBA-Cl: H_2O with molar proportion 1:1:2,75, carbon dioxide saturation, scan rate: 0,1V/s, working window: -1,2 V -2,4 V.

The working window is opened to higher negative potentials, with a fixed lower negative potential, not to compromise the copper electrode (dissolution). This can be seen in Figure 4-25 and Figure 4-26. There is not apparent solvent decomposition with any of the two saturation gases. In Figure 4-26, it can be seen that after the first cycle the feature previously discussed that could be showing carbon dioxide adsorption or reduction, disappears. The current decreases with the cycles and a local pH change is suggested. It is probable that this pH change is due to the use of CO_2 in the electrode surface at very high overpotentials due to its reduction.

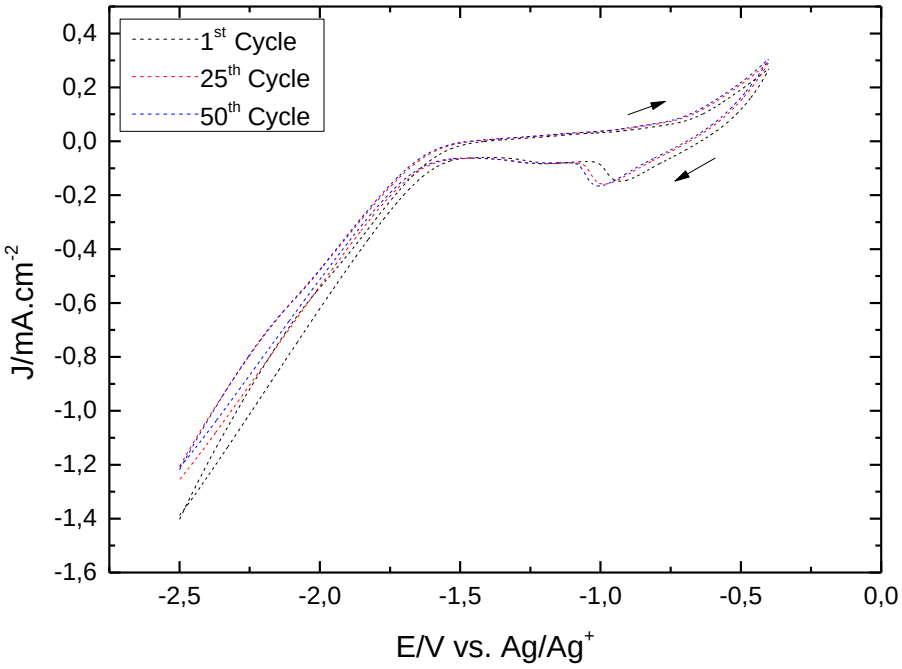

Figure 4-25. Cyclic voltammograms for a polycrystalline copper electrode in DEA:TBA-Cl: H_2O with molar proportion 1:1:1,375, argon saturation, scan rate: 0,1V/s, working window: -0,3 V -2,5 V.

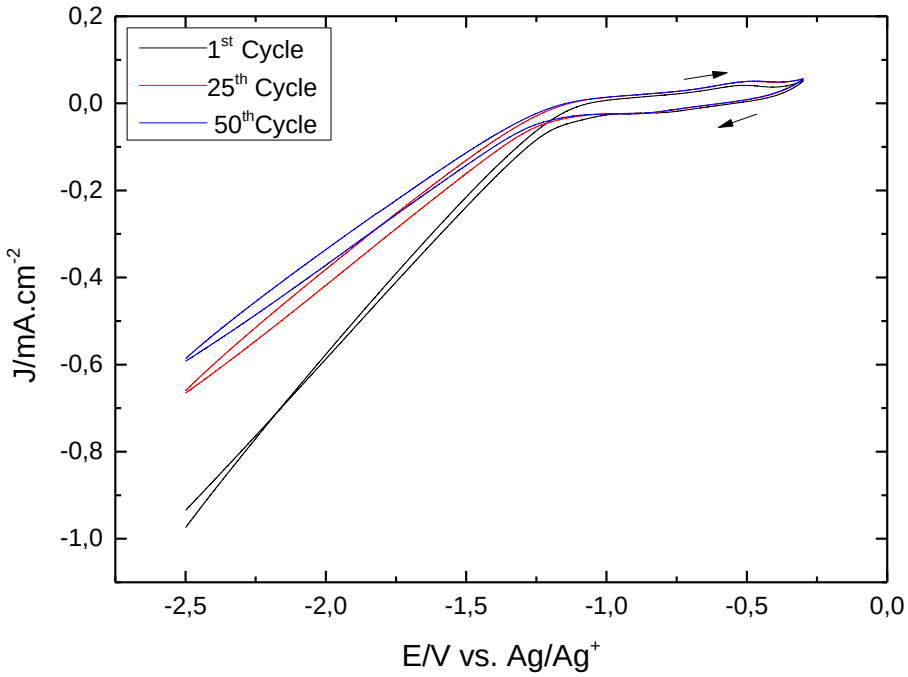

Figure 4-26. Cyclic voltammograms for a polycrystalline copper electrode in DEA:TBA-Cl: H_2O with molar proportion 1:1:1,375, carbon dioxide saturation, scan rate: 0,1V/s, working window: -0,3 V -2,5 V.

Conclusion

In this section, the solvent formed by DEA:TBA-Cl:H_2O was studied with two water quantities in the molar proportions of 1:1:1,375 and 1:1:2,75. The voltammograms presented big differences between Ar and CO_2 for both water quantities studied. It was seen that in presence of Ar there was a bigger window and current than in presence of CO_2. This change in the working window towards positive potentials was suggested to be due to a pH change in presence of CO_2. The shift in the onset potential of the H_2 formation from water was discussed as an evidence that there is a different process in the surface of the electrode which can be caused by the CO_2. A feature in both water quantities in the CO_2 voltammograms which appeared just before the H_2 formation from water, was suggested to be due to carbon dioxide adsorption or reduction. Since the molar proportion 1:1:1,375 showed the requirement of lower overpotentials, this was chosen for further studies.

When the stability was studied cycling fifty times, the solvent was unexpectedly very stable, this suggested that catalysis was not happening at low overpotentials for any of the water quantities. However, when the working window was expanded to high overpotentials and cycled fifty times, a change was clear in the voltammetry in presence of carbon dioxide, it was suggested to be due to pH change, which may indicate that high energy input promotes the release of CO_2 from the solvent for further electroreduction.
In order to confirm this, additional techniques are needed.

4.2 In-situ Electrochemical Spectroscopy

This section presents the spectroscopic in-situ results of the electrocatalytic CO_2 reduction in the solvent formed by DEA:TBA-Cl:H_2O in a molar proportion of 1:1:1,375. As it was previously explained, this was performed with the objective of finding out if the CO_2 is captured by the solvent and further electrocatalytically reduced.

4.2.1 Raman

Initially, the in-situ electrochemical spectroscopic study was planned to do using Raman, using the technique surface enhanced Raman spectroscopy. As it was previously explained, this had the objective of researching how the solvent adsorbs in the surface of the catalyst and how this affects in the formation of CO, which is a key step in the formation of further reduction products. Unfortunately, this could not be done since it was discovered that the available Raman could not be used for this technique. This is further explained in Appendix B.

4.2.2 FTIR ATR-SEIRAS

In order to facilitate the identification of the bands during CO_2 reduction and to help differentiate which bands are due to the presence of CO_2 and which are from the solvent, transmission spectra were collected in both argon and carbon dioxide atmosphere. These spectra can be seen in Figure 4-27.

The spectra presented in this figure go from a wavenumber of 600 cm^{-1} to 1700 cm^{-1}, since this region was considered as the most important to identify interactions between the CO_2 and the electrode. The solvent interactions with the surface are also observed. The full spectra is presented in the Appendix C. In the region from 2534 cm^{-1} to 4000 cm^{-1}, the spectra present bands that are due to the C-H stretching present in the CH_3 coming from the TBA-Cl. In the region around a wavenumber of 3300 cm^{-1} there are bands that are due to the OH vibrations in water. Moreover, around a wavenumber of 3500 cm^{-1} there are bands from the bond N-H from the DEA.

In Figure 4-27, several bands which are characteristic of the spectrum taken under CO_2 can be identified. It can be observed that these bands are absent in the blank spectrum under Ar atmosphere. The stretching vibration of the functional group C-O is identified at the bands with wavenumber 1361 cm^{-1} and 1291 cm^{-1}. Furthermore, COO is identified, which has its stretching mode at a wavenumber of 1402 cm^{-1} and its bending at a wavenumber of 1550 cm^{-1}.

Some bands from functional groups belonging to the solvent can be identified in both spectra. The stretching mode of the functional group C-H can be identified in the argon spectrum at the wavenumbers 1487 cm^{-1}, and at wavenumbers of 1464 cm^{-1} and at 1469 cm^{-1} in the carbon dioxide spectrum, and its bending can be identified in both CO_2 and Ar atmospheres at the wavenumbers 924 cm^{-1}, 880 cm^{-1}, 801 cm^{-1}. In addition, the stretching mode of the functional group C-OH can be observed in both argon and carbon dioxide spectrum at a wavenumber of 1381 cm^{-1}. Stretching mode of the functional group C-N can be identified in the CO_2 spectrum at a wavenumber of 1252 cm^{-1} and in the Ar spectrum at a wavenumber 1244 cm^{-1}. Moreover, the stretching mode of the functional group C-C-N can be identified in both argon and carbon dioxide spectra at a wavenumber of 1149 cm^{-1}. Besides, the stretching from the functional group C-O belonging to -CH_2OH can be observed under argon atmosphere at a wavenumber 1058 cm^{-1}.

A band from the bending of the functional group OH can be identified in the carbon dioxide spectrum at a wavenumber 1428 cm^{-1}. The band at wavenumber 740 cm^{-1} in both argon and carbon dioxide atmosphere that can be attributed to the bending of -CH_2.

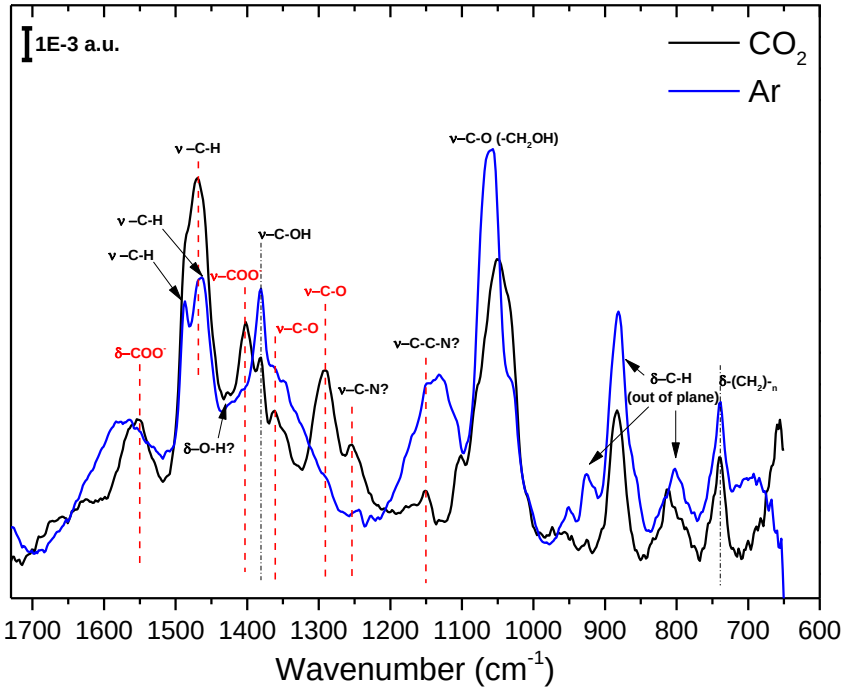

Figure 4-27. Transmission spectra of the solvent DEA:TBA-Cl:H_2O with the molar proportions 1:1:1,375 saturated in both Ar and CO_2.

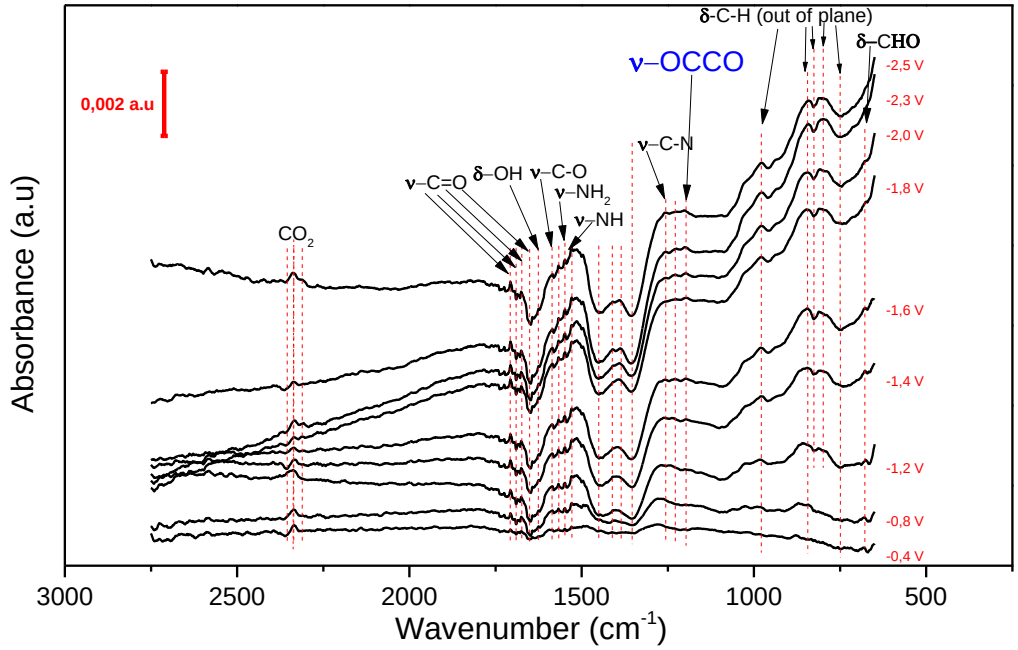

Figure 4-28. SEIRAS spectra for CO_2 reduction in the solvent DEA:TBA-Cl:H_2O in the molar proportions 1:1:1,375 at the indicated potentials.

In Figure 4-28, the SEIRAS spectra for CO_2 reduction at different potentials can be seen. The bands at wavenumber of 2354 cm^{-1}, 2335 cm^{-1} and 2309 cm^{-1} correspond to CO_2. Assigning the band at 2354 which is depleting from the surface as CO_2 a top and to the band 2309 cm^{-1} which starts forming at a potential of -1,4 V as CO_2 probably shifting to bridge position on the electrode surface. These structures can be seen in Figure 4-29. There is also the possibility that the CO_2 is coming from two different solvation spheres.

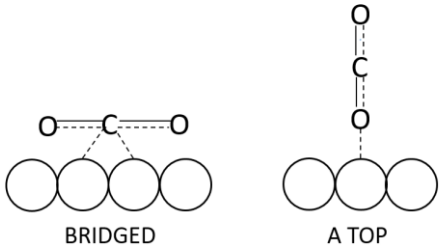

Figure 4-29. Proposed CO_2 adsorbed structures.

Several bands were assigned as stretching of the functional group C=O, positive bands at wavenumbers of 1707 cm^{-1} and 1675 cm^{-1} [81] that can be seen from potential -0,4 V, negative bands at wavenumbers 1690 cm^{-1}, 1645 cm^{-1}[28], which can be seen from potential -0,4 V but they become more evident with more negative potentials.

Some bands were identified as stretching of the functional group C-O, positive bands at wavenumbers of 1584 cm^{-1} and 1388 cm^{-1}, being the last one evident after potentials of -2,3 V.

There is a band at a wavenumber of 1567 cm^{-1} which can be attributed to the stretching of the functional group COO^-, and it can be seen from potentials of -0,4 V.

Negative broad bands can be observed at wavenumbers 1449 cm^{-1} and 1354 cm^{-1} which start at potential of -0,8 V. These bands increase with applied potential, suggesting the N-O interaction. This is believed to be related to the way the CO_2 molecule interacts with the DEA molecule trough the nitrogen group.

In addition, there is a band at wavenumber of 1625 cm^{-1} which was assigned to OH bending [28].

Remarkably, there is a band at a wavenumber 1200 cm^{-1} which was assigned as the CO dimer OCCO stretching, according to calculations done by density functional theory (DFT)[81], and never before observed experimentally. It appears at a potential of -1,4 V and continues till -2.5 V.

A band was identified as the stretching of the functional group N-H, at wavenumber of 1530 cm^{-1} which can be observed since potential -0,4 V. As well a band at a wavenumber of 1548 cm^{-1} can be attributed to the stretching of the functional group NH_2.

Two positive bands were assigned to the stretching of the interaction C-N at wavenumbers of 1410 cm^{-1} , which is evident at potentials of -0,4 V, and 1259 cm^{-1} [81], which is evident after potentials of -0,6 V. As well, there is a band at a wavenumber of 1227 cm^{-1} which is attributed to bending the functional group C-C-N.

There is a band at 1496 cm^{-1} attributed to the stretching of the functional group C=C. This may suggest the formation of ethylene, a common reduction product from CO_2 electro-reduction on Cu [82].

Bands at wavenumbers 978 cm^{-1}, 842 cm^{-1}, 824 cm^{-1}, 803 cm^{-1} are attributed to out of plane C-H vibrations, which indicate the presence of a rigid structure between the CO_2 and the DEA from the solvent. It can also be seen that the bands at 978 cm^{-1}, 842 cm^{-1} and 803 cm^{-1} start at a potential of -0,8 V and increases with applied potential. Band at 822 cm^{-1} is negative and starts at a potential of -1,2 V being more negative with increasing potential.

Besides, there is a band at a wavenumber of 676 cm^{-1} which was attributed to the functional group CHO (aldehyde), it starts forming at potential of -0,4 V and it decreases with applied potential until it disappears at a potential of -2 V. This might happen because it forms another product which unfortunately, it is not possible to distinguish. In Table 5, the assignments for each wavenumber are shown to summarize all the information obtained from the SEIRAS spectrum.

Table 5. SEIRAS spectrum assignments.

Wavenumber (cm^{-1})	**Assignment**
2354	CO_2 Gas
2335	CO_2 Gas
2309	CO_2 Gas
1707	ν-C=O
1690	ν-C=O
1675	ν-C=O
1645	ν-C=O
1625	δ-OH
1584	ν-C-O
1567	ν-COO^-
1548	ν-NH_2
1530	ν-NH
1496	ν-C=C
1449	R-N-O
1410	ν-C-N
1388	ν-C-O
1354	R-N-O
1259	ν-C-C-N
1227	δ-C-C-N
1200	ν -OCCO
978	δ-C-H (out of plane)
842	δ-C-H (out of plane)
824	δ-C-H (out of plane)
803	δ-C-H (out of plane)
676	δ-CHO

Conclusion

In conclusion, it can be seen in the transmission spectra the difference in bands between the spectrum taken under carbon dioxide atmosphere and the one taken under argon, together with the identified vibrations belonging to CO_2 that leads to the confirmation that the solvent has absorbed the CO_2.

In the FTIR spectra, the existence of bands attributed to the presence of CO_2 are suggested to be from CO_2 a-top and bridged. It is important take into account that the CO_2 can be captured in the solvent, being adsorbed in the solvent forming chemical interactions, dissolved in the small amount of water which is also part of the solvent or by London and/or van der Waals forces. So it is also taken into account the possibility to have two different solvation spheres for that CO_2 observed. The presence of this bands can be caused by the break of the bond of the CO_2 with the diethanolamine or any of the previous interactions described further studies are needed to determine that.

An important observation is the change in the bands with applied potential, which is a sign that electrocatalysis is happening. Several bands suggested the formation of ethylene and aldehyde which are common on the reduction of carbon dioxide on copper. However, it was not possible to identify all bands since this requires an improved resolution for gas detection (~0.1 cm^{-1}).

Ultimately, the band 1200 cm^{-1} was assigned to the stretching of the dimer OCCO, which has been predicted by DFT calculations in other studies, but never identified experimentally.

5 CONCLUSIONS AND RECOMMENDATIONS

In this work, the electrochemical characterization performed is considered of utmost importance, since it had not been shown previously to attempt electrocatalytic carbon dioxide reduction in DES or LTTM. A broad and exhaustive study where different metal-catalysts, different solvents and water proportions were evaluated. This electrochemical characterization together with a spectroscopic study show for the first time that it is possible to capture and reduce the carbon dioxide in these solvents.

First, a electrochemical characterization of different metals (Au, Pd, Pt and Cu) in contact with the solvents formed by CA:TBA-Cl:H_2O and F: TBA-Cl:H_2O in the molar proportion 1:1:27,5 was performed. Generally, this study led to the observation that these solvents in the used proportions can be used for electrochemistry and that the working potential windows depend on the interaction between solvent and catalyst.

Regarding the stability of the solvents with each metal, some features were observed. In gold, the formation of oxyhydroxides was recognized, consequently this metal was discarded for this application. In platinum, the presence of underpotential deposited hydrogen was seen for the first time in a solvent with a poor proton dissociation. Regarding palladium, proton reduction and oxidation were observed and as consequence this metal is not convenient for the wanted application. In copper, "cleaner" voltammograms than in the other metals were seen. In the sense that they did not resemble adsorption/desorption of the solvent or proton reduction from the HBD component of the solvent. For this reason, copper was chosen as the optimum option for electrocatalytic reduction of carbon dioxide. However, no significant signs suggesting carbon dioxide reduction were identified in this study for the solvents CA:TBA-Cl:H_2O and F:TBA-Cl:H_2O at any of the metals.

It was determined experimentally that the solvents without water addition were too viscous to perform electrochemistry, this together with the known fact that the water is important as a source of protons to form products from carbon dioxide reduction made clear the necessity of water addition. Following this, a study was done to find out the effect of different water contents in the electrochemistry. The solvent formed by F:TBA-Cl:H_2O was studied first with the different molar proportions of 1:1:6,785; 1:1:13,75; 1:1:27,5. From this study, it was determined that the solvent did not have any decomposition signs with a working potential window from -1 V to -2,5 V and smaller water quantities. But with more water content and expanding working window towards negative potentials, copper was suffering oxidation and there was proton reduction from the fructose. Moreover, there was not any feature suggesting carbon dioxide adsorption or reduction. This also led to the conclusion that a solvent with low pH and high proton availability is not suitable for electrochemical carbon dioxide reduction. Even when multiple carbonyl groups are presented and were expected to help the CO_2 capture.

As a result, a solvent with higher pH was studied, DEA:TBA-Cl:H_2O. This solvent was studied in two molar proportions 1:1:1,375 and 1:1:2,75, in both, big differences were

seen in the working windows between Ar and CO_2, this together with a feature resembling carbon dioxide adsorption or reduction, were proof of the carbon dioxide being captured. When the stability of this solvent was studied, cycling it fifty times, it was noticed that it was very stable and that this could suggest that no catalysis was taking place. Subsequently, in order to study if there could be catalysis at higher overpotentials, the working window was expanded to negative potentials and then, there was a clear change in local pH which could resemble the reduction of CO_2. This presented the need of a spectroscopic analysis.

The solvent, DEA:TBA-Cl:H_2O with the molar proportion 1:1:1,375, was analysed with SEIRAS, since it was not possible to use Raman. The results showed that the solvent had captured the carbon dioxide and that there is also CO_2 'not bonded' to diethanolamine. The not bonded CO_2 has three possible origins, it is captured by the water, it is captured by London or van der Waals interactions or the bond to diethanolamine with which was captured has been broken.

Changes in the bands with applied potential were seen, indicating that catalysis takes place. Exceptionally, the stretching of the dimer OCCO was assigned to the band 1200 cm^{-1} which has been calculated by DFT in other studies but never seen experimentally.

From these studies it was concluded that it is possible to electrocatalytically reduce the carbon dioxide in the presence of DES or LTTMs, this was made possible with the selection of copper as catalyst electrode and the solvent formed by DEA:TBA-Cl with the addition of water forming the proportions 1:1:1,375.

A step further for this system would be to optimize both the electrolyte and the catalyst. Appendix B explained the attempt to characterize the solvent in presence of an improved catalyst. However, this interaction could not be characterized since Raman could not be used due to the lack of plasmon activation on Cu from the monochromatic source. Two different structures, nanocubes and nanowires, were proposed. The procedure to synthesize nanowires need further improvement, since it did not lead to reproducible results. The nanocubes were studied further, analyzing them with SEM microscopy, unfortunately this microscope was not powerful enough to determine how different synthesis conditions affect the morphology, deeper analysis is needed as well. It would be very interesting to know how the different parameters affect their formation and this could be measured in FTIR, since it will give information in the mechanism of their improved performance and in how they behave with the different solvents.

For future work, a physicochemical characterization of the solvent would be necessary. Identifying if the solvent reaches a eutectic point with different proportions, and if with different proportions this solvent could adsorb more CO_2. In addition, it is important that future studies determine the mechanism with which the CO_2 is captured, since some interactions with the DEA molecules capture the CO_2 irreversibly and then all the carbon dioxide captured cannot be released for further reduction.

This thesis also showed the important role of the water in electrochemistry, so a further water content optimization focusing on conductivity, CO_2 content, role in the electrode surface and stability of solvent/water during electrochemistry is recommended to improve this process.

Moreover, further spectroscopic studies would be interesting to acquire more information in how the carbon dioxide is reduced and how the products are formed. In addition, it will be interesting to model the system using molecular dynamics to help understand how the different parameters of the solvent affect the electrocatalytic carbon dioxide reduction and to further explain the experimental results found.

BIBLIOGRAPHY

[1] IPCC, *Climate Change 2014*. 2014.

[2] M. Inman, "Carbon is forever," *Nat. Reports Clim. Chang.*, vol. 2, no. 812, pp. 156–158, 2008.

[3] D. Archer and V. Brovkin, "The millennial atmospheric lifetime of anthropogenic CO2," *Clim. Change*, vol. 90, no. 3, pp. 283–297, 2008.

[4] M. D. D. J. R. Ehleringer, T. E. Cerling, "A history of atmospheric CO_2 and its effects on plants, animals, and ecosystems," *Springer*, pp. 83–113, 2005.

[5] A. Smets, J. Klaus, O. Isabella, V. S. Rne;, and Z. Miro, "Solar Energy."

[6] S. Benson *et al.*, "Underground geological storage," *Ipcc*, pp. 195–276, 2005.

[7] C. Philibert, J. Ellis, and J. Podkanski, "Carbon Capture and Storage in the CDM," *Int. Energy Agency*, no. December, p. 30, 2007.

[8] J. Lefebvre *et al.*, "Renewable Power-to-Gas : A technological and economic review," vol. 85, 2016.

[9] M. Younas, L. Loong Kong, M. J. K. Bashir, H. Nadeem, A. Shehzad, and S. Sethupathi, "Recent Advancements, Fundamental Challenges, and Opportunities in Catalytic Methanation of CO2," *Energy and Fuels*, vol. 30, no. 11, pp. 8815–8831, 2016.

[10] Ş. Neaţu, J. A. Maciá-Agulló, and H. Garcia, "Solar light photocatalytic CO2 reduction: General considerations and selected bench-mark photocatalysts," *Int. J. Mol. Sci.*, vol. 15, no. 4, pp. 5246–5262, 2014.

[11] K. Li, X. An, K. H. Park, M. Khraisheh, and J. Tang, "A critical review of CO2 photoconversion: Catalysts and reactors," *Catal. Today*, vol. 224, pp. 3–12, 2014.

[12] M. Gattrell, N. Gupta, and A. Co, "A review of the aqueous electrochemical reduction of CO2 to hydrocarbons at copper," *J. Electroanal. Chem.*, vol. 594, no. 1, pp. 1–19, 2006.

[13] A. A. J. Torriero, *Electrochemistry in Ionic Liquids*, vol. 1. .

[14] J. Boswell, *Instrumental Methods in Electrochemistry*, no. March. 2007.

[15] Z. Stojek, "The Electrical Double Layer and Its Structure," *Electroanal. Methods*, pp. 3–8, 2005.

[16] Y. Hori, "Electrochemical CO 2 Reduction on Metal Electrodes," *Mod. Asp. Electrochem.*, no. 42, pp. 89–189, 2008.

[17] S. Taguchi and A. Aramata, "Surface-structure sensitive reduced CO2 formation on Pt single crystal electrodes in sulfuric acid solution," *Electrochim. Acta*, vol. 39, no. 17, pp. 2533–2537, 1994.

[18] R. Kortlever, J. Shen, K. J. P. Schouten, F. Calle-Vallejo, and M. T. M. Koper, "Catalysts and Reaction Pathways for the Electrochemical Reduction of Carbon Dioxide," *J. Phys. Chem. Lett.*, vol. 6, no. 20, pp. 4073–4082, 2015.

[19] Y. Hori and A. Murata, "Electrochemical evidence of intermediate formation of adsorbed CO in cathodic reduction of CO2 at a nickel electrode," *Electrochim. Acta*, vol. 35, no. 11–12, pp. 1777–1780, 1990.

[20] Y. Hori, K. Kikuchi, and S. Suzuki, "Production of CO and in CH4 in Electrochemical Reduction of CO2 at metal electrodes in aqueous Hydrogencarbonate Solution," pp. 1695–1698, 1985.

[21] A. A. Peterson, F. Abild-Pedersen, F. Studt, J. Rossmeisl, and J. K. Nørskov, "How copper catalyzes the electroreduction of carbon dioxide into hydrocarbon fuels," *Energy Environ. Sci.*, vol. 3, no. 9, p. 1311, 2010.

[22] E. R. Pugh, K. L. Wray, D. O. E. C. De-, D. W. Dewulf, T. Jin, and A. J. Bard,

"Electrochemical and Surface Studies of Carbon Dioxide Reduction to Methane and Ethylene at Copper Electrodes in Aqueous Solutions," vol. 136, no. 6, pp. 6–8, 1989.

[23] E. S. S. A, J. J. Kim, D. P. Summers, K. W. Frese, and M. Park, "Reduction of CO2, and CO to methane on Cu foil electrodes," vol. 245, pp. 223–244, 1988.

[24] J. Lee, Y. Kwon, R. L. Machunda, and H. J. Lee, "Electrocatalytic recycling of CO2 and small organic molecules," *Chem. - An Asian J.*, vol. 4, no. 10, pp. 1516–1523, 2009.

[25] Y. Hori, W. Vielstich, H. A. Gasteiger, and A. Lamm, "Handbook of Fuel Cells," vol. 2, pp. 720–733, 2003.

[26] Y. Hori, H. Wakebe, T. Tsukamoto, and O. Koga, "Electrocatalytic process of CO selectivity in electrochemical reduction of CO2 at metal electrodes in aqueous media," *Electrochim. Acta*, vol. 39, no. 11–12, pp. 1833–1839, 1994.

[27] T. F. Jaramillo, J. K. Nørskov, J. Varley, L. Grabow, and K. P. Kuhl, "The oxidation of water and the reduction of CO2 to fuels," *Gcep.Stanford.Edu*, pp. 1–22, 2012.

[28] M. C. Figueiredo, I. Ledezma-Yanez, and M. T. M. Koper, "In Situ Spectroscopic Study of CO2 Electroreduction at Copper Electrodes in Acetonitrile," *ACS Catal.*, vol. 6, no. 4, pp. 2382–2392, 2016.

[29] L. V Haynes and D. T. Sawyer, "Electrochemistry of carbon dioxide in dimethyl sulfoxide at gold and mercury electrodes," *Anal. Chem.*, vol. 39, no. May, pp. 332–338, 2002.

[30] A. Gennaro, A. A. Isse, M.-G. Severin, E. Vianello, I. Bhugun, and J.-M. Savéant, "Mechanism of the electrochemical reduction of carbon dioxide at inert electrodes in media of low proton availability," *J. Chem. Soc., Faraday Trans.*, vol. 92, no. 20, pp. 3963–3968, 1996.

[31] C. Amatore and J. M. Saveant, "Mechanism and kinetic characteristics of the electrochemical reduction of carbon dioxide in media of low proton availability," *J. Am. Chem. Soc.*, vol. 103, no. 17, pp. 5021–5023, 1981.

[32] D. A. Tyssee, J. H. Wagenknecht, M. M. Baizer, and J. L. Chruma, "Some cathodic organic syntheses involving carbon dioxide," *Tetrahedron Lett.*, vol. 13, no. 47, pp. 4809–4812, 1972.

[33] G. A. Baker, S. N. Baker, S. Pandey, and F. V. Bright, "An analytical view of ionic liquids," *Analyst*, vol. 130, no. 6, p. 800, 2005.

[34] S. Sarmad, J.-P. Mikkola, and X. Ji, "Carbon Dioxide Capture with Ionic Liquids and Deep Eutectic Solvents: A New Generation of Sorbents," *ChemSusChem*, vol. 10, no. 2, pp. 324–352, 2017.

[35] M. Armand, F. Endres, D. R. Macfarlane, H. Ohno, and B. Scrosati, "Ionic-liquid materials for the electrochemical challenges of the future," *Nat. Publ. Gr.*, vol. 8, no. 8, pp. 621–629, 2009.

[36] E. Board and T. B. M. Trost, *Ionic Liquids*. .

[37] A. G. Fadeev and M. M. Meagher, "Opportunities for ionic liquids in recovery of biofuels," no. July 2000, pp. 295–296, 2001.

[38] C. Wang, H. Luo, D. Jiang, H. Li, and S. Dai, "Carbon Dioxide Capture by Superbase-Derived Protic Ionic Liquids," *Angew. Chemie Int. Ed.*, vol. 49, no. 34, pp. 5978–5981, 2010.

[39] S. M. Mahurin, J. S. Yeary, S. N. Baker, D. en Jiang, S. Dai, and G. A. Baker, "Ring-opened heterocycles: Promising ionic liquids for gas separation and capture," *J. Memb. Sci.*, vol. 401–402, pp. 61–67, 2012.

[40] S. M. Mahurin, J. S. Lee, G. A. Baker, H. Luo, and S. Dai, "Performance of nitrile-

containing anions in task-specific ionic liquids for improved CO2/N2 separation," *J. Memb. Sci.*, vol. 353, no. 1–2, pp. 177–183, 2010.

[41] V. Pino, M. Germán-Hernández, A. Martín-Pérez, and J. L. Anderson, "Ionic Liquid-Based Surfactants in Separation Science," *Sep. Sci. Technol.*, vol. 47, no. 2, pp. 264–276, 2012.

[42] M. Alvarez-guerra, J. Albo, E. Alvarez-guerra, and A. Irabien, "Ionic liquids in the electrochemical valorisation of CO2," *Energy Environ. Sci.*, vol. 8, pp. 2574–2599, 2015.

[43] B. a Rosen *et al.*, "Ionic Liquid – Mediated Selective," *Science (80-.).*, vol. 334, no. November, pp. 643–645, 2011.

[44] S. Zhang, J. Sun, X. Zhang, and J. Xin, "Chem Soc Rev Ionic liquid-based green processes for," *Chem. Soc. Rev.*, vol. 43, pp. 7838–7869, 2014.

[45] L. Overpotentials *et al.*, "Ionic Liquid – Mediated Selective," pp. 2–4.

[46] M. C. Buzzeo, R. G. Evans, and R. G. Compton, "Non-Haloaluminate Room-Temperature Ionic Liquids in Electrochemistry – A Review," pp. 1106–1120, 2004.

[47] M. Antonia *et al.*, "(Eco) toxicity and biodegradability of selected protic and aprotic ionic liquids," vol. 261, pp. 99–105, 2013.

[48] L. Chen, M. Sharifzadeh, N. Mac Dowell, and T. Welton, "Inexpensive ionic liquids: [HSO4]-based solvent production at bulk scale," pp. 1–3, 2013.

[49] D. A. Alonso, A. Baeza, R. Chinchilla, G. Guillena, I. M. Pastor, and D. J. Ramon, "Deep Eutectic Solvents: The Organic Reaction Medium of the Century," *European J. Org. Chem.*, vol. 2016, no. 4, pp. 612–632, 2016.

[50] R. Craveiro *et al.*, "Properties and thermal behavior of natural deep eutectic solvents," *J. Mol. Liq.*, vol. 215, pp. 534–540, 2016.

[51] G. García, S. Aparicio, R. Ullah, and M. Atilhan, "Deep Eutectic Solvents: Physicochemical Properties and Gas Separation Applications," *Energy & Fuels*, vol. 29, no. 4, pp. 2616–2644, 2015.

[52] A. Paiva, R. Craveiro, I. Aroso, M. Martins, R. L. Reis, and A. R. C. Duarte, "Natural Deep Eutectic Solvents − Solvents for the 21st Century," 2014.

[53] M. Francisco, A. Van Den Bruinhorst, and M. C. Kroon, "Low-transition-temperature mixtures (LTTMs): A new generation of designer solvents," *Angew. Chemie - Int. Ed.*, vol. 52, no. 11, pp. 3074–3085, 2013.

[54] L. F. Zubeir, M. H. M. Lacroix, and M. C. Kroon, "Low Transition Temperature Mixtures as Innovative and Sustainable CO2 Capture Solvents," 2014.

[55] Y. Dai, G. J. Witkamp, R. Verpoorte, and Y. H. Choi, "Tailoring properties of natural deep eutectic solvents with water to facilitate their applications," *Food Chem.*, vol. 187, pp. 14–19, 2015.

[56] D. J. G. P. Van Osch, L. F. Zubeir, A. Van Den Bruinhorst, M. A. A. Rocha, and M. C. Kroon, "Hydrophobic deep eutectic solvents as water-immiscible extractants," *Green Chem.*, vol. 17, pp. 4518–4521, 2015.

[57] A. P. Abbott, G. Capper, D. L. Davies, R. K. Rasheed, and V. Tambyrajah, "Novel solvent properties of choline chloride / urea mixtures †," no. November 2002, pp. 70–71, 2003.

[58] H. G. Morrison, C. C. Sun, and S. Neervannan, "Characterization of thermal behavior of deep eutectic solvents and their potential as drug solubilization vehicles," vol. 378, pp. 136–139, 2009.

[59] B. S. Singh, H. R. Lobo, and G. S. Shankarling, "Choline chloride based eutectic solvents : Magical catalytic system for carbon – carbon bond formation in the rapid synthesis of β -hydroxy functionalized derivatives," *CATCOM*, vol. 24, pp. 70–74,

2012.
[60] Y. Hou, Y. Gu, S. Zhang, F. Yang, H. Ding, and Y. Shan, “Novel binary eutectic mixtures based on imidazole,” vol. 143, pp. 154–159, 2008.
[61] K. Shahbaz, S. Baroutian, F. S. Mjalli, M. A. Hashim, and I. M. Alnashef, “Thermochimica Acta Densities of ammonium and phosphonium based deep eutectic solvents : Prediction using artificial intelligence and group contribution techniques,” *Thermochim. Acta*, vol. 527, pp. 59–66, 2012.
[62] F. Saadat, G. Bagh, F. S. Mjalli, M. A. Hashim, M. K. O. Hadj-kali, and I. M. Alnashef, “Solubility of Sodium Salts in Ammonium-Based Deep Eutectic Solvents,” 2013.
[63] A. Hayyan, M. Ali, F. S. Mjalli, M. Hayyan, and I. M. Alnashef, “A novel phosphonium-based deep eutectic catalyst for biodiesel production from industrial low grade crude palm oil,” *Chem. Eng. Sci.*, vol. 92, pp. 81–88, 2013.
[64] E. L. Smith, A. P. Abbott, and K. S. Ryder, “Deep Eutectic Solvents (DESs) and Their Applications,” *Chem. Rev.*, vol. 114, no. 21, pp. 11060–11082, 2014.
[65] T. J. Trivedi, J. H. Lee, H. J. Lee, Y. K. Jeong, and J. W. Choi, “Deep eutectic solvents as attractive media for CO 2 capture,” *Green Chem.*, vol. 18, no. 9, pp. 2834–2842, 2016.
[66] L. L. Sze *et al.*, “Ternary Deep Eutectic Solvents Tasked for Carbon Dioxide Capture,” 2014.
[67] T. J. Trivedi, J. H. Lee, H. J. Lee, Y. K. Jeong, and J. W. Choi, “Deep eutectic solvents as attractive media for CO 2 capture,” *Green Chem.*, vol. 18, no. 9, pp. 2834–2842, 2016.
[68] G. R. Pazuki and H. Pahlavanzadeh, “Correlation and Prediction of the Solubility of CO2 in a Mixture of Organic Solution Solvents 1,” vol. 39, no. 3, pp. 240–245, 2005.
[69] “PubChem.” [Online]. Available: https://pubchem.ncbi.nlm.nih.gov/. [Accessed: 02-Jun-2017].
[70] “SIGMA-ALDRICH.” [Online]. Available: https://www.sigmaaldrich.com/nederland.html. [Accessed: 02-Jun-2017].
[71] A. Nacci, A. Monopoli, and A. Fanizzi, “Cyclic Carbonate Formation from Carbon Dioxide and Oxiranes in Tetrabutylammonium Halides as solvents and catalysts,” *Org. Lett.*, vol. 4, no. 15, pp. 1552–1554, 2002.
[72] University of Cambridge, “Cyclic Voltammetry Principles.” [Online]. Available: http://www.ceb.cam.ac.uk/research/groups/rg-eme/teaching-notes/linear-sweep-and-cyclic-voltametry-the-principles. [Accessed: 02-Jun-2017].
[73] Ferraro and J. R, *Introductory raman spectroscopy*. Academic press, 2003.
[74] E. Le Ru and P. G. Etchegoin, *Principles of Surface-Enhanced Raman Spectrocopy*. Elsevier Science, 2008.
[75] M. Osawa, “Surface-enhanced infrared absorption,” pp. 163–187, 2001.
[76] I. Ledezma-Yanez and M. T. M. Koper, “Influence of water on the hydrogen evolution reaction on a gold electrode in acetonitrile solution,” *J. Electroanal. Chem.*, 2016.
[77] R. Gómez, J. M. Orts, B. Álvarez-Ruiz, and J. M. Feliu, “Effect of Temperature on Hydrogen Adsorption on Pt(111), Pt(110), and Pt(100) Electrodes in 0.1 M HClO 4,” *J. Phys. Chem. B*, vol. 108, no. 1, pp. 228–238, 2004.
[78] A. J. Bard, G. Inzelt, and F. Scholz, *Electrochemical Dictionary*. Springer, 2008.
[79] V. Artero, M. Chavarot-Kerlidou, and M. Fontecave, “Splitting water with cobalt,” *Angew. Chemie - Int. Ed.*, vol. 50, no. 32, pp. 7238–7266, 2011.
[80] I. Ledezma-Yanez, O. Díaz-Morales, M. C. Figueiredo, and M. T. M. Koper,

"Hydrogen Oxidation and Hydrogen Evolution on a Platinum Electrode in Acetonitrile," *ChemElectroChem*, vol. 2, no. 10, pp. 1612–1622, 2015.

[81] E. Perez-Gallent, M. C. Figueiredo, F. Calle-Vallejo, and M. T. M. Koper, "Spectroscopic Observation of a Hydrogenated CO Dimer Intermediate During CO Reduction on Cu(100) Electrodes," *Angew. Chemie - Int. Ed.*, vol. 56, no. 13, pp. 3621–3624, 2017.

[82] K. J. P. Schouten, Z. Qin, and M. T. M. Koper, "Two Pathways for the Formation of Ethylene in CO Reduction on Single-Crystal Copper Electrodes," 2012.

[83] F. S. Roberts, K. P. Kuhl, and A. Nilsson, "Electroreduction of Carbon Monoxide over a Copper Nanocube Catalyst: Surface Structure and pH Dependence on Selectivity," *ChemCatChem*, vol. 8, no. 6, pp. 1119–1124, 2016.

[84] F. S. Roberts, K. P. Kuhl, and A. Nilsson, "High selectivity for ethylene from carbon dioxide reduction over copper nanocube electrocatalysts," *Angew. Chemie - Int. Ed.*, vol. 54, no. 17, pp. 5179–5182, 2015.

[85] J. M. Chem, Z. Zhang, and P. Wang, "Highly stable copper oxide composite as an effective photocathode for water splitting via a facile electrochemical synthesis strategy †," no. 1, pp. 2456–2464, 2012.

APPENDIX A FUTURE PROSPECTS

This section collects some work that needs to be finished, and presents a line of research that could be followed in the future.

The aim of this research was to try reported nanostructures, benchmark them using surface enhanced Raman Spectroscopy in an aqueous solution and then evaluate their performance with the home-made solvent. Unfortunately, our Raman setup did not work for the electrochemical measurements for several reasons which escape our scope, and the reasons are explained in Appendix B. Furthermore, the method reported for the formation of nanowire like-structures proved to be irreproducible under the conditions given, and it needs further optimization before trying these surfaces as electrocatalysts.

Nanocubes

Roberts, F. Sloan, Kendra P. Kuhl, and Anders Nilsson reported a cubic nanostructured copper surface which shows high selectivity for multicarbon products, especially ethylene. It is reported that oxidative-reduction cycles in a solution containing KCl, causes the formation of this cubic structures. They reported a electrolyte formed by 0,1 M $KHCO_3$ with pH 6,8 and a scan rate of 5 mV/s. Moreover, they reported this structures had a size of 100-30 nm [83], [84].

Experimental

In order to grow these nanocubes, first, the electrode was polished manually with sand paper grain 4000 and alumina suspensions with different grain sizes of 1 µm, 0,3 µm and 0,05 µm. The electrodes were subject of an ultrasonic bath for ten minutes in ultrapure water for removing alumina traces. After it, it was placed in a solution of 0,2 M K_2CO_3, 0,2 M $KHCO_3$, 0,004 M KCl. This solution is used because a good buffer capacity is wanted.

The structures were growth in a copper electrode doing cyclic voltammetry with a scan rate of 5 mV/s and a working window from 0,8 V to -1,2 V. The copper electrode, consisting of a copper disc welded to a copper wire, all of it covered by a non-conductive gel Omega bond. For the SEM samples, a commercial copper sheet was attached to a copper conducting tape.

Discussion

It is important to mention that since the aim of the study was to characterize the nanostructures using Raman in presence of aqueous solution and the solvent, no capacitance experiment was done to find out the active surface area.

In Figure A- 1, a cyclic voltammetry obtained for the growth of nanocubes can be seen. At 0 V there is a feature that is identified as reduction from Cu(II) to Cu (I), this feature is sharp, indication of an oriented structure. At -0,3 V there is a feature identified as reduction from Cu(I) to Cu and in the reverse cycle at around 0,1 V there is oxidation from Cu(I) to Cu(II) [85].

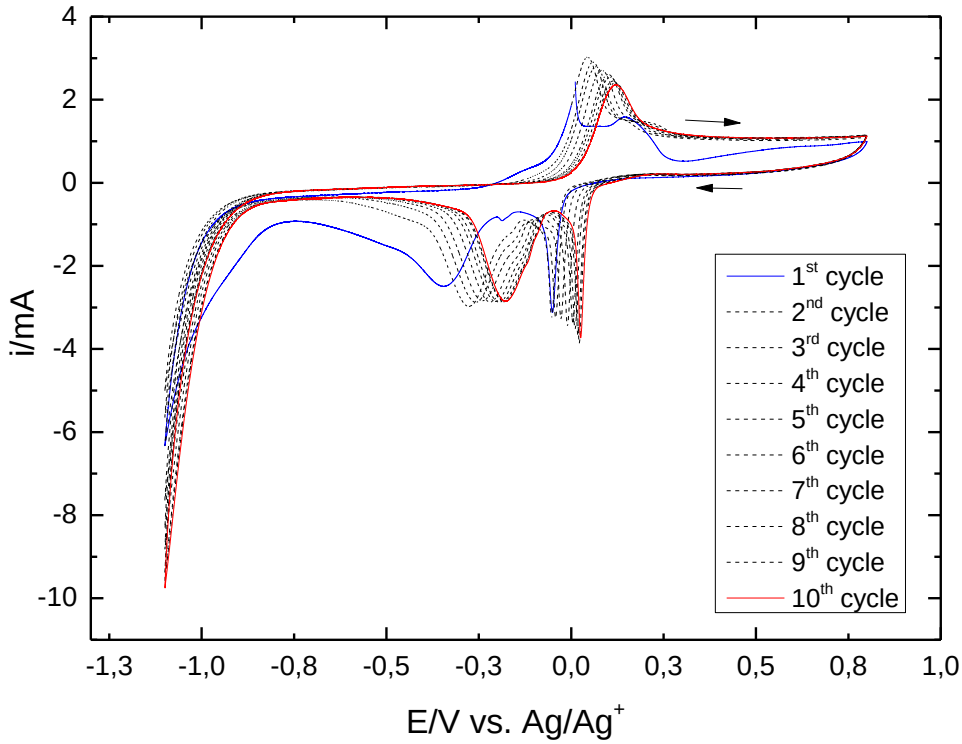

Figure A- 1. Cyclic voltammograms to generate nanostructures in copper, working window 0,8 V - 1,2 V. Scan rate: 5 mV/s.

In order characterize the nanocubic structures generated, and to know which parameters affect in the formation, three samples were grown with varying characteristics to be examined under SEM microscopy. The different characteristics used can be seen in Table 6. As well, the voltammetries to form these structures can be seen in Figure A- 2. On it, comparing Sample 1 and Samples 2, when the scan rate is increased changes can be seen. The features correspond to copper oxidation and reduction as previously explained for Figure A- 1. On Sample 3, it can be seen three features that resemble oxidation at -0,2 V from Cu to Cu (I), 0 V from Cu (I) to Cu (II) and 0,3 V $CuO/Cu(OH)_2$ and three that resemble reduction at -0,2 V from Cu(II) to Cu(I), at -0,6 V from Cu(I) to Cu and -0,8 V Cu.

Table 6. Parameters used in the samples.

	Scan rate(mV/s)	Nº Cycles	Atmosphere	Working Window
SAMPLE 1	5	10	CO_2	0,5 V -1,2 V
SAMPLE 2	10	5	CO_2	0,5 V -1,2 V
SAMPLE 3	10	5	Ar	0,5 V -1,2 V

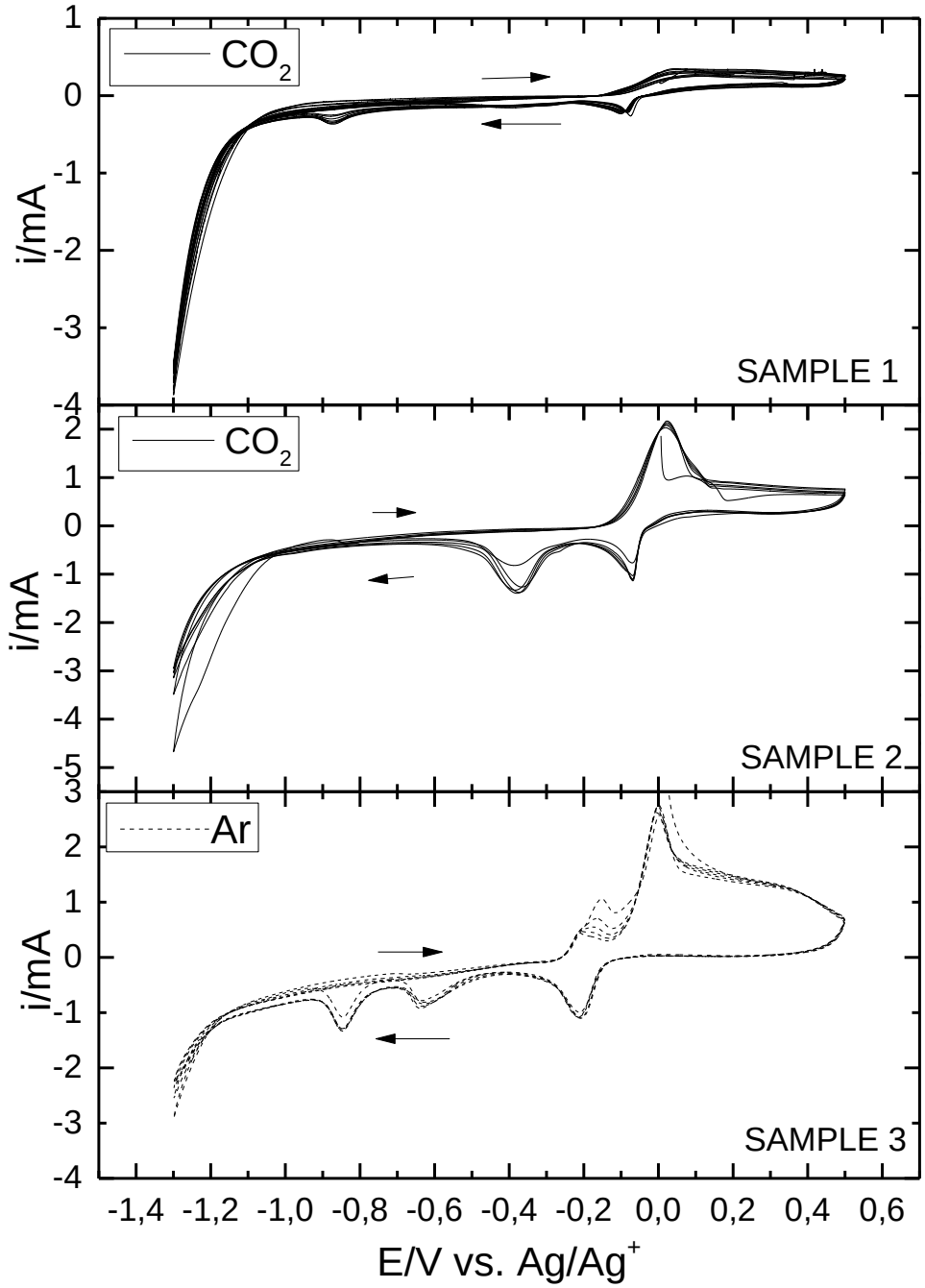

Figure A- 2. Cyclic voltammograms to generate nanostructures in copper electrode varying conditions.

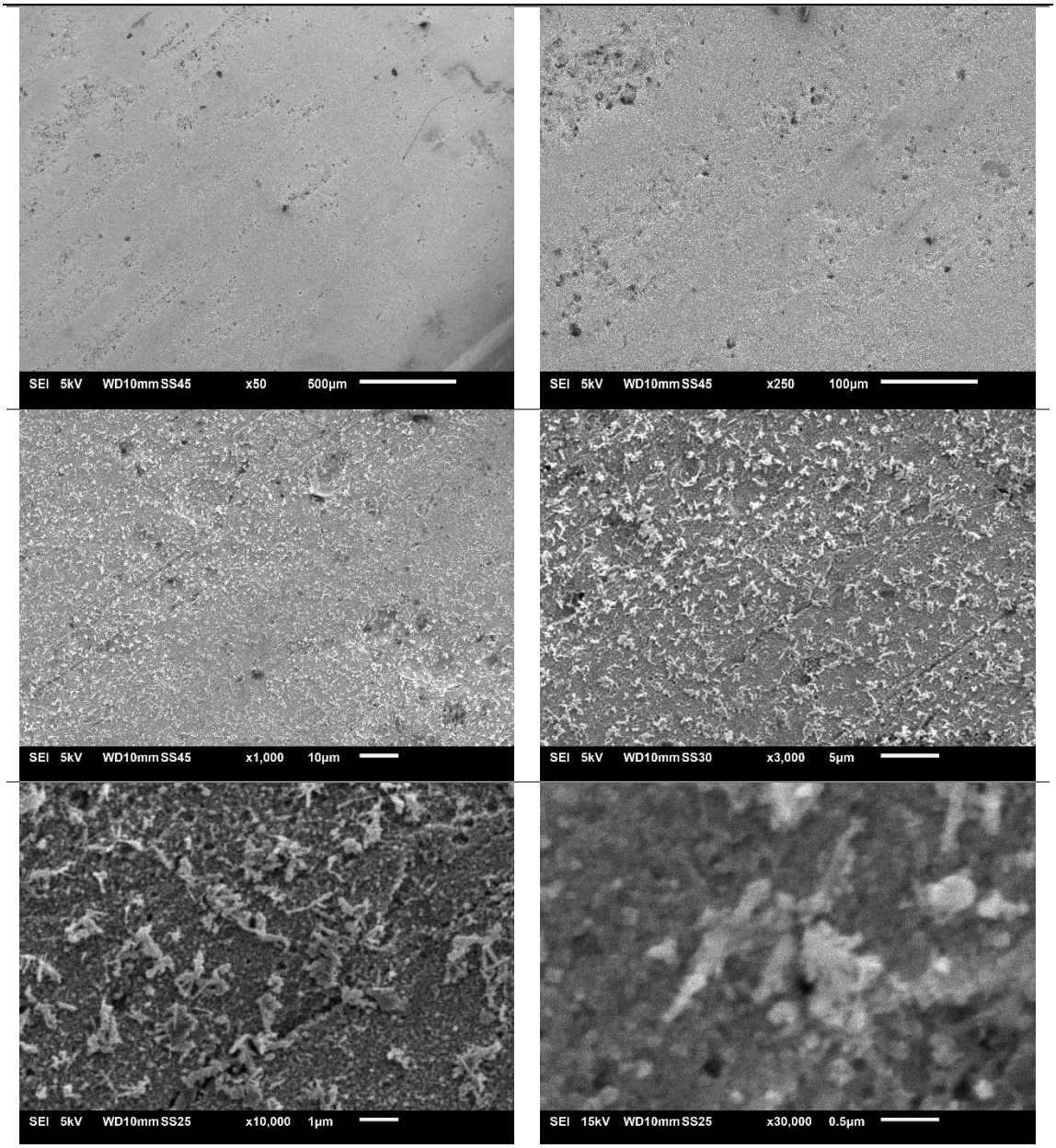

Figure A- 3. SAMPLE 1 under different magnifications of 500 µm, 100 µm, 10 µm, 5 µm, 1 µm and 0,5 µm.

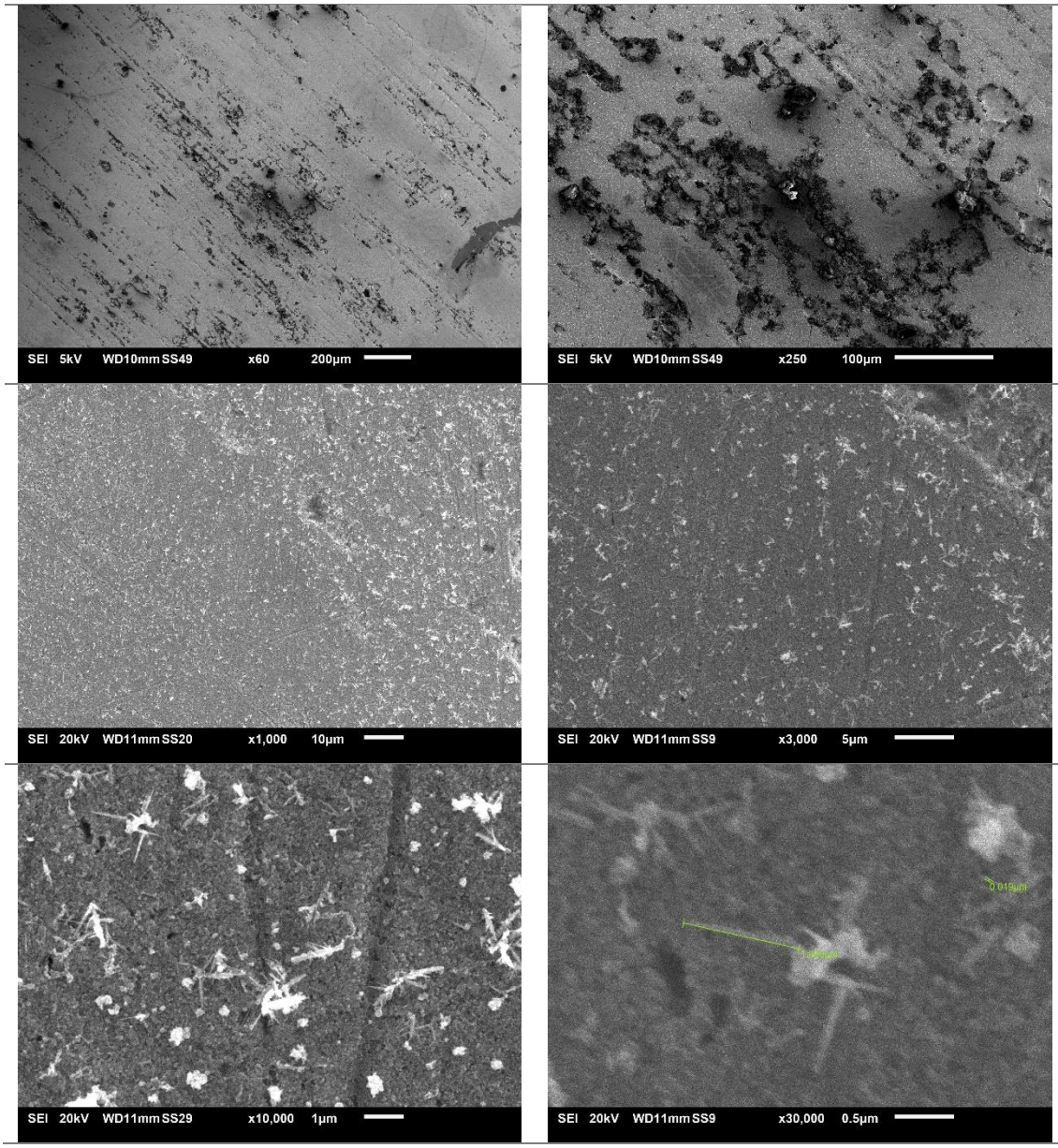

Figure A- 4. SAMPLE 2 under different magnifications of 200 µm, 100 µm, 10 µm, 5 µm, 1 µm and 0,5 µm.

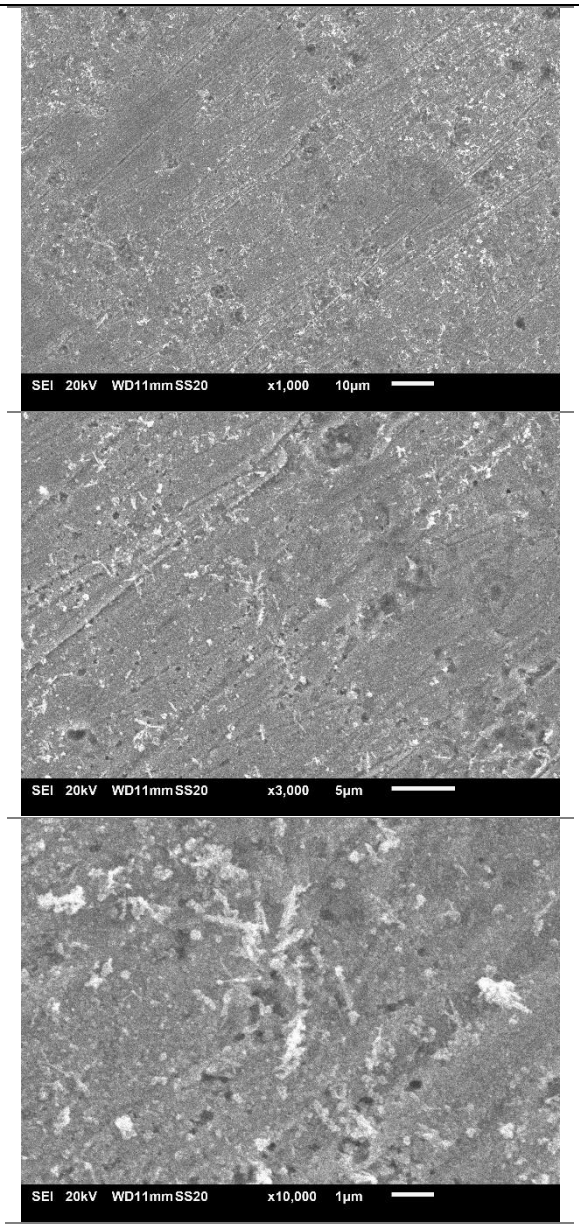

Figure A- 5. SAMPLE 3 under different magnifications of 10 µm, 5 µm and 1 µm.

When comparing the different SEM images shown in Figure A- 3, Figure A- 4 and Figure A- 5, structures can be seen. Unfortunately, the expected nanocubes cannot be seen because the SEM microscope is not powerful enough, since these structures should be in the nano range.

Sample 1 has a bigger population of structures than the Samples 2 and 3, this can be because it was cycled 5 times more and with a slower scan rate than in the other two samples. Besides, it can be seen that there is carbonate formation as well under argon atmosphere. Moreover, in Figure A- 4, the crystallite needle has a size of 1 µm and if the structures that can be seen in the background would be nanocubes, they would have a size of 19 nm.

Nanowires

Experimental

The first aim for the nanostructures was to measure them using Raman. They were done in a copper electrode, consisting of a copper disc welded to a copper wire, all of it covered by a non conductive gel Omega bond. This electrode has a geometrical surface area of 2,5 cm. The electrode was electropolished, this was done using a solution of 30% (v/v) H_3PO_4, this process was done with stirring in order to remove the bubbles that can form porous structures on the electrode.

For the cathode a platinum mesh was used, this grid was bended so it stayed parallel to the electrode surface. A voltage of 7,5 V and a current of 10 A were applied during 60 s. This procedure was repeated if the surface obtained did not look polished enough. After the procedure, the electrode was rinsed with water to eliminate the possible electrolyte residues.

The nanostructures were grown after polishing the electrode. For this, the same setup was used. The electrolyte used was a solution of 0,2 M K_2CO_3 and 0,2 M $KHCO_3$. Using the same cathode, cleaned to remove residues of the polishing electrolyte. A voltage of 3 V and a current of 10 A was applied during a variable time which would be explained after.

Discussion

As mentioned previously, no capacitance experiment was done in order to find out the real area, since the first aim was to measure them with Raman.

The reproducibility of the structures was low, since the samples presented different colour and coverage each time they were formed, just by looking with the naked eye. The growth time of the nanostructures was first set to 30 minutes. With this growth time blue oxides were formed. When longer exposure time the blue oxides detached from the surface, during this time. The experiment was repeated with an exposure time of 3 hours, but still the surface had different colour and coverage as appearance to eye. Besides, the nanostructures were let to grown for a long time (24 hours), the surface observed was completely different as well. This can be seen in Figure A- 6.

It was suggested that there were significant changes, when the growing of the surface is done just after electropolishing, without having the electrode any contact with the air. Or when after electropolished, the electrode was left in contact with air for one day and then, the nanostructures were growth. This could be due to the fact that the supposed nanowires might be grown by nucleation from a oxide formed by the contact of the copper with the air.

In Figure A- 7 a cyclic voltammogram using the electrode surface under a growth of 24 hours can be seen. It was done under CO_2 saturation with a scan rate of 0,1 V/s and a working window from 0,3 V until -1,2 V. On it, significant changes can be seen between the first and second cycles which could mean that there are notable changes in the surface during the process.
This presents, an interesting option for future work, since first the nanostructures should be able to be growth with reproducibility.

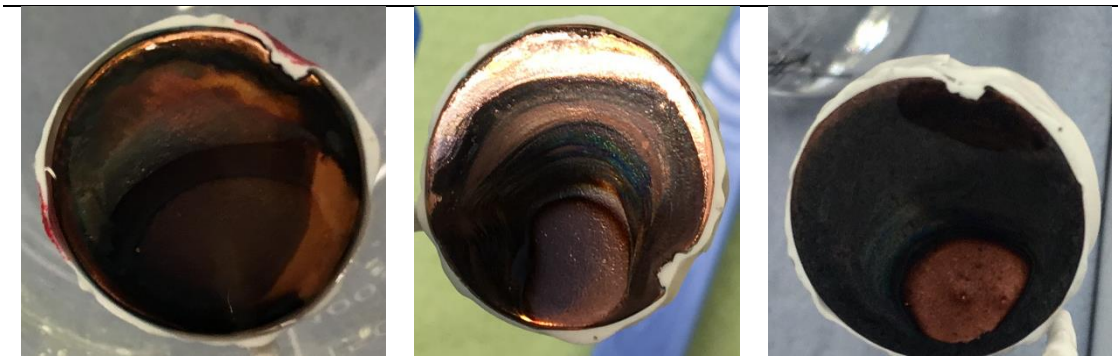

Figure A- 6. Pictures of the copper electrode surface after growing nanostructures for 30 m (left), 3 h (middle) and 24 h (right).

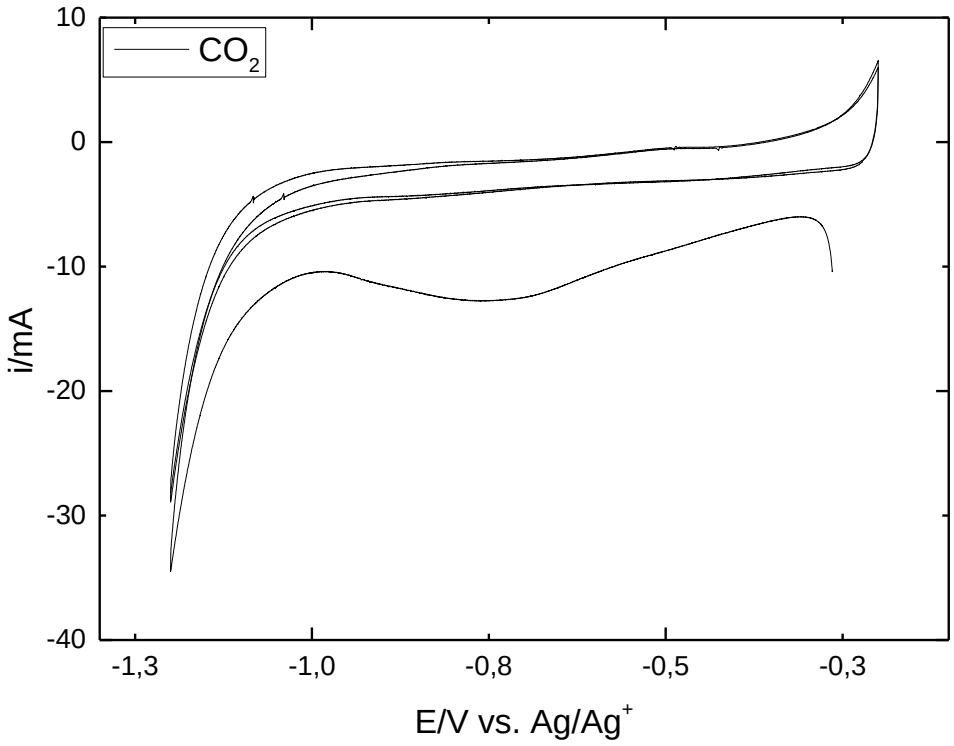

Figure A- 7. Cyclic voltammograms for a nanostructured copper electrode in a solution 0,2 M K_2CO_3 0,2 M $KHCO_3$, under CO_2 atmosphere. Scan rate: 0,1 V/s. Working window: 0,3 V -1,2 V.

Conclusions

Both nanostructures present promising new options, unfortunately they could not be analyzed in Raman.

The cubic nanostructure would need a more powerful microscope to study, how the growing parameters affect the formation. The nanocubes were tried to be used in the FTIR, since it was not possible in Raman, but when the nanocubes were formed in the film deposited above the germanium crystal, even depositing a thicker copper film and reducing the working window and the cycles to form them, the film broke. If it would be known how the growing parameters affect maybe it would be possible how to do this process which will result very interesting to know the pathway of how this nanostructures has such a higher selectivity for ethylene.

The possible nanowires presented as well a promising option, but first their growing characteristics need to be studied to obtain reproducibility.

APPENDIX B RAMAN

Problems

In numerous occasions, SERS was tried to be performed on a copper electrode with nanostructures on its surface (nanocubes and nanowires), as well as with the usual roughening of its surface and with just the metal. In all the cases the probe was moved to re-focus manually, trying to point to different places of the electrode surface.

Every time, when the probe was positioned far from the surface, spectra looked normal and with high intensity as if the enhanced was working using SERS. But after, doing electrochemistry in-situ on a large range of potentials, the results did not change. Bands were at the same position all the times, which could happen. However, different enhancements were done with different solutions, and always it was observed that the bands did not present Stark effect, even in a large potential region.

On the contrary, when the probe was situated close to the surface of the electrode there was a deformation in the middle of the spectra. This was tried and repeated with different solutions and surface enhancements. It was concluded that the laser is too powerful and when the enhancement is added there is a saturation in the probe, which makes impossible to be used for SERS in the electrode surface used and with the used configuration.

Together with the above described, other small complications were encountered. At high potential, bubbles formed during the reaction were deposited on the probe, making it impossible to keep measuring. This is shown in Figure B- 1, where the WE and the laser probe with the bubbles attached can be seen.

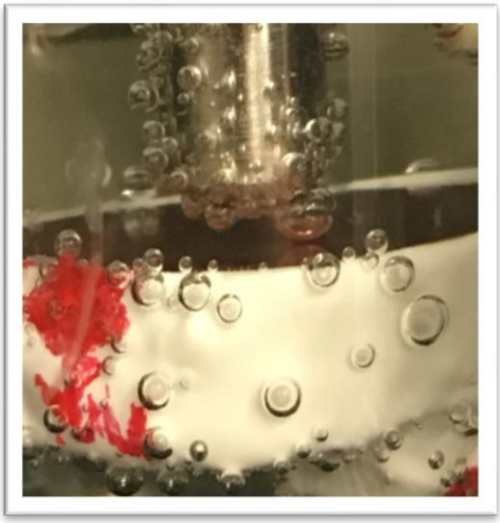

Figure B- 1. Raman probe and WE.

In aqueous solutions, there were some peaks that at first were identified as Cl, but blank experiments were performed to find out that these bands were still present and its relationship with Cl was discarded. At first, it was though the instruments could be contaminated but after cleaned everything these peaks were still there. Then measurements were taken with just water and just silicon and the peaks were still there, so it was concluded that they belong to the probe, which is made of stainless steel.

Ex-situ Raman

Figure B- 2, the different spectra between the DEA and the solvent formed by DEA:TBA-Cl:H_2O is shown. For the solvent, some bands were identified, some of this bands are also present in the diethanolamine pure, sometimes with some displacement, which could be caused by the interactions between DEA and TBA-Cl once the solvent is formed. For the DES some bands were identified. A band at a wavenumber of 3315 cm^{-1} was attributed to the vibration of the functional group N-H. Several wavenumber are assigned to the functional group C-H, stretching at wavenumber of 2929 cm^{-1}, 2869 cm^{-1}, 1323 cm^{-1} and bending at wavenumber of 1312 cm^{-1}, 1301 cm^{-1}, 1270 cm^{-1}, 1029 cm^{-1}. Band at a wavenumber of 2744 cm^{-1} was identified as the functional group CHO. Several wavenumber were assigned as the functional group C-C at 1156 cm^{-1}, 1126 cm^{-1}, 1149 cm^{-1}, 1131 cm^{-1} and 1108 cm^{-1}. Band at a wavenumber of 879 cm^{-1} was attributed to the stretching of the functional group C-N-C.

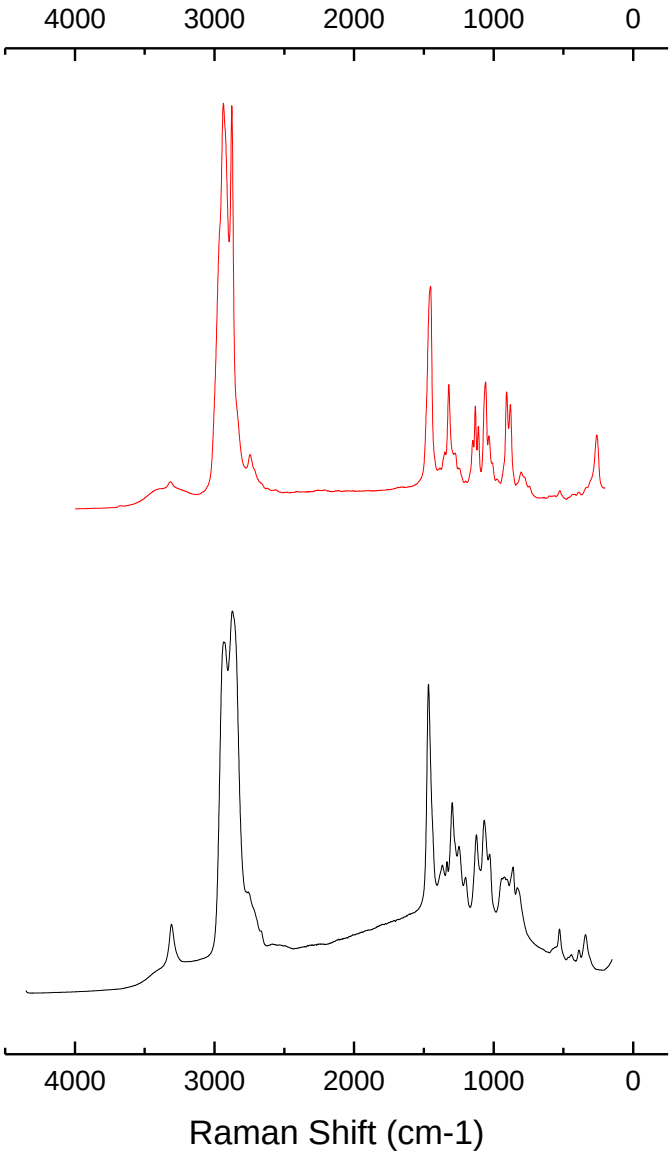

Figure B- 2. Solvent DEA:TBA-Cl:H_2O with molar proportions 1:1:1,375 spectra (in red) and DEA spectra (in black).

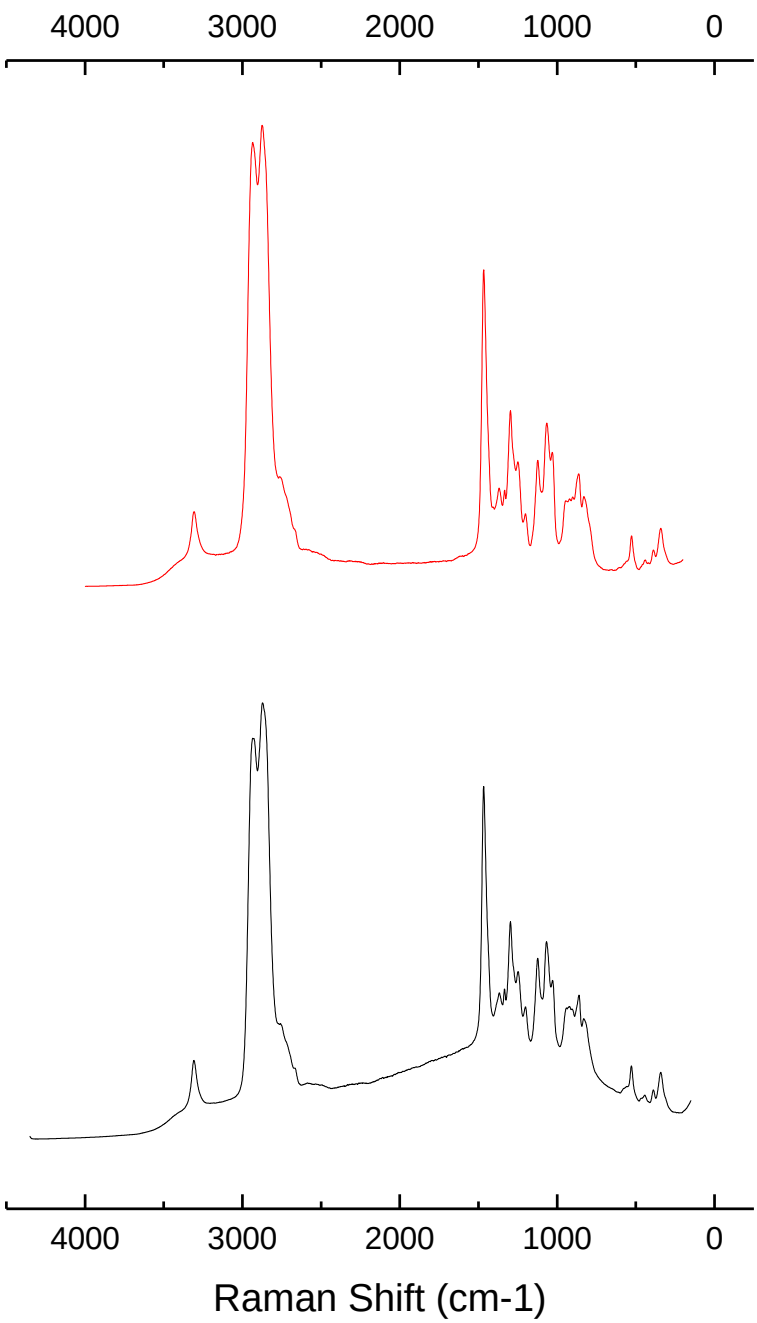

Figure B- 3. DEA (black) and DEA after bubbling CO_2 (red).

Diethanolamine was measured before and after bubbling CO_2, this can be seen in Figure B- 3. This was done in order to know if the CO_2 bonds to the N forming an amide. However, it can be seen that there is no change due to carbon dioxide presence.

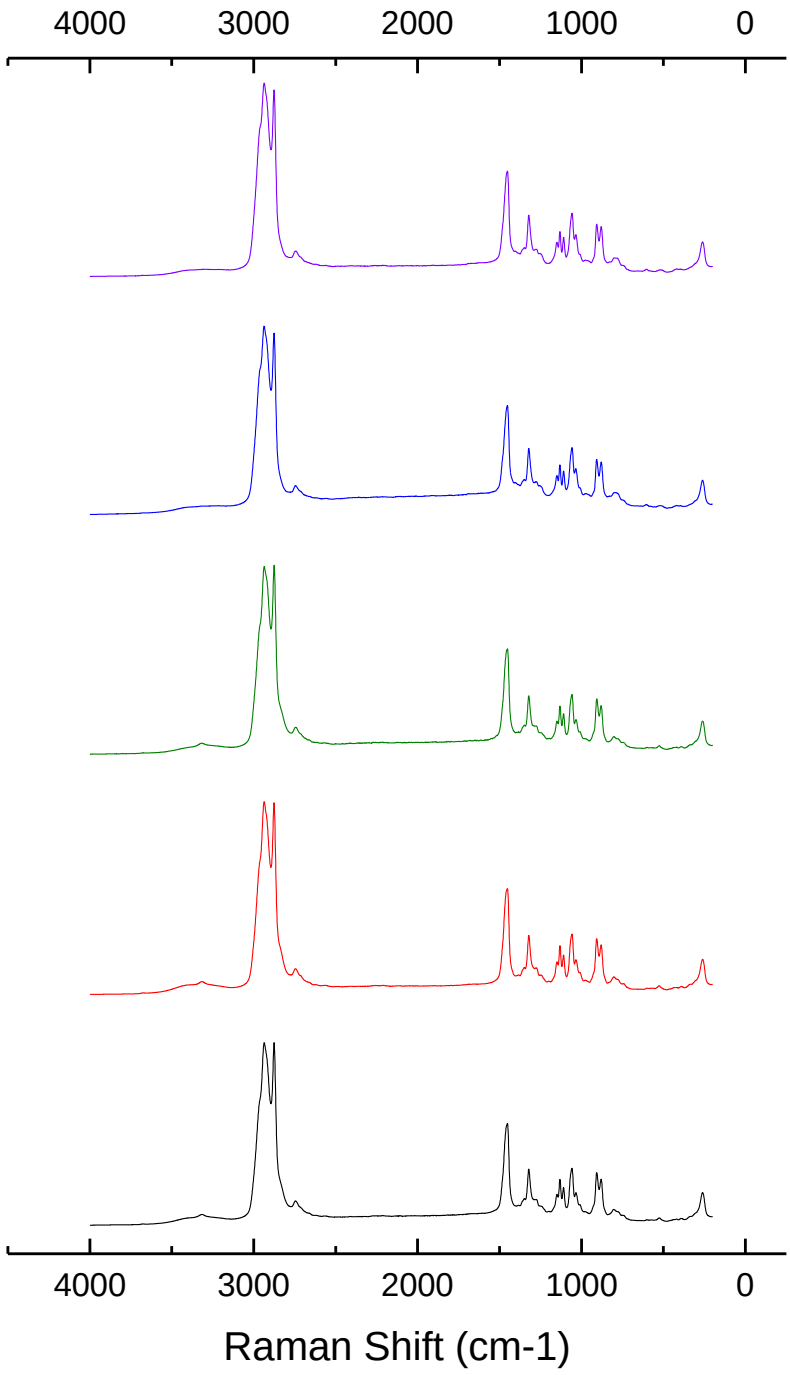

Figure B- 4. Solvent DEA:TBA-Cl:H_2O in the molar proportions 1:1:1,375 under different conditions: Solvent (black), after bubbling Ar (red), after 50 cycles (green), after applying -0,8 V for 1 h (blue) and after applying -2,5 for 30m (purple).

In Figure B- 4 is shown different trials that were done using normal ex-situ Raman. First the solvent after preparation was measured, after the solvent was saturated with argon and measured again. Another portion of the solvent was saturated with carbon dioxide and fifty cycles with the working window -0,3 V 1,4 V were applied with a scan rate of 0,1 V/s. After this the solvent was measured with Raman again, but as it can be seen there is no difference in the bands compare to the fresh solvent or the solvent under argon atmosphere. Besides, it was decided to apply a potential of -0,8 V during 1 h to see if

there was possible to see any product of CO_2 reduction or decomposition of this solvent, but as it can be seen the spectra is the same that in the previous cases. After this, with the same purpose as previously expressed, a potential of -2,5 V was applied during 30 minutes and again the spectra does not change. This suggested at first that the solvent is very stable under carbon dioxide atmosphere since no decomposition can be seen and there is not carbon dioxide reduction. However, as it was explained in the previous section the Raman was used several times with carbon dioxide in aqueous solutions and copper electrode and this is known to generate products but no change in bands was detected. So it is determined that these measurements are not conclusive, therefore, it was decided to use the available FTIR which can be seen in Section 4.

APPENDIX C FTIR DATA

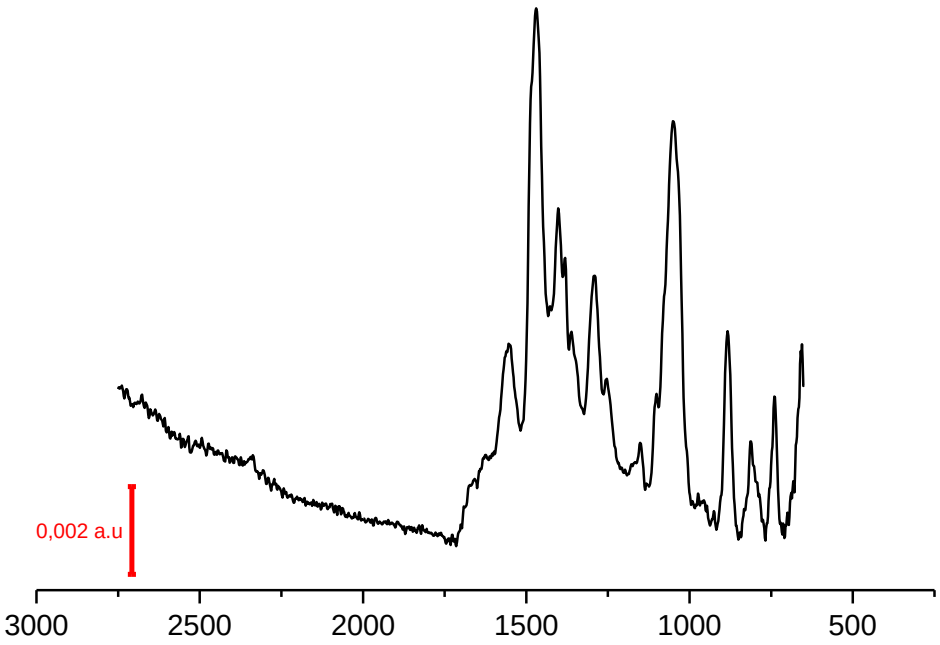

Figure C- 1. Transmission spectrum for the solvent DEA:TBA-Cl:H_2O in the molar proportion 1:1:1,375 saturated with CO_2.

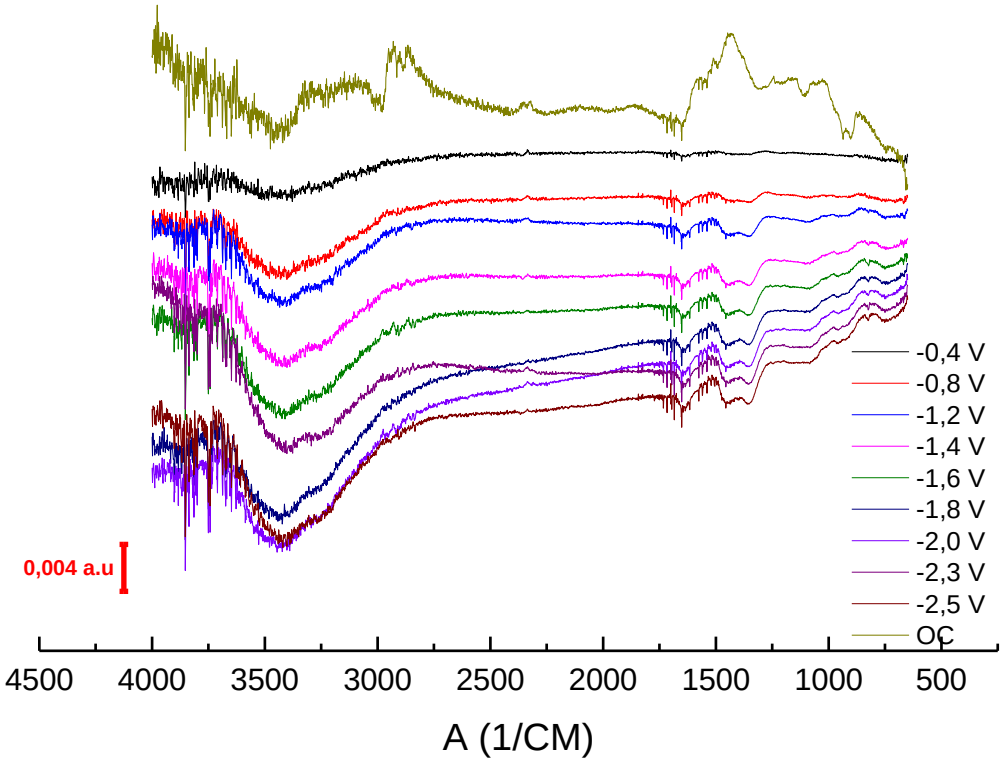

Figure C- 2. SEIRAS raw data.

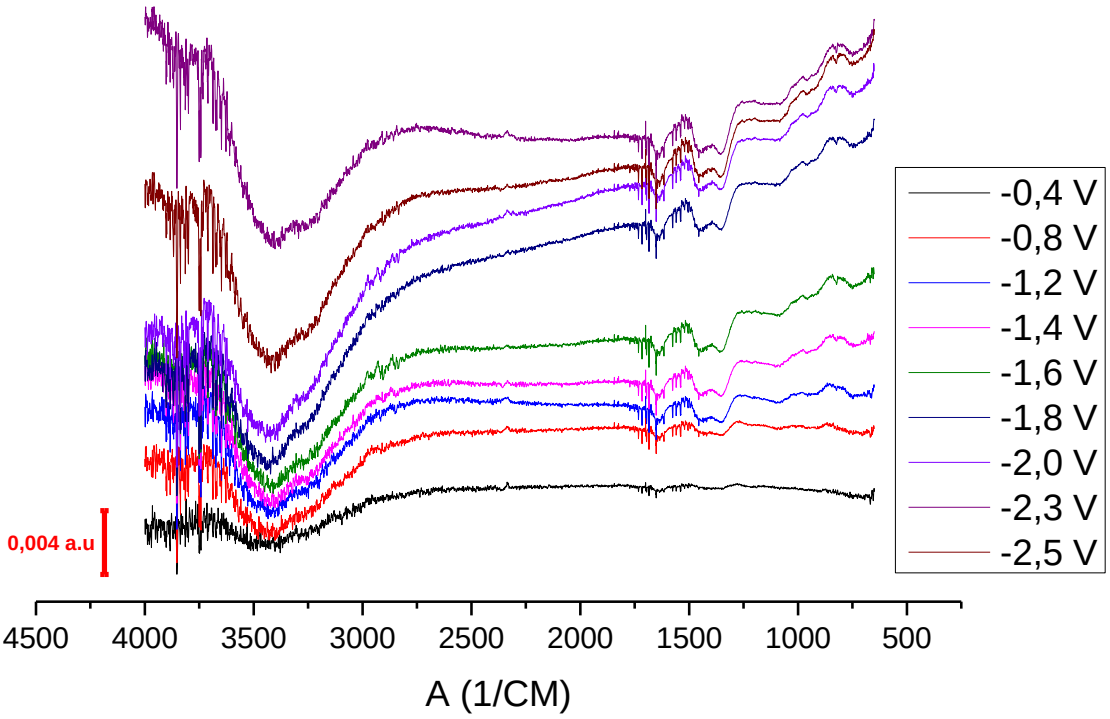

Figure C- 3. SEIRAS processed data.